CNS1-dependency of *in vivo* peptide-induced $CD4^+Foxp3^+$ regulatory T cells

CNS1-Abhängigkeit von *in vivo* Peptid-induzierten $CD4^+Foxp3^+$ regulatorischen T-Zellen

Doctoral thesis for a medical doctoral degree
at the Graduate School of Life Sciences,
Julius-Maximilians-Universität Würzburg,
Section Infection and Immunity

submitted by

Franziska Jonas

from Fulda

Würzburg 2021

Submitted on:

Members of the Thesis Committee:

Chairperson: Prof. Dr. Wolfgang Kastenmüller

Primary Supervisor: Prof. Dr. Manfred Lutz

Supervisor (Second): Dr. Stephan Kissler

Supervisor (Third): Prof. Dr. Martin Fassnacht

Date of Public Defence:

Date of Receipt of Certificates:

Contents

List of Figures

List of Tables

Abbreviations

General abbreviations

APC	antigen-presenting cell
bp	basepair(s)
Cas9	CRISPR associated protein 9
CD	cluster of differentiation
CM	complete media
CNS	conserved non-coding sequence
CRISPR	Clustered Regularly Interspaced Short Palindromic Repeats
CTLA-4	cytotoxic T-lymphocyte-associated protein 4
d	day(s)
DC	dendritic cell
DMSO	dimethyl sulfoxide
DNA	deoxyribonucleic acid
dNTPs	deoxynucleotide triphosphates
EDTA	ethylenediaminetetraacetic acid
FACS	fluorescence activated cell sorting
Fc	Fragment, crystallizable
FCS	fetal calf serum
Foxp3	Forkhead box P3
g	acceleration due to gravity
h	hour
i.p.	intraperitoneal
i.v.	intravenous
IL-2	Interleukin-2
IL-2Rα	Interleukin-2 receptor α chain
kb	kilobase(s)
KO	knockout
LN	lymph node
MACS	magnetic activated cell sorting
MHC	Major Histocompatibility Complex
min	minute
MLN	mesenteric lymph node

mRNA	messenger RNA
NOD	non-obese diabetic
PBS	phosphate-buffered saline
PCR	polymerase chain reaction
PLN	pancreatic lymph node
PTPN22	protein tyrosine phosphatase, non-receptor type 22
pTreg	Periphery-derived regulatory T cell
RPMI CM	Roswell Park Memorial Institute cell culture medium
RT	room temperature
s.c.	subcutaneous
SP	Single positive
T1D	type 1 diabetes
TCR	T cell receptor
Teff	effector T cell
tg	transgenic
Treg	regulatory T cell
tTreg	Thymus-derived regulatory T cell
V	Volt
WT	wild type

Nucleotide abbreviations

A	adenine
C	cytosine
G	guanine
T	thymine

1. Introduction

1.1. Innate and adaptive Immunity

Throughout human life, we are permanently confronted with foreign, potentially hazardous pathogens such as bacteria, viruses or funghi [5]. Intrinsic risks i.e. neoplastic transformation add on to these threats. Thus, survival is very much dependent on the integrity of host defense mechanisms to counteract this threat [5]. This defense is provided by the immune system of higher organisms. It provides potent protection through a complex network of lymphoid organs, immune cells, cytokines and humoral factors. In the first place, protection of the host organism is ensured by physical, chemical and microbial barrier mechanisms [5]. If these barriers fail, in the second place, innate immunity takes action. Hereto, cellular innate immune cells such as neutrophils, monocytes, macrophages as well as complement factors, cytokines and acute phase proteins attack invading pathogens [2]. Herewith, a rapid but unspecific reaction against a broad spectrum of pathogens is ensured.

Specific reactions, however, require recognition of pathogen-specific epitopes by T and B cells bearing antigen-specific receptors. Yet, this adaptive response occurs somewhat delayed as antigen specificity takes several days or weeks to develop [2]. In contrast to innate immunity where no memory can be established, adaptive immune responses can result in a memory response, which enables more rapid antigen-specific defense in case of subsequent exposition with the same antigens [6, 7].

Antigen-specific B and T cell receptor formation relies on a recombination process. Here, multiple DNA segments are cut, modified and spliced together. More specific, in humans a variety of 25 x 10^6 T cell receptors (TCRs) in the blood and 1×10^5 to 2×10^5 receptor variants in the T cell memory subset has been estimated to exist [8]. As part of their development, naïve T cells leave the bone marrow and migrate to the thymus where they undergo positive and negative selection. T cells with a receptor that recognizes self-MHC in the thymic cortex are positively selected. The remaining CD4 or alternatively CD8 single positive T cells pass on to the corticomedullary junction where negative selection takes place. T cells highly reactive to self-antigens undergo clonal deletion by apoptosis [9]. Less than 10 % of thymocytes withstand this strict positive and negative selection process [7]. Emerging naïve T cells are competent to recognize their specific antigen when presented with self MHC but tolerant to self-antigens [2]. Yet, autoantigens that are insufficiently expressed in the primary lymphoid tissue do not contribute to central tolerance. As a consequence, some cognate autoreactive T cells will emerge from the thymus (Figure 1) [10].

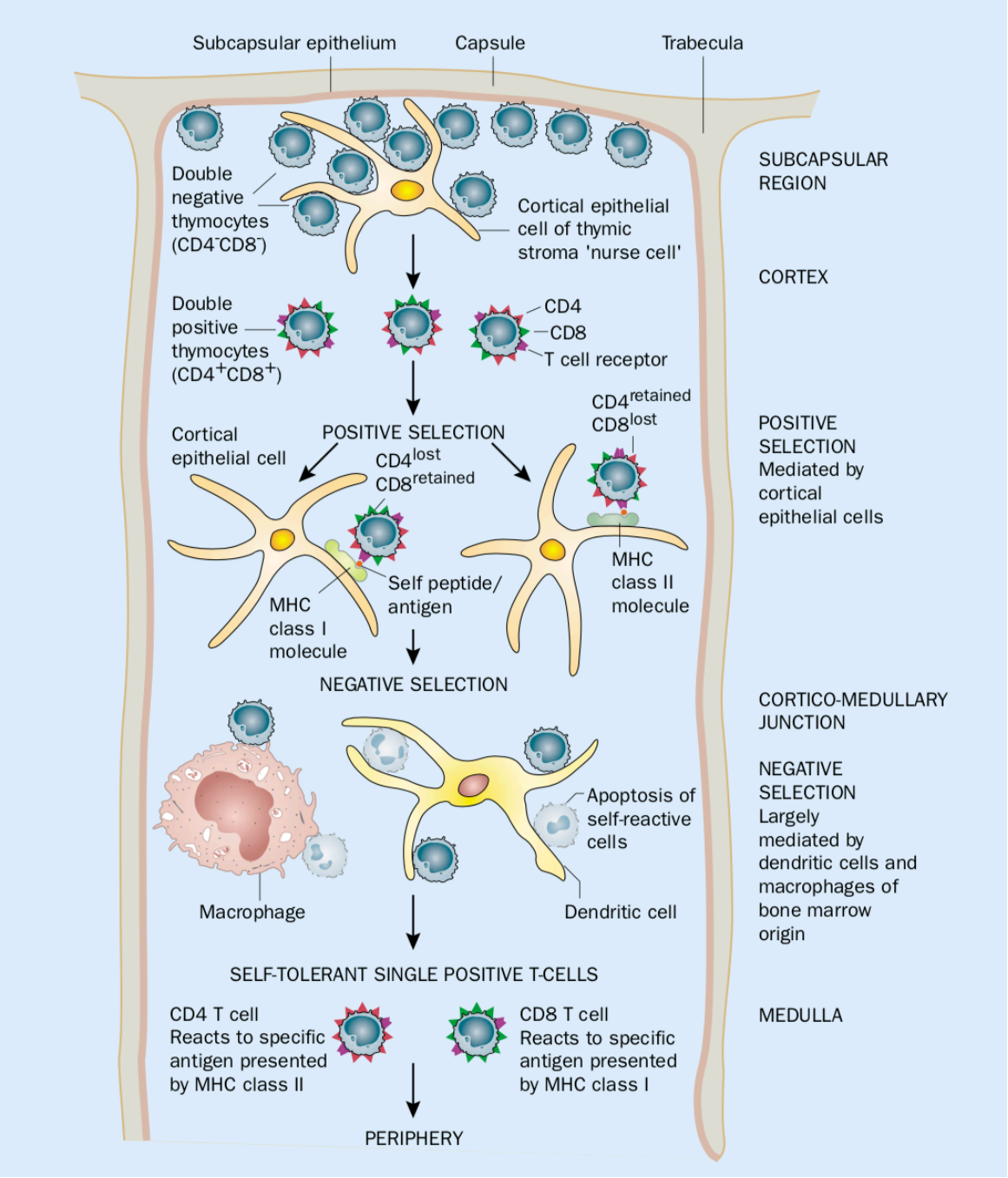

Figure 1: T cell development in the thymus

Early T cell progenitor cells from the blood stream enter the thymus in the subcapsular region. T cells that recognize antigens presented from cortical epithelial cells undergo positive selection and pass from the cortex into the cortico-medullary junction where negative selection takes place. Here, T cells recognizing self-antigens are eliminated. Emerging T cells are thus capable to react to specific antigens presented via MHC molecules but are tolerant towards self-antigens. Figure and description adopted from [2].

Antigen-naïve T cells home to peripheral lymph nodes where antigen-presenting cells (APCs) present corresponding foreign antigens through surface MHC II molecules. However, presentation of self-antigens such as peptide fragments is performed by all nucleated cells

through surface MHC class I molecules. Depending on the mode of antigen-presentation either CD4 positive T helper cells or CD8 positive cytotoxic T cells are activated and trigger further immune responses (reviewed in [6]).

1.2. Autoimmunity

Excessive immune responses to pathogens, but also reactivity against self-antigens can be harmful for the host organism [11]. However, autoreactive receptors occur naturally when immunologic responses take place. This is as a broad spectrum of receptor affinities is required to protect from external pathogens [9, 12]. Yet, in the vast majority of cases, exposition of immune cells with an autoreactive receptor to auto-antigens does not lead to autoimmunity. Various security-mechanisms emerged throughout evolution to control excessive immune reactions and to avoid damage to the host: First of all, priming of emerging naïve T cells is restricted to antigen-presentation with MHC molecules. This ensures that only pathogenic antigens invading host cells or inducing an inflammatory response can trigger an immune response. Innocuous self-antigens thus should be spared. Besides, a T cell receptor binding to the antigen-MHC complex alone is not sufficient for T cell activation. Signal transmission into the cell is highly dependent on coreceptor stimulation. The main coreceptors for T cell signaling are CD80, CD86 and CD40 on APCs that bind to CD28, CTLA-4 and CD40 ligand located on the T cell [2]. Mediators that are present in an inflammatory environment induce upregulation of these costimulatory molecules and thus render T cell activation more likely [13]. In contrast to an inflammatory environment, healthy tissue cannot provide adequate co-stimulation for T cell activation. Therefore, subthreshold stimulated T cells become anergic instead [2]. Finally, immune homeostasis is performed by so called regulatory T cells (Tregs) that dampen proinflammatory reactions (see below). However, if central and peripheral tolerance mechanisms fail autoimmunity can occur [14].

1.3. Type I Diabetes

If immunosuppressive capacities fail, immune responses get shifted towards autoimmunity [14]. Due to the low prevalence of individual disease, heterogenous clinical presentations and varying diagnostic criteria over time, epidemiologic studies on autoimmunity in general are difficult to conduct [15]. Yet, Cooper and colleagues estimated a prevalence of autoimmune

diseases of 7.6 % - 9.4 % [15] which is considerably higher than the seminal calculations from Jacobson et al. in 1997, who estimated a prevalence of 3.2 % [16].

For instance, type I diabetes is considered to be an immune-associated, if not directly immune-mediated disease [17, 18]. Even though wide variations in disease incidence can be witnessed between countries, the overall incidence has increased continuously over the last decades (Figure 2) [1, 19, 20].

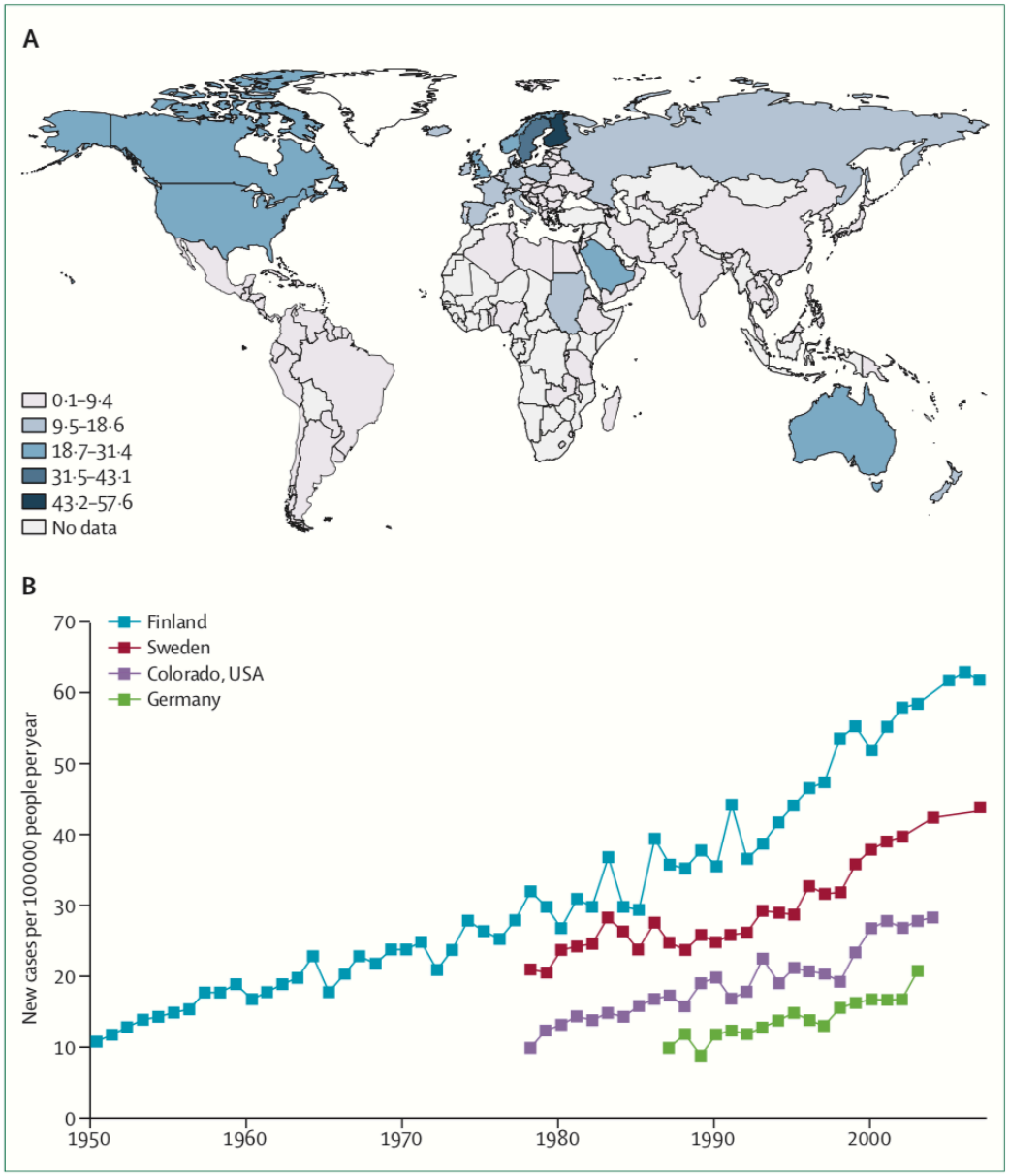

Figure 2: Incidence of Type I Diabetes in 0-14 years old children

A) Estimated global incidence of type I diabetes, by region, in 2011.

B) Incidences of type I diabetes in 0-14 years old children in indicated regions.

Figure and description adopted from [1].

However, the cause of this global trend is still unknown. Next to genetic changes, environmental influences such as certain diets, vitamin pathways or viral infections are currently subject to a controversial discussion [1, 21, 22]. Central to type I diabetes are dysregulated blood glucose levels due to a selective destruction of insulin-producing pancreatic β-cells [22]. Acute dysregulation of blood glucose levels can result in potentially life-threatening periods of hypoglycemia or periods of hyperglycemia such as ketoacidosis or hyperosmolar hyperglycemic coma. Long-term complications include macrovascular pathologies such as cardiovascular disease, peripheral artery occlusive disease and stroke. Microvascular complications include diabetic glomerulosclerosis, retinopathy and neuropathy [23]. To restrain blood glucose levels, patients are dependent on supplementation of exogenous insulin for the rest of their lives. However, long-term micro- and macrovascular complications due to hyperglycemia cannot be avoided completely [24-26]. Disease-onset is classically seen in children and adolescents. Typical symptoms include polydipsia, polyphagia and polyuria. Central criteria for diagnosis in humans are pathologic fasting blood glucose levels (higher than 7 mmol/L (126 mg/dL)), any blood glucose level of 11.1 mmol/L (200 mg/dL) or higher with symptoms of hyperglycemia, or an abnormal 2 h oral glucose-tolerance test. Since 2009 the American Diabetes Association has been approving pathologic levels of glycated hemoglobin (HbA1c > 6.5 %) as a diagnostic criterion [27]. Despite these criteria, diagnosis of type I diabetes is not trivial. Especially the discrimination between the autoimmune-driven type I diabetes and other diabetes subtypes like type II diabetes that entails a metabolic syndrome and primarily affects adults can be difficult in some cases [1].

However, as type I diabetes is thought to be immune mediated, also immunological changes can be observed: Chronic inflammation of pancreatic islets causes β-cell damages. Regeneration, if any, is insufficient and thus cannot prevent the loss of endogenous insulin production over time. However, characteristic disease symptoms do not occur until 90 – 95 % of β-cells are lost [28]. Causes for this progredient β-cell destruction are seen in disturbed processes in bone marrow and thymus, as well as in the immune system and the β-cells themselves [1]. Within the insulitis lesions several components of the immune system take action. $CD8^+$ cytotoxic T cells are the most predominant population, followed by macrophages, $CD4^+$ T helper cells, B lymphocytes and plasma cells [29]. In contrast, regulatory T cells as well as natural killer cells (NK cells) are rare [1]. Notably, there are as well serological changes in patients with type I diabetes. More than 90 % of newly diagnosed individuals have one or more of the following autoantibodies at the time of disease onset: Those reactive to insulin (IAA), glutamic acid decarboxylase (GADA), insulinoma-associated autoantigen 2 (IA2A) and

zinc transporter 8 (ZnZ8A). These autoantibodies can appear months to years before symptomatic onset and might thus also be useful for early diagnosis or even disease prevention [21, 30-32].

Although it is not yet fully understood what exactly triggers disease onset, some genetic associations are known to affect disease susceptibility by contributing to an aberrant immune response [33] or to a misguided reactions towards environmental stimuli [34-36]. So far, around 60 susceptibility loci have been mapped. The strongest association can be found for the human leucocyte antigen (HLA) [13]. Other associations can be found for proteins affecting T cell activation such as PTPN22 (protein tyrosine phosphatase, non-receptor type 22), CTLA-4 (cytotoxic T-lymphocyte-associated protein 4) and IL-2Rα (Interleukin-2 receptor α chain) [13, 21]. This finding supports the hypothesis that $CD4^+$ and $CD8^+$ T cells play a fundamental role for the type I diabetes pathology [13].

Standard treatment protocols for diabetes type I rely on the supplementation of exogenous insulin via multiple daily injections or by the use of continuous subcutaneous insulin infusions (CSII). Improvements in existing therapy strategies include the advanced insulin pump systems, the development of specifically designed long-acting insulin analogues and modulation of incretins [1]. However, today's clinical strategies mainly focus on a symptomatic control of dysregulated blood glucose levels rather than treatment of the underlying autoimmune-mediated destruction of insulin-producing β-cells. Current approaches for the treatment of other autoimmune disease such as Hashimoto's disease, Grave's disease or Myasthenia gravis rely on symptomatic control and unspecific immunosuppression to globally dampen autoimmune reactions as well [37, 38]. However, unspecific immunosuppression as well reduces immune responses against foreign pathogens. Lethal infections may result from this practice. Toxicity and side effects of this medication add on to the negative side of such a treatment [37]. Strategies, that instead target the dysregulated immune response specifically are of interest to find a curative approach for the treatment of autoimmune diseases including type I diabetes [38, 39].

To date, multidirectional approaches to specifically suppress β-cell autoimmunity in T1D are being tested in clinical trials with the object of disease modulation at different stages [38]. Windows for therapeutic intervention are see at an early prodromal stage, at the time of clinical disease onset and for the protection of residual β cell function in long-term T1D patients [40]. Antigen-independent immunotherapies include the administration of depleting antibodies against effector T cells (Teff) [41, 42] or B cells [43] and antibody-derivatives such as immunoglobulin fusion molecules like CTLA-4-Ig (Abatacept) [44, 45]. Neutralization of

proinflammatory effector molecules like TNFα [46] or IL-21 [47] has been considered as a therapy as well. More recently, the microbiome and its potential for disease treatment due to its impact on the normal function of the immune system got into focus of interest [48-54].
Although today's clinical application of targeted immunotherapy for T1D is still limited [39], some therapeutic strategies showed promising results. In particular, $CD4^+$ regulatory T cells (Tregs) have already been shown to prevent autoimmunity and rejections of transplants in clinical studies [55] (see below). For instance, encouraging protocols for T1D-treatment for instance rely on a low dose administration of IL-2 for *in situ* Treg induction [56-58]. Alternatively, application of a whole antigen or peptide antigens is carried out to selectively tolerize autoreactive Teff and promote antigen-specific Tregs [38, 59].

1.4. $CD4^+Foxp3^+$ Regulatory T cells (Tregs)

1.4.1. $CD4^+Foxp3^+$ Tregs as regulators of excessive immune responses

As mentioned above, at the one hand adaptive immune responses constitute potent defense mechanisms against harmful pathogens. On the other hand, negative consequences from an overwhelming immune response against host tissues must be prevented. Such regulation of immune responses is, among others, conducted by a subset of $CD4^+$ T cells with potent immunosuppressive properties. Studies from the 1960s demonstrated the key role of the thymus as the site of generation of immunosuppressive T cells, as thymectomy performed on mice before day 3 of life lead to wasting disease due to autoimmunity [60]. Subsequent studies showed that the thymus is critical for establishing and maintaining immunologic self-tolerance [61-64]. In 1995, Sakaguchi and colleagues [65] identified a subset of $CD4^+$ T lymphocytes expressing high amounts of interleukin 2 receptor α-chain (CD25) on the cell surface that showed sufficient immunosuppression to prevent autoimmunity in thymectomized mice and in other autoimmunity models (reviewed in [66-68]). Whether these so called regulatory T cells (Tregs) represent a stable lineage rather than just an activated state of T cells has been highly controversial for decades [69]. The first Treg marker identified - CD25 - is not only highly expressed on Tregs but also upregulated by activated T cells [70]. It became apparent, that additionally to the fact that CD25 is not specific for Tregs, this surface marker is not necessarily upregulated on all Tregs: To a certain extent, there are $CD25^-$ Tregs with transcriptional signatures and suppressive function. These operate similarly to what is observed for $CD25^+$ Tregs that can be found in secondary lymphoid organs and other nonlymphoid tissue [70, 71]. Other Treg markers such as CTLA-4 or GITR (glucocorticoid-induced TNFR-related protein)

are as well not specific for Tregs only [70]. As a consequence, much effort was made to identify more reliable Treg markers. In 2003, Fontenot, Khattri and Hori described Foxp3 (Forkhead box P3), an X-chromosome-encoded member of the forkhead transcription factor family, to be Treg-lineage-determining [71-73]. Mice lacking functional Foxp3 show a specific phenotype. The so-called scurfy mice develop widespread early-onset autoimmunity that is fatal [74]. Accordingly, also acute ablation of Tregs *in vivo* causes severe autoimmunity [75]. Mutations in the Foxp3 gene in humans cause the IPEX-syndrome (immunodysregulation polyendocrinopathy, enteropathy X-linked syndrome) [76]. Affected patients suffer from a disease phenotype equivalent to what is observed among scurfy mice - including diabetes, thyroiditis, hemolytic anemia, hyper-IgE syndrome, exfoliative dermatitis, splenomegaly, lymphadenopathy and cytokine storm [76-78]. Experimental upregulation of Foxp3 expression in $CD4^+CD25^-$ T cells results in the acquisition of a Treg cell phenotype including immunosuppressive capacities, as well as the upregulation of other Treg markers like CD25, CLTA-4 and GITR [71-73]. Notably, at least in humans Foxp3 expression can be upregulated during conventional T cell activation [65, 79]. However, this just reflects a temporary state and is not to be compared to stable, high level Foxp3 expression as it occurs in Tregs [80].

Foxp3 expression is not only lineage-defining but also essential for Treg differentiation and functioning [81, 82]. On a molecular level, Foxp3 can be integrated into different multimolecular complexes defining its context-depending activity. To this day, it is not completely understood how exactly Foxp3 regulates its target genes. Presumably, it mostly acts as an activator for transcription. However, it may also act as a passive repressor of transcription depending on the exact nature of the complex being formed. This is at it tunes down enhancer activity or even acts as an active repressor when associated with major repressor complexes. Beyond that, other modes of action including effects that are independent of DNA-binding are likely to take place [83].

Nevertheless, Foxp3 is not an ideal Treg marker in terms of practicability. For instance, as a transcription factor, Foxp3 is localized intracellularly and therefore cell sorting on living cells is not possible [84]. Yet, it is still the most commonly used and most accurate marker for Treg lineage known to date [85].

Over the last decades, the biologic importance of Tregs in multiple biological contexts became evident (Figure 3). Dysfunctional islet-resident Tregs are thought to be a key factor in the pathogenesis of autoimmune diabetes onset in NOD mice [86]. Beyond this, dysfunctional Tregs are also part of the pathogenesis of other models of excessive immune responses such as rheumatoid arthritis [87], multiple sclerosis [88], inflammatory bowel disease [89-91],

allogeneic transplantation [92, 93], and allergy [94]. However, augmented Treg-mediated tolerance has been shown to potentially facilitate tumor growth [95]. Treg based modulation of the immune system is a promising step towards future personalized medicine [55]. Initial clinical phase I studies were promising: Therapeutic administration of polyclonal Tregs reduced the incidence of acute graft-versus-host disease (GVHD) in patients that received hematopoietic stem cell transplantation for the treatment of hematologic malignancies. Tregs were either freshly isolated [96] or expanded *ex vivo* [97]. Subsequent phase I and II studies tested clinical administration of Tregs in various settings including hematopoietic stem cell transplantation, solid organ transplantation and autoimmunity [98]. These studies confirmed therapeutic efficacy and safety of Treg administration [55]. However, adverse events such as infections [99] and tumors [100] have been reported occasionally and remain to be addressed by current studies. Multi-directional approaches yielding to implement Treg-based immunotherapy protocols investigate adoptive Treg cell therapies as well as biologics, microbial stimulation or small-molecule based approaches to boost Tregs *in vivo* [3, 92, 98]. Prior to clinical approval, major issues in Treg manufacturing regarding optimal cellular source, cell purity and numbers of cells required for therapeutic effect need to be solved [55]. Moreover, biological questions concerning the identification of disease-specific antigens, Treg activation status and phenotypical stability as well as homing, long-term survival, and impact on immunity against opportunistic pathogens remain to be addressed [92].

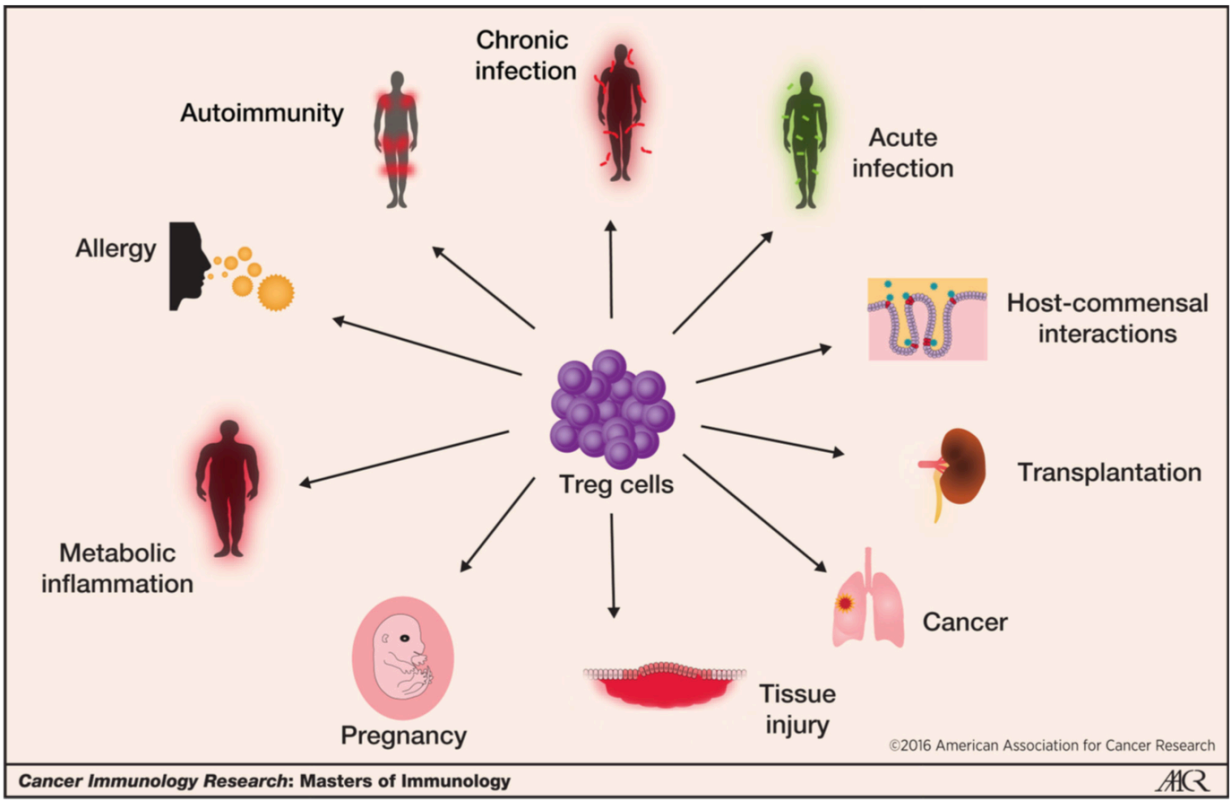

Figure 3: Treg cells modulate immune responses in many contexts

$CD4^+Foxp3^+$ Tregs play a major role in downregulating excessive immune responses in various biological contexts, including autoimmunity as well as cancer, infections, host-commensal interactions and inflammation at barrier sites, allergy, pregnancy, tissue repair, metabolic inflammation and allo-transplantation.

Figure and description adopted from [3].

1.4.2. Thymic vs. peripheral differentiation of $CD4^+Foxp3^+$ Tregs

The discovery of Foxp3 as a specific Treg marker initiated a wave of research in the field. As a consequence, a multitude of Treg cell subpopulations as well as new terminology and abbreviations were introduced that led to a consensus on Treg nomenclature in 2013 [101]: Hereafter, Tregs are classified as "thymus-derived Treg cells" (tTregs) or "peripherally-derived Treg cells" (pTregs) depending on their anatomical location of differentiation. If in any doubt, the general term "$Foxp3^+$ Treg cell" should be employed. By contrast, *in vitro* generated Tregs were suggested to generally be referred to as "*in vitro* induced Tregs".

Not only does this provide a standardized terminology between different research groups. In addition, it also informs about important Treg subgroups: The majority of Tregs develop from CD4 single positive T cells in the thymus (so-called thymus-derived tTregs). TCR signaling characteristics are central determinants of T cell lineage fate. tTreg differentiation requires high-avidity interactions with self-peptide/MHC class II complexes that range between low

signal strength mediating positive selection of conventional CD4$^+$ T cells and stronger signals which favor negative selection instead [4, 102] (Figure 4).

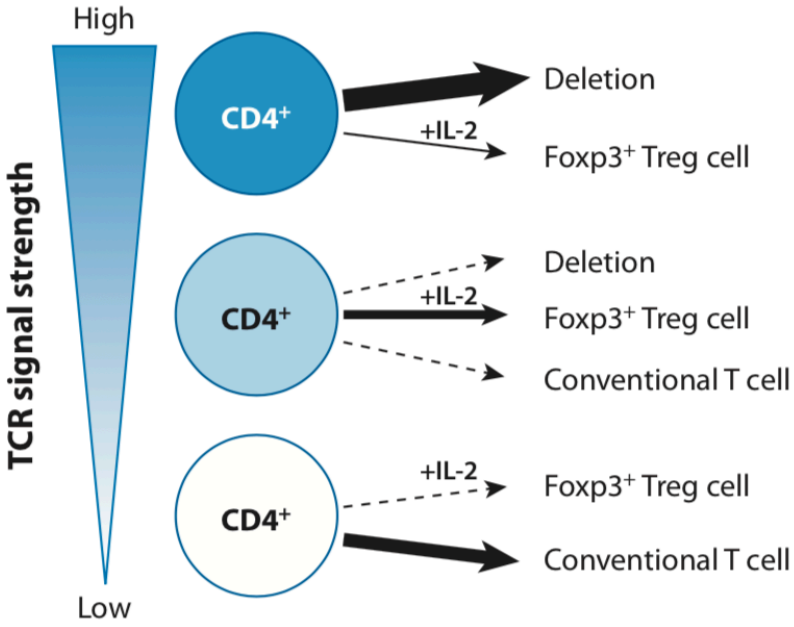

Figure 4: TCR signal strength determines CD4$^+$ T cell fate

Thymic differentiation of T cells is determined by TCR-mediated interactions with peptide-MHC-complexes presented by antigen-presenting cells. During this process high avidity interactions favor deletion of potentially hazardous autoreactive T cells. By contrast, low TCR signal strength allows for conventional T cell differentiation. Intermediate TCR signaling strength however enables Foxp3$^+$ Treg formation. Weight of arrows reflects relative probability of indicated outcomes.

Figure and description adopted from [4].

However, TCR-signaling alone is not sufficient to enable Foxp3 upregulation and Treg cell differentiation. Additional signals required for tTreg differentiation and maintenance include IL-2 and to a lesser extent IL-7 and IL-15 [4].

A smaller proportion of Foxp3$^+$ Tregs does not develop in the thymus but in the periphery (pTregs) from mature CD4$^+$Foxp3$^-$ T cells upon tolerogenic exposure to non-self antigens such as allergens, food and the commensal microbiota [3, 103, 104]. pTreg induction is higher when strong TCR signaling, suboptimal co-stimulation (e.g. increased CTLA-4 and decreased CD28 signaling) and high amounts of TGF-β and retinoic acid are present [4, 105]. The highest frequency of pTregs is found in the gut where non-self antigens are abundant and microbial stimulation through short-chain fatty acids is possible [106-108].

Remarkably, Foxp3 expression is regulated differently between tTregs and pTregs. Whereas pTreg differentiation is dependent on CNS1 (conserved noncoding sequence 1), an intronic Foxp3 cis-regulatory element with binding sites for Smad3 and retinoic acid receptor (RAR)

[109], CNS1 is dispensable for tTreg generation [110]. The observation that CNS1 and herewith pTregs formation occurs in placental mammals only, raises the question whether pTreg formation emerged during evolution to enforce materno-fetal tolerance [109]. Notably, mice with a selective defect for pTreg differentiation suffer from a late onset allergic and asthma-like inflammation in the gut and lung. However, these mice do not succumb to wasting disease which is seen in scurfy mice lacking the entire Treg compartment [111]. Thus, biological functions of tTregs and pTregs are thought to be distinct [109, 110]. Presumably, tTregs mediate peripheral tolerance against self-antigens, whereas pTregs restrain immune responses to harmless non-self antigens like allergens, commensal microbiota, dietary antigens and paternal alloantigens [3].

1.4.3. Discrimination between tTregs and pTregs

In 2010 Thornton and colleagues proposed Helios, an Ikaros transcription factor family member, as a marker for differentiation between tTregs and pTregs in mice [112]. The Ikaros transcription factor family is made up of five DNA-binding proteins that are expressed in a variety of tissues and thought to regulate gene transcription through chromatin remodeling. Helios, though, seems to be specifically expressed on T cells [113, 114]. Yet, its exact function is not fully clear. It is highly expressed on tTregs. Whereas pTregs lack Helios expression without any effect on Foxp3 expression [112]. As for Foxp3, Helios is not suitable for cell sorting on living cells due to its intracellular localization [103]. Another drawback is that independently from the subset being involved, Tregs can upregulate Helios expression upon activation and proliferation, thereby undermining its use to distinguish tTregs from pTregs [115-117].

Neuropilin-1 (Nrp-1) was suggested to be another marker for differentiation between tTregs and pTregs simultaneously by Yadav and Weiss in 2012 [104, 118]. However, its role in Treg biology is not yet fully clear [118]. It has been hypothesized that Nrp-1 expression on Tregs supports peripheral immunoregulatory activities under various conditions [119-121]. Yet, mice harboring Nrp-1 deficient T-cells do not show any pathology [122].

Neuropilin-1 expression is reduced on pTregs compared to tTregs analogous to Helios expression. In contrast to Helios, Neuropilin-1 is expressed on cell surfaces and thus can be used for separation of living cells. Yet, Nrp-1 and Helios expression patterns do not fully overlap [104]. Additionally, upregulation of Neuropilin-1 has been observed in pTregs as well, for example in an inflammatory environment or by positive regulation through TGF-β [118].

Another drawback is that Neuropilin-1, in contrast to Helios, is not expressed on human Tregs. Thus, its use as a specific tTregs marker is limited to murine models only [123].

1.4.4. Mechanisms of $CD4^+Foxp3^+$ Treg mediated immunosuppression

Numerous operating principles of Treg mediated suppression have been suggested [124]. Presumably, Tregs employ multiple mechanisms to fulfill their full suppressive repertoire [3, 125]: CD25, the first Treg marker being used, has been found to be required for $CD8^+$ T cell suppression mediated by extracellular Il-2 depletion [126, 127]. However, transcriptional profiling of $CD4^+Foxp3^+$ Tregs revealed considerably more candidate genes with immunosuppressive function: CD39 and CD73 represent highly expressed ectoenzymes on Tregs that deprive extracellular ATP availability by conversion to Adenosine which has direct inhibitory effects on conventional effector T cells, dendritic cells (DCs) and myeloid cells [3]. High CTLA-4 expression on Tregs can induce downregulation of CD80 and CD86 expression on DCs and herewith indirectly inhibits DCs due to insufficient co-stimulation [128]. Less DC activity subsequently leads to impaired priming of effector T cells. Independently, effector T cell trafficking to the target organ is hypothesized to be regulated by Tregs as well [103]. Importantly, Tregs also produce and secrete immunomodulatory proteins including IL-10, granzymes and TGF-β with well-known immunosuppressive effects [4, 129-131] (Figure 5).

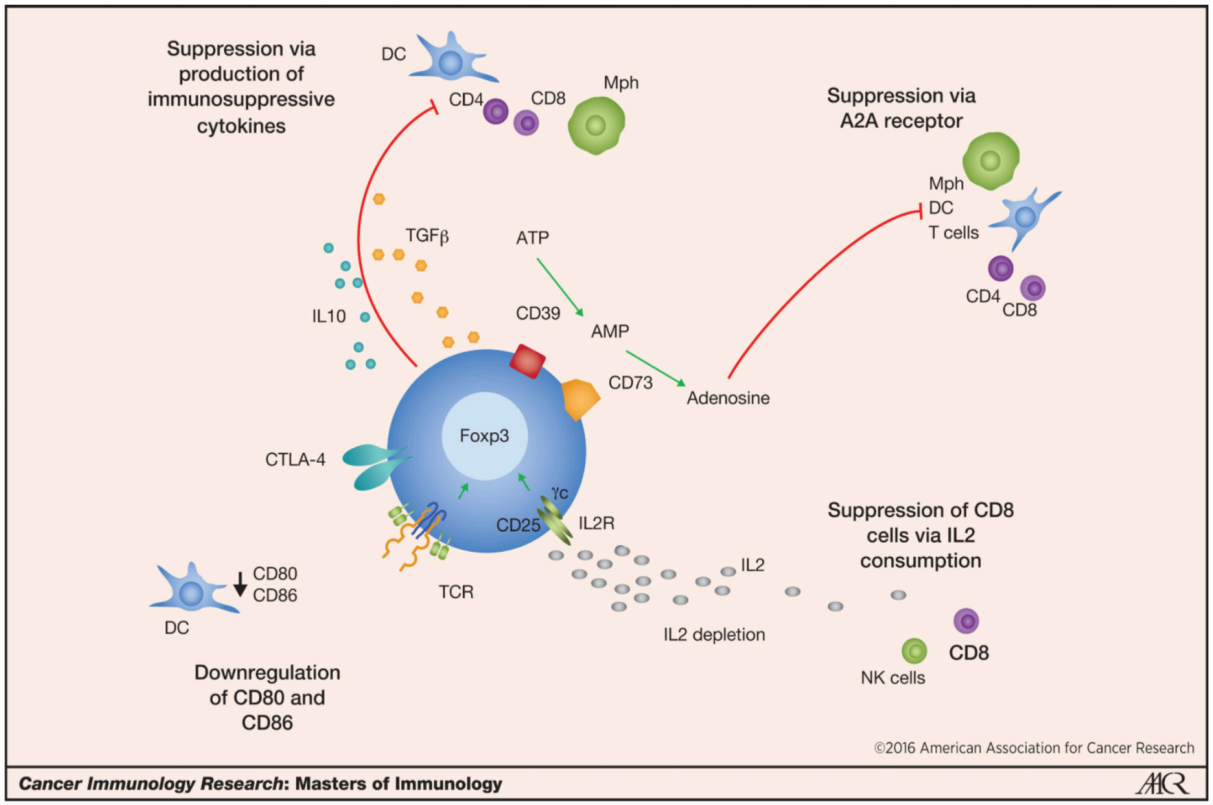

Figure 5: Mechanisms of Treg-mediated immunosuppression

Tregs dampen immune responses through various mechanisms including the production and secretion of immunosuppressive cytokines such as IL-10 and TGF-β, downregulation of CD80 and CD86 by expression of high levels of CTLA-4 as well as extracellular deprivation of ATP and IL-2.

Figure and description adopted from [3].

1.4.5. Peptide-induced CD4$^+$Foxp3$^+$ Tregs

CD4$^+$Foxp3$^+$ Tregs have been studied extensively *in vitro* and *in vivo*. In this context, various protocols have been established for experimental induction of CD4$^+$Foxp3$^+$ Tregs in rodents. Polyclonal Treg expansion for example is seen after transfer into lymphopenic hosts [132, 133]. Subimmunogenic administration of agonist antigen however converts naïve TCR tg CD4$^+$ T cells into antigen-specific CD4$^+$Foxp3$^+$ Tregs [134, 135]. In murine models antigen-specific CD4$^+$Foxp3$^+$ Tregs have been induced by various protocols including oral [136-138], subcutaneous [136], intravenous [138], intranasal [139] or intraperitoneal [137] antigen administration. Targeting of peptide-agonist ligands to dendritic cells may as well induce CD4$^+$Foxp3$^+$ Tregs [140]. Current approaches also apply DNA vaccinations to transiently express disease-specific antigens via DNA vectors [141].

Antigen-specific CD4$^+$Foxp3$^+$ Tregs have been shown to prevent autoimmunity in various experimental settings of autoimmunity in rodents [137, 142]. As mentioned above, peptide-

induced $CD4^+Foxp3^+$ Tregs are currently being tested in clinical trials for prevention and treatment of autoimmune diseases such as T1D, multiple sclerosis, arthritis and celiac disease in humans (reviewed in [38]). Although various clinical trials have shown no substantial safety issues, peptide-based therapies for autoimmunity in humans are still at the very beginning [38]. Incomplete knowledge of pathogenic mechanisms and a complex variety of antigens that trigger and maintain autoimmunity in humans, still hinder the translation of peptide-induced tolerance approaches in animals into effective treatment strategies in humans [38].

1.5. Type I diabetes mouse models

1.5.1. The non-obese diabetic strain (NOD)

The NOD mouse strain is commonly used to model autoimmunity in preclinical studies as it shares many similarities in disease pathology of type I diabetes with humans [143, 144]. Shared characteristics between humans and rodents include the presence of autoreactive $CD4^+$ and $CD8^+$ T cells as well as disease-specific autoantibodies with reactivity against insulin, GAD65 (glutamic acid decarboxylase), IGRP (islet-specific glucose-6-phosphatase catalytic subunit-related protein), IA-2 (insulinoma-associated protein 2), ZNT8 (zinc transporter in β-cells) or other pancreatic self-antigens [145, 146]. Spontaneous autoimmune diabetes in NOD mice occurs due to a summation of multiple defective tolerance mechanisms interfering with both central and peripheral tolerance [147]. The NOD strain harbors the unique major histocompatibility complex (MHC) haplotype $H\text{-}2^{g7}$ which is considered to be the main genetic contributor to disease susceptibility [148, 149]. However, over 20 additional non-MHC insulin-dependent diabetes loci were found to mediate disease risk [150]. Autoreactive T cells are thought to be the primary cause for insulitis and β-cell destruction. Yet, pathogenesis in NOD mice is multifactorial, including defective macrophage maturation and function [151], impaired NK cell function and the absence of C5a and hemolytic complement [145]. Moreover, self-reactive antibodies contribute to disease progression as well [152, 153]. When a critical mass of > 95 % of β-cells has been destroyed, endogenous insulin-production becomes insufficient and overt diabetes develops [154]. Diabetes incidence in NOD mice ranges from 60 - 80 % in females to 20 – 30 % in males [155, 156]. Disease onset is not only genetically predetermined but also dependent on environmental factors, such as housing conditions. Female mice usually succumb to diabetes at 12 to 14 weeks of age whereas male mice are affected slightly later. Prior to overt diabetes, severe insulitis occurs by 10 weeks of age for both sexes [145].

Translation of experiences from this animal model into clinical applications has not always been straightforward [143, 157]. Yet, the NOD mouse strain has fundamentally contributed to the current expertise about disease pathology and progression and still continues to be the basis for the development of new therapeutic approaches [143].

1.5.2. The NOD CNS1 KO mouse model

The Foxp3 enhancer conserved non-coding sequence 1 (CNS1) has been shown to be required for pTreg but not for tTreg differentiation (see above) [110]. CNS1 KO mice show exclusively impaired pTreg frequencies whereas the overall Treg level in general remains unchanged [110, 111]. CNS1 KO mice on the NOD background were generated previously by CRISPR-Cas9 genome editing [158]. Along with decreased pTreg levels, NOD CNS1 deficient mice show increased incidences of autoimmune diabetes in both female and male mice [158].

1.5.3. NOD BDC2.5 tg mice

BDC2.5 transgenic (tg) mice were originally generated by Katz and colleagues in 1993 [154]. This strain harbors rearranged TCR α- and β-genes from a diabetogenic T cell clone that was isolated from a NOD mouse. BDC2.5 is an islet-antigen specific, H-2g7 restricted and diabetogenic $CD4^+$ T cell clone. Transgenic T cells with BDC2.5 specifity undergo regular thymic development and in particular do not succumb to clonal deletion [154]. As a result, BDC2.5 transgenic TCR αβ T cells with islet cell-specific reactivity appear in the periphery of transgenic mice. BDC2.5 transgenic mice on a NOD genetic background show generalized and extensive islet pathology after a few weeks of age. However, overt diabetes does not occur for several months [159]. Such genetically and phenotypically well-described mice provide a suitable context for studying the development and control of autoimmunity in the context of type I diabetes [154, 160].

1.5.4. NOD CNS1 KO BDC2.5 tg mice

BDC2.5 TCR tg mice contain a large mass of naïve monoclonal T cells [154] allowing for an induction of a sufficient number of antigen-specific $Foxp3^+$ Tregs upon stimulation with the agonist antigen [134, 135]. To investigate the impact of CNS1 deficiency for *in vivo* induction of antigen specific $Foxp3^+$ Tregs, BDC2.5 tg mice were bred with NOD CNS1 KO mice.

1.5.5. NOD SCID mice

These mice carry the severe combined immunodeficiency (SCID) mutation on the *Prkdc* gene. As a result, SCID mice lack functional T and B cells due to defective DNA repair mechanisms and abrogated rearrangement of genes that code for T and B cell receptors [161]. Mutants on the NOD/ShiLtSz background are commonly used for diabetes and obesity research. In particular, transfer of splenocytes from prediabetic or diabetic NOD females induces diabetes in NOD SCID immunodeficient mice [162]. Comparison of diabetes incidence and progression after transfer of gene-WT and KO splenocytes allows to determine gene variants that increase disease susceptibility [13, 160].

1.6. Aim of the study

Numerous studies have demonstrated that immunosuppressive $CD4^+Foxp3^+$ Tregs can be induced *in vitro* as well as *in vivo*. *In vivo* Treg induction is already tested in clinical trials for the treatment of autoimmune diseases such as T1D [56]. It is also a useful tool for basic research to gain further insights into Treg subsets and their physiology.

We hypothesize that *in vivo* peptide-induced antigen specific $CD4^+Foxp3^+$ Tregs share characteristics with naturally occurring $CD4^+Foxp3^+$ pTregs.

The aims of the project are:

- to validate the dependency of *in vitro* induced $CD4^+Foxp3^+$ Tregs on CNS1
- to establish a murine model for *in vivo* peptide-induction of antigen-specific $CD4^+Foxp3^+$ Tregs
- to investigate CNS1 dependency of *in vivo* peptide-induced Tregs

2. Material and Methods

2.1. Chemicals and Reagents

Product	Provider	Cat. No.
2-,2-2-Tribromoethanol	Sigma	T48402-25G
2-Methyl-2-butanol	Sigma	240486-100ML
Agarose	Fisher Scientific	BP160-500
Ammoniumchloride	Fisher Scientific	A649-500
$CaCl_2$	Fisher Scientific	C70-500
DMSO	Fisher Scientific	ICN19481980
dNTP	Thermo Scientific	R0192
DPBS	Fisher Scientific	SH30028FS
DreamTaq Green Buffer	Fisher Scientific	B71
Fetal Bovine Serum	Atlanta Biologicals	S11150
GeneRuler Low Range DNA Ladder	Fisher Scientific	SM1193
Glycerol	Fisher Scientific	AC32725-5000
HEPES	Invitrogen	15630-080
KCl	Fisher Scientific	P217-500
$KHOC_3$	Fisher Scientific	P235-500
L-Glutamine	Invitrogen	25030081
Na_2EDTA	Bio Basic	6381-92-6
Penicillin/ Streptomycin	Invitrogen	15140122
Sodium Pyruvate	Invitrogen	11360070
TAE	Fisher Scientific	B49
Tris-HCl pH 8.0	Fisher Scientific	BP1758-100
Tris-HCl pH 9.0	Invitrogen	15567027
Triton X-100	Fisher Scientific	AC32737-2500
UltraPure Distilled Water	Invitrogen	10977-015
β-Mercaptoethanol	Invitrogen	21985023

Table 1: Chemicals and Reagents

2.2. Media and buffers

ACK buffer	155 mM NH_4Cl
	1 mM $KHOC_3$
	0.1 mM Na_2EDTA
	pH = 7.2 – 7.4
Avertin Stock Solution	3.54 mM 2-,2-2-Tribromoethanol dissolved
	in 2-Methyl-2-butanol
Ear lysis buffer	50 mM KCl
	10 mM Tris-HCl pH = 9.0
	0.1 % Triton X-100
MACS buffer	PBS supplemented with
	0.5 % FBS
	2 mM Na_2EDTA
Proteinase K Stock Solution	20 mg/mL Proteinase K
	50 mM Tris-HCl pH = 8.0
	3 mM $CaCl_2$
	50 % glycerol
RBC buffer	144 mM NH_4Cl
	17 mM TrisHCl
	pH = 7.2
RPMI CM	RPMI supplemented with:
	10 % FBS
	2 mM L-Glutamine
	50 U/µg/ml Penicillin/Streptomycin
	55 µM beta-Mercaptoethanol
	10 mM HEPES
	1 mmM Sodium Pyruvate

Table 2: Media and buffers

2.3. Mice

2.3.1. General

NOD/ShiLtJ, NOD BDC2.5 tg and NOD SCID were purchased from The Jackson Laboratory (Bar Harbor, ME).

NOD CNS1 KO mice were previously generated by Schuster and colleagues [158]. NOD CNS1 KO BDC2.5 tg mice were generated by mating male NOD BDC2.5 tg mice (The Jackson Laboratory, Bar Harbor, ME) with female NOD CNS1$^{-/-}$ KO mice. The first filial generation of NOD BDC2.5 tg CNS1 hemizygous males were used for induction of antigen-specific Foxp3^{+} Tregs. For confirmation of this genotype, all progenies underwent genotyping prior to any experiment.

All mice were housed and bred under specific pathogen-free conditions in the animal facility of Joslin Diabetes Center. If not otherwise indicated, experiments were performed on sex-matched adult mice at age of 4 to 12 weeks. For organ harvest mice were sacrificed by carbon dioxide asphyxiation followed by cervical dislocation.

All experiments were approved by the Institutional Animal Care and Use Committee at the Joslin Diabetes Center.

2.3.2. Genotyping

Genotyping was done at weaning age. Ear punches were taken and digested for 2 hours in 200 µl of a 1:100 dilution of Proteinase K in lysis buffer. After deactivation of residual Proteinase K activity via heat shock, PCR was performed to amplify DNA fragments. The amplification reaction contained the sample of template DNA, corresponding primers, dNTPs, reaction buffer as well as DreamTaq DNA Polymerase. Depending on the gene of interest, different PCR protocols were used. PCR conditions are listed in Table 3-Table 7.

		Sequence (5'→ 3')	Primer Type
BDC2.5	Primer 1	CAT GTT TCC CTG CAC ATC AG	Transgene
	Primer 2	CCA GAT CCA AAG ATG AGT TGC	Transgene
	Primer 3	CAA ATG TTG CTT GTC TGG TG	Internal Positive Control Forward
	Primer 4	GTC AGT CGA GTG CAC AGT TT	Internal Positive Control Reverse
CNS1 KO	Primer 5	GGA AGC CAA CAT GGG GTG AA	CNS1 KO
	Primer 6	GGC GCT TAT GTG GCT TCT TTC	Internal Positive Control Forward
	Primer 7	GAG GTA GCT TCT CAT TTT CAA GTG G	Internal Positive Control Reverse

Table 3: List of primers for genotyping

Primers were purchased from Eurofins Scientific and dissolved in water yielding a stock concentration of 10 µM.

Component	Volume	Final Concentration
Template DNA	2 µl	~100 ng
DreamTaq Green Buffer 10X	2.5 µl	1X
dNTP	0.4 µl	0.16 mM
Primer 1	0.25 µl	100 µM
Primer 2	0.25 µl	100 µM
Primer 3	0.25 µl	100 µM
Primer 4	0.25 µl	100 µM
DreamTaq DNA Polymerase	0.25 µl	0.05 U/µl

Table 4: Preparation scheme for BDC2.5 PCR

Step	Temperature (°C)	Time	Number of cycles
Initial denaturation	95	3 min	1
Denaturation	95	30 s	35
Annealing	55	1 min	
Extension	72	1 min	
Final Extension	72	2 min	1

Table 5: PCR protocol for BDC2.5 amplification

Component	Volume	Final Concentration
Template DNA	4 ul	~200 ng
DreamTaq Green Buffer 10X	2.5 µl	1X
dNTP	0.4 µl	0.16 mM
Primer 5	0.5 µl	0.2 µM
Primer 6	0.5 µl	0.2 µM
Primer 7	0.5 µl	0.2 µM
DreamTaq DNA Polymerase	0.25 µl	0.05 U/µl
ddH_2O	adjust to 25 µl	

Table 6: Preparation scheme for CNS1 KO PCR

Step	Temperature (°C)	Time	Number of cycles
Initial denaturation	95	3 min	1
Denaturation	95	30 s	35
Annealing	51.2	30 s	
Extension	72	1 min	
Final Extension	72	5 min	1

Table 7: PCR protocol for CNS1 KO amplification

PCR products were separated via agarose gel electrophoresis. 1.5 % agarose (mass/volume) was melted in pre-heated 1x TAE buffer for BDC2.5 PCR fragment analysis. For CNS1 PCR analysis, 2.5 % agarose gels were used. GreenGlo safe DNA dye (Cat. No. CA3600, Denville) was added for visualization of DNA fragments. To the wells next to 10 µl PCR product samples,

6 µl low range DNA ruler was loaded. The electrophoresis was carried out for 25 min at 120 V. Subsequently, DNA fragments were visualized using a FluorChem8000 imager (ProteinSimple) and AlphaEaseFC (Genetic Technologies) software.

BDC2.5 PCR leads to an expected WT band at 200 bp and, if applicable, a transgenic band at 100 bp (Figure 6). In contrast, CNS1 PCR leads to a 72 bp control band next to an additional band at 447 bp in WT mice (Figure 7).

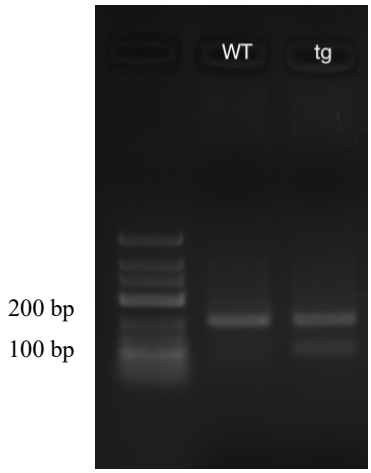

Figure 6: Gel electrophoresis for BDC2.5 genotyping

BDC2.5 PCR leads to an expected WT band at 200 bp and, if applicable, a transgenic band at 100 bp.

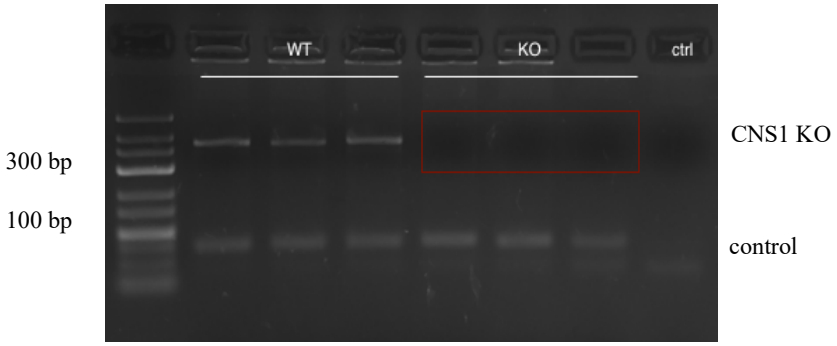

Figure 7: Gel electrophoresis for CNS1 genotyping

CNS1 PCR leads to a 72 bp control band next to an additional band at 447 bp in WT mice

2.3.3. Detection of glycosuria

Mice being followed up for diabetes onset were monitored by weekly measurements of glycosuria using Diastix (Fisher Scientific, Cat. No. AM-2803). Mice with two consecutive glucose values > 250 mg/dL were considered diabetic.

2.4. *In vitro* Treg induction

CNS1 WT and CNS1 KO NOD spleens were harvested in cold PBS. Single cell suspensions were prepared as described in 2.5.1.1. Naïve $CD4^+$ T cells were purified by MACS using the Miltenyi Biotec $CD4^+CD62L^+$ T cell isolation Kit (mouse) kit (Cat. No. 130-093-227). Hereto, non-$CD4^+$ T cells were magnetically labelled with a Biotin-Antibody Cocktail (100 µl per 10^8 cells for 10 min at 4 °C) and subsequently incubated with Anti-Biotin MicroBeads (200 µl per 10^8 cells for 15 min at 4 °C). Labelled non-$CD4^+$ T cells were depleted by manual magnetic separation with LS columns (Miltenyi Biotec, Cat. No. 130-042-401). Columns were washed three times. Subsequently, naïve $CD4^+$ T cell were labelled with CD62L MicroBeads (15 min at 4 °C) and positively selected with MS columns (Miltenyi Biotec, Cat. No. 130-042-201). Columns were washed three times. All intermediate washing steps were performed with MACS buffer followed by centrifugation (300 g, 10 min, 4 °C).

In vitro stimulation was performed with 5 x 10^4 naïve $CD4^+$ cells and 5 µg/ml anti-CD28 antibody, 100 U/mL IL-2, in anti-CD3 coated (coated with 5 µg/ml for 2 h at 37 °C) 96 well, flat-bottom plates for 96 hours at 37 °C and 4 % CO_2 in RPMI CM. Various concentrations of additional TGF-β were tested.

In a second set of experiments, naïve $CD4^+$ T cells (isolated as described in 2.5.1.2.) were co-cultured with NOD WT irradiated non-proliferative splenocytes (100 kV, 4 mA, 10 min (=4710 Rad)). 3.5 x 10^5 naïve $CD4^+$ T cells were co-cultured with 5 times more splenocytes in 24 well plates for 3 days. Stimulation was performed with 2 µg/mL anti-CD3, 200 U/mL IL-2. When indicated, 2 ng/mL of additional TGF-β was added.

Media changes were performed whenever necessary (indicated by color change of the media). Treg frequency was measured by flow cytometry. Cell culture reagents are listed in Table 8.

Reagent	Clone	Provider	Cat. No.
anti-mouse CD3ε	145-2C11	Biolegend	100331
anti-mouse CD28	3751	Biolegend	102102
Il-2		Peprotech	12-212
TGF- β		Peprotech	100-21

Table 8: Cell culture reagents

2.5. *In vivo* Treg induction

2.5.1. Preparation of donor cells

2.5.1.1. Donor organ harvest and preparation of single-cell suspension

Donor animals were sacrificed as described in 2.3.1. Spleens were harvested and kept in ice cold PBS. Within groups, organs were pooled. All further steps were performed under sterile conditions. Single cell suspensions were obtained by mechanical disruption using frosted microscope slides (Fisher Scientific, Cat. No. 12-550-343). Erythrocytes were lysed by 500 µl ACK buffer for 1 min at RT. All washing steps were performed with cold PBS followed by centrifugation (400 g, 5 min, 4 °C). Conglomerates and remains of connective tissue were removed by filtration through a 70 µm nylon mesh (Fisher Scientific, Cat. No. 22363549). Cells were resuspended in ice cold PBS.

2.5.1.2. $CD4^+$ T cell isolation

$CD4^+$ T cells were positively selected with CD4 MicroBeads (Miltenyi Biotec, Cat. No. 130-049-201). Cells were magnetically labelled with 10 µl MicroBeads per 10^7 cells for 15 min at 4 °C. All washing steps were performed with sterile filtered (Millipore, Cat. No. SCGPT02RE) MACS buffer followed by centrifugation (300 g, 10 min, 4 °C). Cells were resuspended in adequate amounts of MACS buffer and manually separated using MACS LS columns (Miltenyi Biotec, Cat. No. 130-042-401). Magnetically labelled $CD4^+$ T cells were removed from the columns by firmly pushing the plunger into the column. Prior to transfer, cells were washed and resuspended in PBS.

2.5.1.3. $CD25^+$ Treg depletion

Initially, a purpose-adapted, shortened MACS-protocol from the $CD4^+CD25^+$ Regulatory T Cell Isolation Kit from Miltenyi Biotec (Cat. No. 130-091-041) was used for the depletion of $CD25^+$ Tregs: $CD25^+$ cells were labelled with 10 µl CD25-PE per 10^7 cells for 10 min at 4 °C. All washing steps were performed with sterile filtered (Millipore, Cat. No. SCGPT02RE) MACS buffer followed by centrifugation (300 g, 10 min, 4 °C). After incubation with 20 µl Anti-PE MicroBeads for another 10 min at 4 °C, the cell suspensions were applied onto LS columns (Miltenyi Biotec, Cat. No. 130-042-401) for manual magnetic separation. Columns were washed three time with MACS buffer. The flow-through, representing unlabeled, $CD25^-$ cells was collected and used for further steps.

In subsequent experiments, the full $CD4^+CD25^+$ Regulatory T Cell Isolation Kit (Miltenyi Biotec, Cat. No. 130-091-041) protocol was performed: Prior to labelling of $CD25^+$ cells, the mouse splenocytes were preselected for non-$CD4^+$ T cells. Cells were resuspended in MACS buffer and subsequently incubated with 10 µl of the $CD4^+CD25^+$ Regulatory T Cell Biotin-Antibody Cocktail per 10^7 cells (10 min, 4°C) followed by incubation with Anti-Biotin Microbeads (15 min, 4 °C). Herewith, non-$CD4^+$ T cells were indirectly magnetically labelled. Subsequently, manual magnetic separation was performed with LD columns (Miltenyi Biotec, Cat. No. 130-042-901). Columns were washed three time with MACS buffer. The flow-through, containing unlabeled $CD4^+$ T cells, was collected for further steps. In contrast, labelled non-$CD4^+$ T cells were collected by adding 1 ml of MACS buffer onto the column, followed by firmly pushing the plunger into the column. Unlabeled $CD4^+$ T cells then were labeled with CD25-PE (10 µl per 10^7 cells, 15 min, 4 °C). 10 µl of Anti-PE MicroBeads was added. After incubation (15 min at 4 °C), the cell suspensions were applied onto MS columns (Miltenyi Biotec, Cat. No. 130-042-201) for manual magnetic separation. Columns were washed three time with MACS buffer. The flow-through, representing unlabeled $CD4^+CD25^-$ T cells, was pooled with the non-$CD4^+$ T cells which were obtained as described above. Cells were washed and resuspended in PBS.

2.5.1.4. Fluorescent labelling of transferred cells

Long term tracking of transferred cells into NOD WT mice was accomplished by labelling cells with fixable Cell Proliferation Dye eFluor™ 670 (eBioscience™ Thermo Fisher Scientific Cat. No. 65-0840). After reconstitution with anhydrous DMSO, the dye was diluted in PBS. As indicated in the manufacturer's protocol, labeling was performed with a final dilution of 5 µM dye for 10 min at 37 °C. To stop labeling, cells were incubated and washed once with RPMI CM (400 g, 5 min, 4 °C). Two final washing steps were performed with ice cold PBS.

2.5.2. Intravenous cell transfer

Prior to any adoptive transfer, aliquots were taken and put aside for future flow cytometry analysis. The remaining cells were adjusted for cell numbers and resuspended in 200 µl PBS per mouse and injection.

Cells (depending on the experiment either $CD4^+CD25^+$ depleted splenocytes or $CD4^+$ T cells) were applied intravenously in the tail vein. Hereto, recipient mice were exposed to an infrared

lamp for 30 seconds to improve peripheral blood circulation. For injection, mice were restrained in a specifically designed plexiglass tube. With a wide diameter syringe (27 Gauge), five to ten million cells were injected per mouse.

2.5.3. Peptide administration

For *in vivo* Treg induction, mice were exposed to subimmunogenic administered BDC2.5 mimetope (Anaspec) via single shot i.v. injection or by using subcutaneous osmotic minipumps over a time course of 14 days, respectively (Table 9). Unless otherwise noted, i.v. injections were performed in tail veins. A total dose of 5 µg mimetope was dissolved in 200 µl sterile PBS per mouse. Intravenous injections were performed as described above.

In contrast, osmotic minipumps were implanted subcutaneously. Depending on the model (Alzet, model 1002 Cat. No. 0004317/ model 2002 Cat. No. 0000296), osmotic minipumps held a total volume of 100 µl or 200 µl. Either way, 5 µg peptide was administered daily for 14 days (70 µg total dose). Pre-surgery, mice were given a dose of buprenorphine (0.05 – 0.1 mg/kg) followed by anesthesia with weight-adjusted amounts of 2-2-2-Tribromoethanol (for adult mice starting from 5 µg 2-2-2-Tribromoethanol). Prior to incision, the site of implantation was shaved and disinfected with 70 % Ethanol (Joslin Diabetes Center, Cat. No. INV70EAGL). Implantations in the back were performed in the mid-scapular region: The subcutaneous tissue was spread to create a suitable pocket for the pump. Following insertion of the pump, wounds were closed using a surgical stapler. Post-surgery mice were placed on a heat pad (~37 °C) to prevent hypothermia. Additionally, mice were observed every 12 h during the first 48 h after surgery and were given repeated doses of buprenorphine as needed if visual inspection indicated signs of distress and discomfort were observed. In all experiments described in this thesis, implanted pumps stayed in place for 14 days. Rather than pump explantation, mice were sacrificed, and organs of interest were harvested after 14 days.

Peptide Name	Sequence (N-Term → C-Term)	Provider	Cat. No.
BDC2.5 Mimetope	H – RTR PLW VRM E – OH	ANASPEC	AS-63774

Table 9: BDC2.5 mimetope specifications

The mimetope was dissolved in sterile PBS yielding a stock concentration of 0.5 µg/µl.

2.5.4. *In vivo* TGF-β-blockade

Following intravenous peptide administration on day 1 after cell transfer, 300 µg anti-TGF-β (InVivoMAb anti-mouse/human/rat/hamster/canine/bovine TGF-β, BioXCell, clone: 1D11.16.8, Cat. No. BE0057) were injected intraperitoneally. On day 4 after cell transfer, another 300 µg of anti-TGF-β were injected intraperitoneally yielding a final dose of 600 µg anti-TGF-β per mouse.

2.5.5. Detection of *in vivo* induced $CD4^+Foxp3^+$ Tregs

2.5.5.1. Preparation of blood samples

Blood samples were taken from living mice in ongoing experiments, as well as after sacrifice once the experimental endpoint was reached: Living mice were bled by incision of the tail vein using a scalpel blade. Two to three drops of blood were collected in 500 µl ice-cold PBS supplemented with 2 mM EDTA to prevent clotting. Prior to blood withdrawal, mice were exposed to an infrared lamp for 30 seconds to improve peripheral blood circulation. For blood collection, mice were restrained in a specifically designed plexiglass tube. As opposed to this, mice that were sacrificed prior to blood withdrawal were bled from the inferior vena cava after surgical opening of the abdomen. Akin to blood samples from living donors, two to three drops of blood were collected in 500 µl ice-cold PBS supplemented with 2 mM EDTA to prevent clotting. To remove erythrocytes, samples were incubated with 4.5 ml RBC lysis buffer at 37 °C until the fluid got clear, followed by a washing step with PBS and centrifugation (400 g, 5 min, 4 °C).

2.5.5.2. Preparation of solid organ samples

Mice were sacrificed once the experimental endpoint was reached. Spleens, PNL and MLN were harvested in ice cold PBS. Single cell suspensions were obtained as described above.
In some experiments, single cell suspensions were analyzed with flow cytometry directly. In contrast, in other experiments samples were enriched for $CD4^+$ T cells prior to FACS analysis. Isolation of $CD4^+$ T cells was performed with MACS using the $CD4^+$ T Cell Isolation Kit from Miltenyi Biotec (Cat. No. 130-104-454).

2.6. FACS analysis of induced Tregs

Analysis of Treg induction *in vitro* and *in vivo* was performed by flow cytometry (LSR II/ Fortessa, BD Biosciences) followed by interpretation using FlowJo™ 10 (Tree Star).

Cell suspensions from *in vitro* and *in vivo* Treg induction experiments, respectively, were washed with PBS once and incubated for 10 min at 4 °C with anti-CD16/CD32 (Biolegend, Cat. No. 101302, Clone 93, diluted 1:200) to block unspecific binding of antibodies to Fc-receptors. Following a washing step with PBS and subsequent centrifugation (400 g, 5 min, 4 °C), dead cells were labelled with Zombie Fixable Viability dye (Zombie green diluted 1:800, Biolegend, Cat. No. 423111/ Zombie NIR diluted 1:200, Biolegend, Cat. No. 423105) for 10 min 4 °C. Surface marker staining was performed right afterwards without washing for 15 min at 4 °C (dilution 1:400). Cells were washed with PBS and subsequently fixed using the Transcription Factor Staining Buffer Set from Thermo Fisher Scientific (Cat. No. 00-5523-00). Fixation was achieved by incubation in fixation buffer for 1 h at 4 °C. Intracellular staining for Foxp3 and Helios was performed for 30 min at RT (diluted 1:200 in permeabilization buffer). Another washing step with permeabilization buffer was performed followed by resuspension in adequate amounts of PBS. Fixation and permeabilization buffer both are included in the Transcription Factor Staining Buffer Set from Thermo Fisher Scientific (Cat. No. 00-5523-00). All staining steps were performed in the dark to protect conjugated fluorochromes from bleaching. All antibodies used for this project can be found in Table 10.

Antibody	Clone	Providor	Cat. No.
CD25- PerCP/Cy5.5	3C7	Biolegend	101911
CD4- Brilliant Violet 605	GK1.5	Biolegend	100451
CD4- Brilliant Violet 785	RM4-5	Biolegend	100552
CD8a- APC	53-6.7	Biolegend	100712
CD8a- APC/Cy7	53-6.7	Biolegend	100714
CD8a- Brilliant Violet 711	53-6.7	Biolegend	100759
Foxp3- eFluor450	FJK-16s	eBioscience	48-5773-82
Foxp3- PE	FJK-16s	eBioscience	12-5773-82
Helios- Alexa Fluor 488	22F6	Biolegend	137213
Helios- Pacific Blue	22F6	Biolegend	137220
Nrp-1- PE-Cyanine7	3DS304M	eBioscience	25-3041-82

Table 10: List of FACS antibodies

2.7. Gating strategies

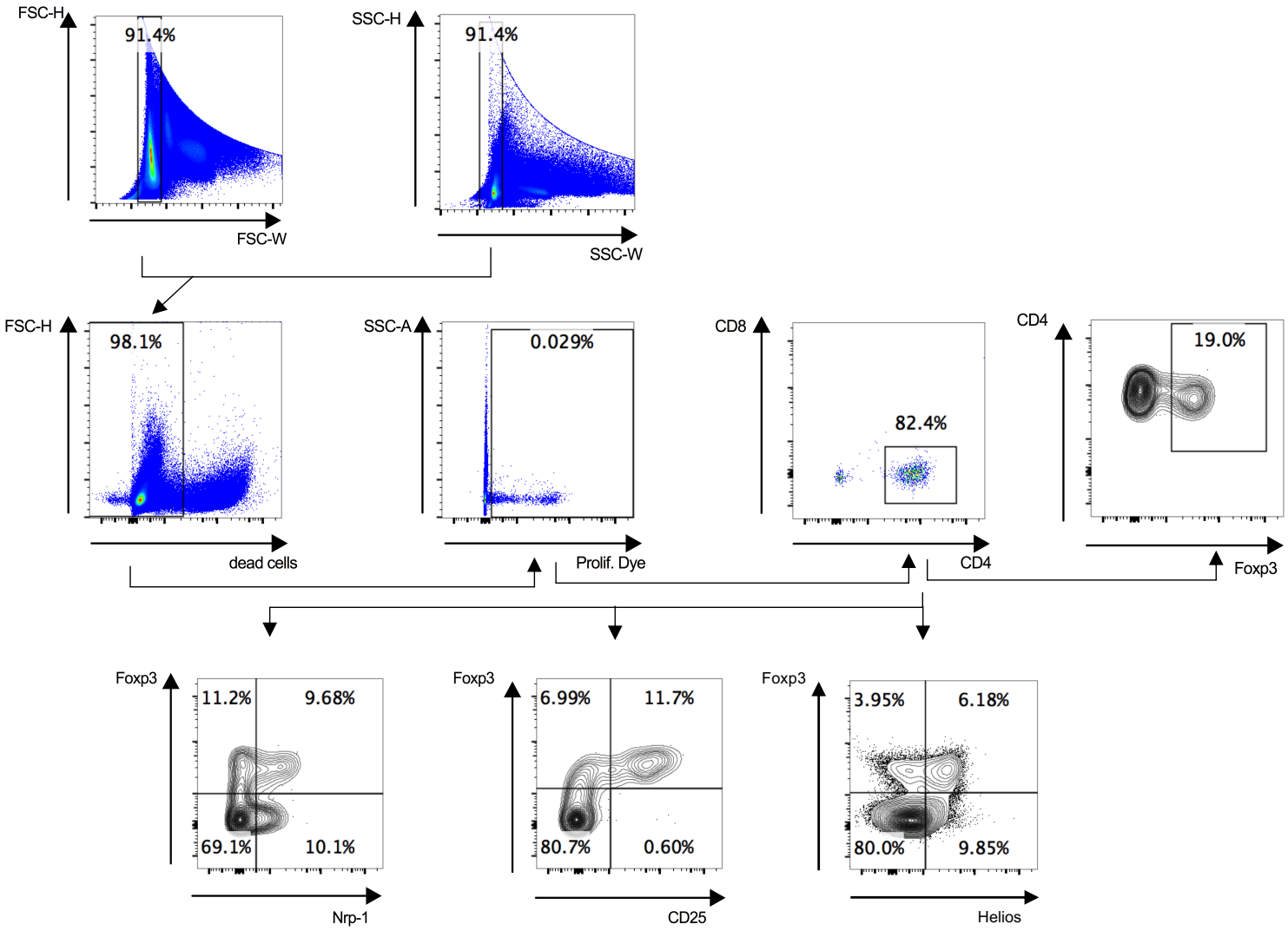

Figure 8: Gating strategy: Transfer of labelled CD4$^+$ T cells into NOD recipients

Isolated cells were gated on a forward and side scatter for doublet-exclusion. Dead cells were excluded as only cells with low fluorescence in the dead cell stain were included. Whenever donor cells were labelled with Proliferation Dye prior to transfer in recipient mice, cells were gated on positivity for this Proliferation Dye. CD8$^-$ CD4$^+$ lymphocytes were analyzed for Foxp3, CD25, Nrp-1 and Helios expression.

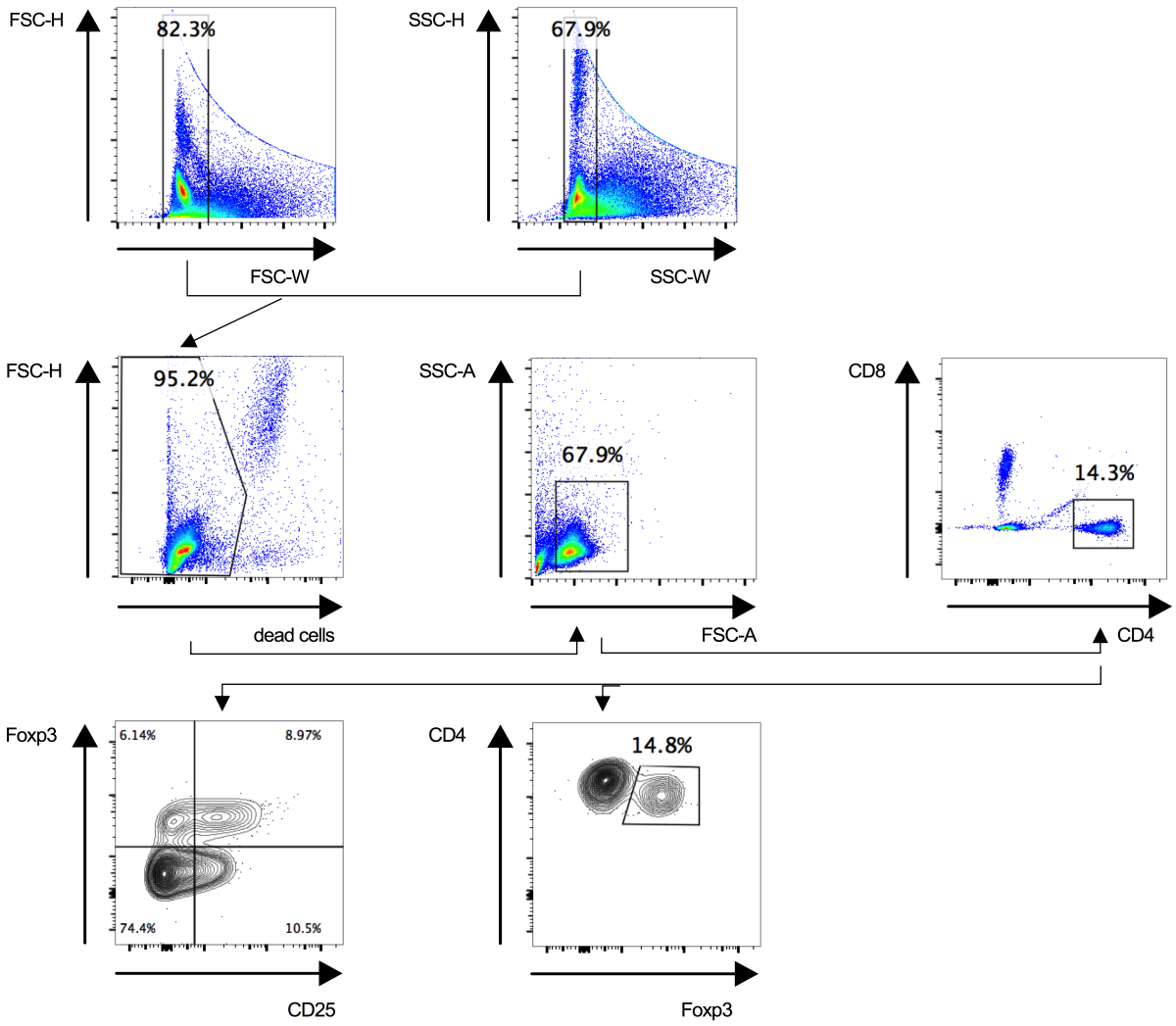

Figure 9: Gating strategy: Transfer of CD4$^+$ T cells into SCID recipients

Isolated cells were gated on forward and side scatter for doublet-exclusion. Dead cells were excluded as only cells with low fluorescence in the dead cell stain were included. Lymphocytes were identified on the basis of size and granularity. CD8$^-$CD4$^+$ cells were analyzed for Foxp3, and CD25 expression.

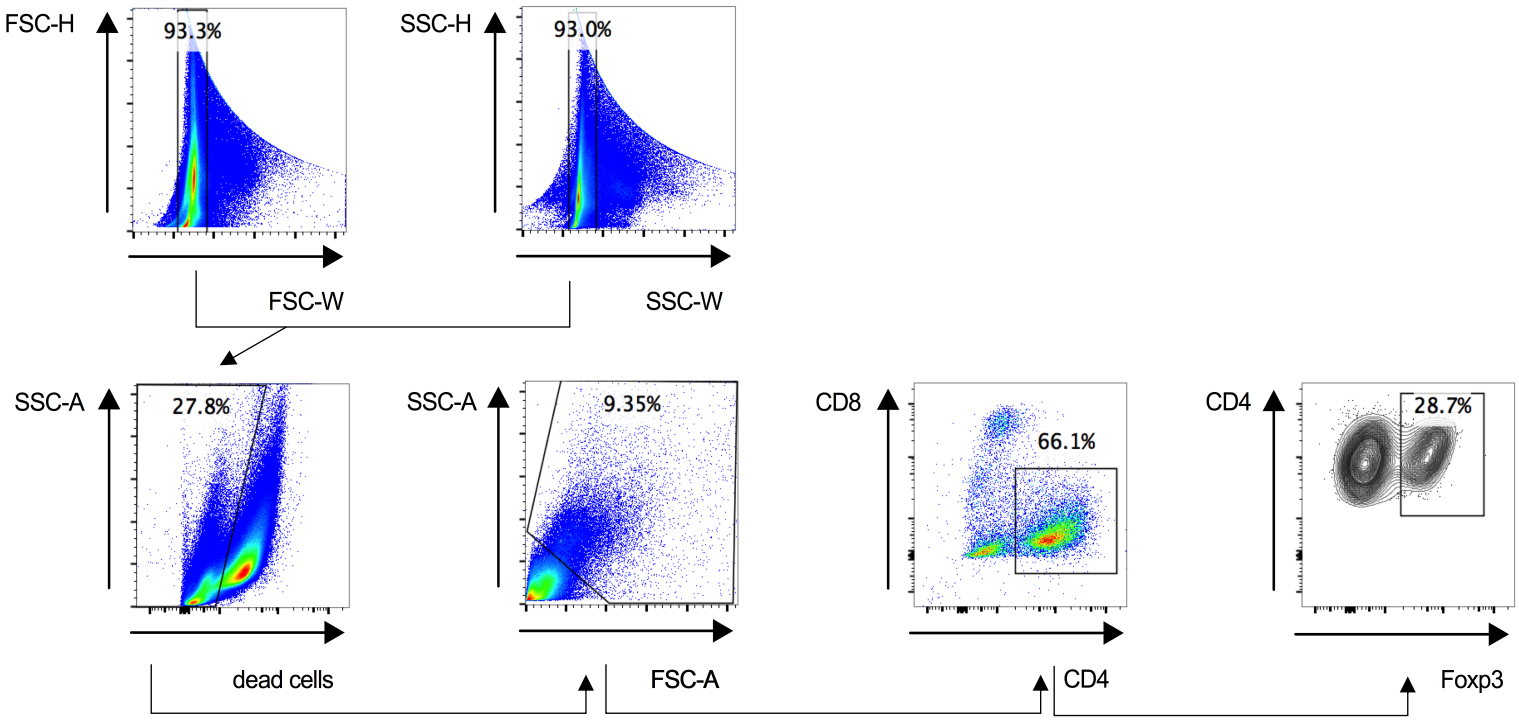

Figure 10: Gating strategy: *In vitro* Foxp3 induction

Isolated cells were gated on forward and side scatter for doublet-exclusion. Dead cells were excluded as only cells with low fluorescence in the dead cell stain were included. Lymphocytes were identified on the basis of size and granularity. $CD8^{-}CD4^{+}$ cells then were analyzed for Foxp3 expression.

2.8. Statistics

Statistical analyses were performed using GraphPad Prism (Version 6 and 7, GraphPad Software Inc.). For comparison of two experimental groups at a single time point, unpaired two-samples t-tests were performed. Paired t-tests were used for observational studies to compare experimental groups over time. Two-way ANOVA correction for multiple comparisons using Holm-Sidak method was used to analyze *in vitro* assays for Foxp3 induction. Log-rank tests and Gehan-Breslow-Wilcoxon tests were utilized for comparison of survival distributions.

If not indicated otherwise, figures show mean values and SEM (standard error of the mean). Significance levels are given as $p < 0.05$ (*), $p < 0.01$ (**), $p < 0.001$ (***).

3. Results

3.1. Dependency of *in vitro* induced CD4$^+$Foxp3$^+$ Tregs on CNS1 and TGF-β

Previous work [110, 111] demonstrated an impaired capability of CNS1 deficient naïve T cells for Foxp3 induction *in vitro*. For this work, naïve CD4$^+$ T cells were isolated from NOD WT or CNS1 KO mice and stimulated with anti-CD3, IL-2 and TGF-β. *In vitro* assays either were performed in the absence (Figure 11 A) or presence (Figure 11 B) of co-stimulatory, non-proliferative splenocytes.

In the absence of APC, *in vitro* induction of CD4$^+$Foxp3$^+$ T cells was observed for both CNS1 WT and CNS1 KO donor cells. Induction efficacy was clearly dependent on the amount of additionally added TGF-β (Figure 11A). When no additional TGF-β was applied, 21.30 % of CD4$^+$ CNS1 WT cells in culture were positive for Foxp3. Stepwise addition of TGF-β yielded up to 83.32 % Foxp3$^+$ of CD4$^+$ CNS1 WT cells (0.50 ng/ml TGF-β). Similar results were seen for CNS1 KO cells (no additional TGF-β: 16.05 % Foxp3$^+$ of CD4$^+$ CNS1 KO cells vs. 0.50 ng/ml TGF-β: 70.35 % Foxp3$^+$ of CD4$^+$ CNS1 KO cells). Notably, levels of CD4$^+$Foxp3$^+$ T cells in CNS1 deficient donor cells constantly remained below levels of CD4$^+$Foxp3$^+$ T cells in CNS1 WT when stimulated with TGF-β ($p = 0.0020$).

Similar results were obtained when an *in vitro* culture was performed in the presence of co-stimulatory APCs (Figure 11B). When no additional TGF-β was applied, 11.02 % ± 1.19 % SEM of CD4$^+$ CNS1 WT cells in culture were positive for Foxp3. The addition of 2 ng/ml TGF-β yielded up to 29.12 % ± 0.45 % SEM Foxp3$^+$ of CD4$^+$ CNS1 WT. Similar results were seen for CNS1 KO cells (no additional TGF-β: 9.86 **%** ± 1.07 % SEM Foxp3$^+$ of CD4$^+$ CNS1 KO cells vs. 2 ng/ml TGF-β: 19.35 % ± 0.55 % SEM Foxp3$^+$ of CD4$^+$ CNS1 KO cells). In accordance with what was seen in the absence of co-stimulatory APCs, levels of CD4$^+$Foxp3$^+$ T cells in CNS1 deficient donor cells remained below levels of CD4$^+$Foxp3$^+$ T cells in CNS1 WT when stimulated with an equivalent amount of TGF-β ($p = 0.0052$).

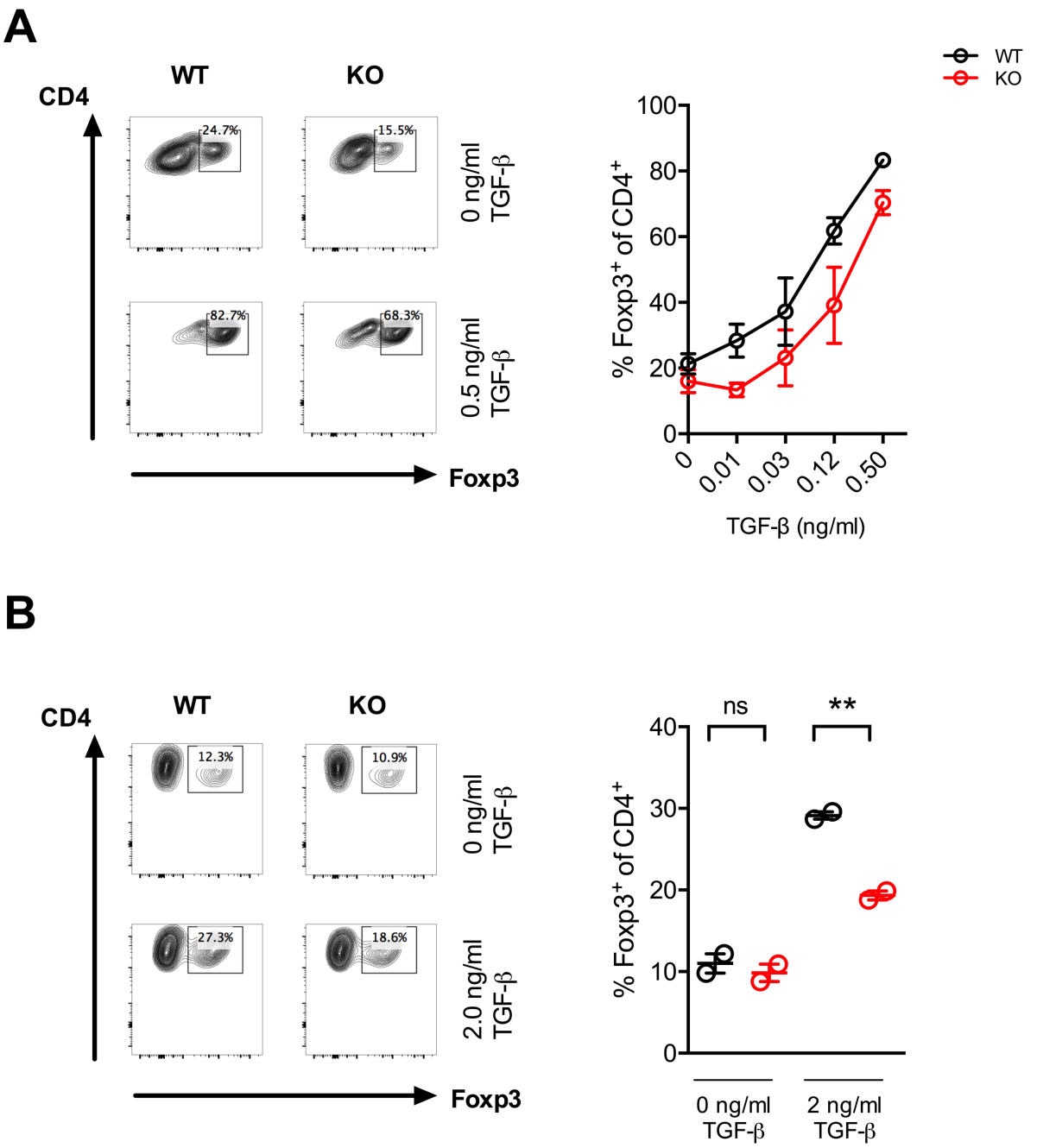

Figure 11: Dependency of *in vitro* Foxp3 induction on CNS1 and TGF-β

A) Naïve $CD4^+$ T cells were isolated from NOD CNS1 WT or NOD CNS1 KO mice and stimulated *in vitro* with anti-CD3, IL-2 and TGF-β. $CD4^+Foxp3^+$ Tregs were measured by flow cytometry after four days. Representative plots (left panels) and cell frequencies for percentage of $Foxp3^+$ cells among $CD4^+$ T cells (mean ± SEM, right panel) are shown. n = 2 mice/group, the value for each mouse was averaged from 3 technical replicates. The full gating strategy is reported in Material and Methods.
B) Naïve $CD4^+$ T cells from NOD CNS1 WT or NOD CNS1 KO mice were stimulated *in vitro* in the presence of irradiated splenocytes, anti-CD3, IL-2 and TGF-β. $CD4^+Foxp3^+$ Treg frequency was measured by flow cytometry after 3 days. Representative plots (left panels) and cell frequencies (mean ± SEM, right panel) for percentage of $Foxp3^+$ cells among $CD4^+$ T cells are shown. n = 2 mice/group, the value for each mouse was averaged from 3 technical replicates. All results are representative for three similar experiments. * ($p < 0.05$), ** ($p < 0.01$)

3.2. *In vivo* induction of antigen-specific CD4$^+$Foxp3$^+$ Tregs

3.2.1. *In vivo* induction of Foxp3 expression by single intravenous application of agonist BDC2.5 peptide

Induction of Foxp3 was performed in NOD BDC2.5 tg mice. Hereto, mice were exposed to 5 µg BDC2.5 mimetope in PBS by a single intravenous injection. Control mice were injected with an equivalent volume of PBS (Figure 12). In this setting, mice were followed up for Foxp3 expression in CD4$^+$ T cells, as well as for Nrp-1 and Helios as Treg markers. Blood was taken in four-day intervals. On day 12 after injection, all mice were sacrificed and analyzed for changes in the Treg compartment in blood and lymphatic organs like spleen, mesenteric (MLN) and pancreatic lymph nodes (PLN). Flowcytometry was used for analysis (Figure 13 A).

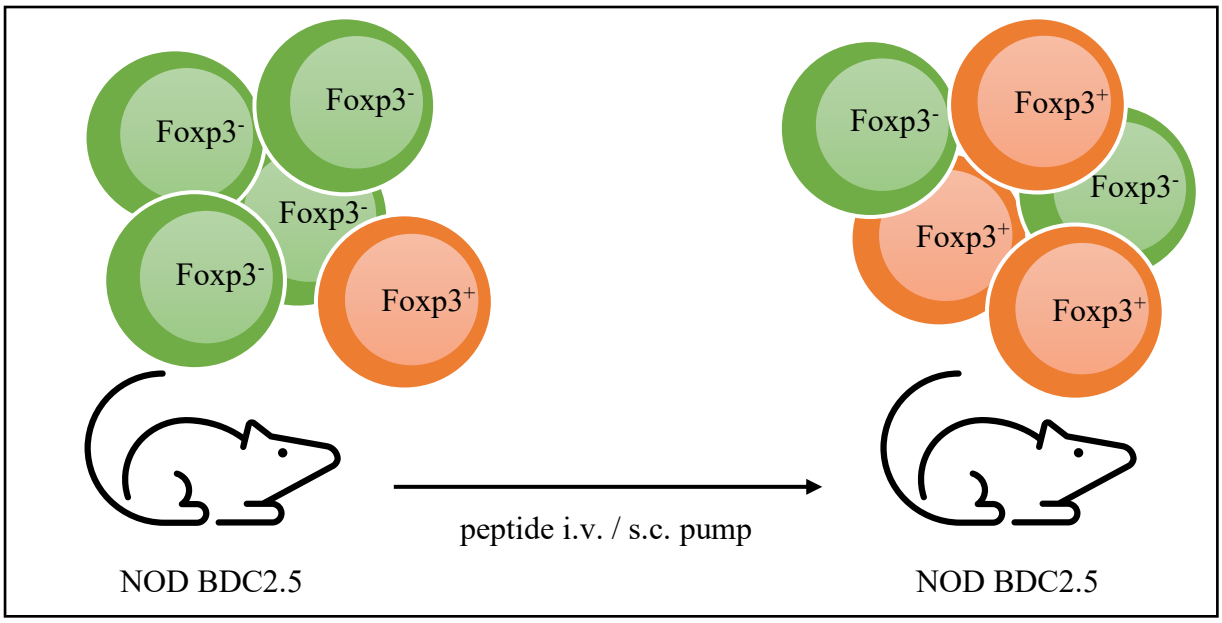

Figure 12: Experimental design: *In vivo* induction of CD4$^+$Foxp3$^+$ Tregs in BDC2.5 tg NOD by subimmunogenic stimulation with agonist peptide

NOD BDC2.5 tg mice were exposed to BDC2.5 peptide under subimmunogenic conditions. 5 µg peptide was applied as a single shot i.v. injection. Alternatively, a daily dose of 5 µg peptide was applied continuously for 14 days using a subcutaneously implanted osmotic minipump. Control mice were treated with PBS instead. Foxp3 expression within CD4$^+$ cells was analyzed in blood, spleen, mesenteric and pancreatic lymph nodes by flow cytometry.
Symbols: Orange: CD4$^+$Foxp3$^+$ T cells; green: CD4$^+$Foxp3$^-$ T cells.

Blood samples from PBS treated control animals showed a relatively stable fraction of 8.08 % ± 0.05 % SEM Foxp3$^+$ of CD4$^+$ T cells at day 4 and 5.88 % ± 0.74 % SEM Foxp3$^+$ of CD4$^+$ T cells at day 12 ($p = 0.0874$). Comparisons between control animals and peptide treated groups at equivalent time points revealed significant increases in CD4$^+$Foxp3$^+$ T cells. In particular, as early as 4 days after peptide injection Foxp3$^+$CD4$^+$ T cells yielded a mean of 15.33 % ± 1.35 % SEM. This absolute increase of 7.25 % ± 1.35 % SEM was significant

($p = 0.0058$). This trend of increased Treg frequencies through peptide stimulation was preserved until the experimental endpoint. However, the absolute increase of $CD4^+Foxp3^+$ Tregs upon peptide stimulation declined at later time points (absolute increase at 8 days: 3.46 % ± 0.10 % SEM, $p = 0.0180$/ at 12 days: 2.30 % ± 0.89 % SEM, $p = 0.0492$). Accordingly, levels of $CD4^+Foxp3^+$ Tregs in peptide-treated animals decreased over time and approached levels of $CD4^+Foxp3^+$ Tregs in control animals (paired students t-test: % $Foxp3^+$ of $CD4^+$ at day 4 vs day 8: $p = 0.1151$; paired students t-test: % $Foxp3^+$ of $CD4^+$ at day 8 vs day 12: $p = 0.0259$). As expected, there was no significant change in $Foxp3^+$ Tregs in untreated mice over time (paired students t-test: % $Foxp3^+$ of $CD4^+$ at day 4 vs day 12: $p = 0.0874$) (Figure 13 B, left panel).

Similar to what was seen in blood, solid organ samples from spleen, PLN and MLN showed increases in $Foxp3^+$ cells within $CD4^+$ T cells upon peptide treatment. 12 days after injection, spleens from peptide treated animals showed an absolute increase of 4,45 % ± 1.11 % SEM of $CD4^+Foxp3^+$ T cells (from 8,150 % in control animals to 12.63 % in peptide treated animals; $p = 0.0099$). $CD4^+Foxp3^+$ T cells in MLN showed an absolute increase of 2.54 % ± 0.64 % SEM (from 5.700 % in control animals to 8.24 % in peptide treated animals; $p = 0.0108$) and $CD4^+Foxp3^+$ T cells in PLN increased by 3.60 % ± 1.32 % SEM (from 4.45 % in control animals to 8.04 % in peptide treated animals; $p = 0.0523$) (Figure 13 B, middle and right panel).

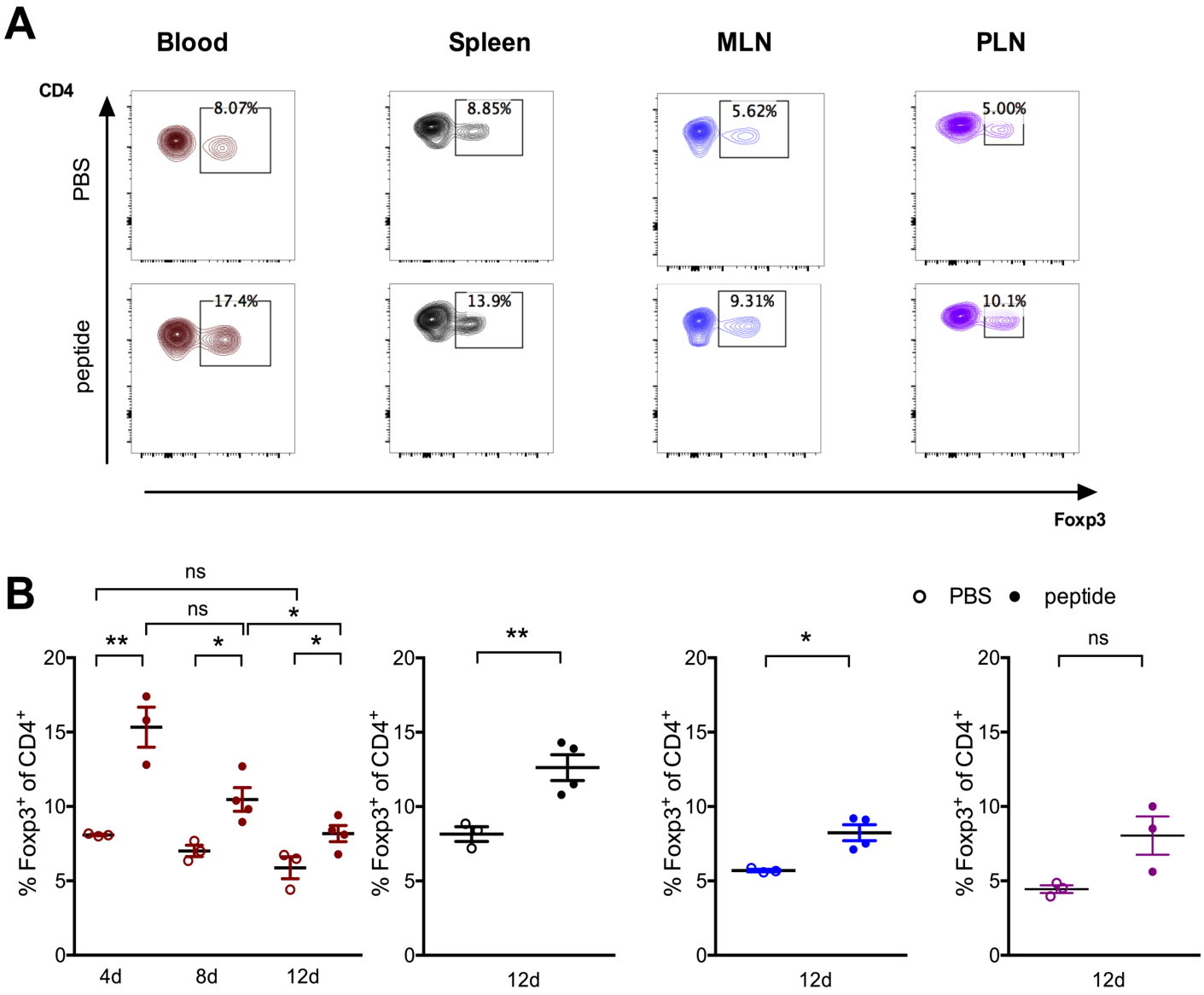

Figure 13: *In vivo* induction of CD4$^+$Foxp3$^+$ Tregs in BDC2.5 tg NOD mice by single intravenous peptide administration

Tregs were characterized as CD4$^+$ Foxp3$^+$ cells. For induction of Foxp3 expression a single dose of 5 µg BDC2.5 mimetope peptide was applied intravenously. Samples from blood, spleen, MLN and PLN were taken at indicated time points and analyzed by flow cytometry. The full gating strategy is reported in Material and Methods. All samples were gated on live CD4$^+$CD8$^-$ lymphocytes.
A) Representative FACS plots are shown.
B) Cell frequencies (mean ± SEM) for percentage of Foxp3$^+$ cells among CD4$^+$ cells at indicated time points are shown. Analyzed organs are color-coded just like A). Each circle represents one experimental animal. Empty circles represent control animals, full circles depict the experimental group.
The depicted results are representative for two similar experiments. * ($p < 0.05$), ** ($p < 0.01$)

To address the question whether peptide administration specifically boosts p- or tTregs, samples were co-analyzed for the expression of Helios and Nrp1. The expression pattern for samples from blood, spleen, MLN and PLN are shown in Figure 14.

12 days after injection, no significant difference for Helios expression between control and peptide treated animals was found in the $CD4^+Foxp3^+$ population in blood samples ($p = 0.9014$), spleen ($p = 0.2388$) and PLN ($p = 0.3079$). In MLN, however, an absolute increase of 10.93 % ± 3.40 % SEM $Helios^-$ of $CD4^+Foxp3^+$ was observed ($p = 0.0237$) (Figure 14 A).

Equivalently, Nrp1 expression patterns remained stable upon peptide administration (blood: $p = 0.0946$, spleen: $p = 0.9344$, MLN: $p = 0.9086$, PLN: $p = 0.9703$) (Figure 14 B).

The expression levels of Helios and Nrp1 as redundant markers for discrimination of different Treg subsets mostly were equivalently distributed between samples from the same organ. However, expression patterns of Helios and Nrp-1 within $CD4^+Foxp3^+$ cells were not fully identical: Blood and spleen samples from 12 days after control treatment showed significantly higher levels of $Nrp\text{-}1^-$ of $CD4^+Foxp3^+$ compared to $Helios^-$ of $CD4^+Foxp3^+$ (blood: difference between means 13.45 % ± 3.84 % SEM, $p = 0.0249$, spleen: difference between means 8.29 ± 2.11 % SEM, $p = 0.0171$). No significant difference in expression patterns of $Helios^-$ and $Nrp\text{-}1^-$ within $Foxp3^+CD4^+$ cells was found in any other group.

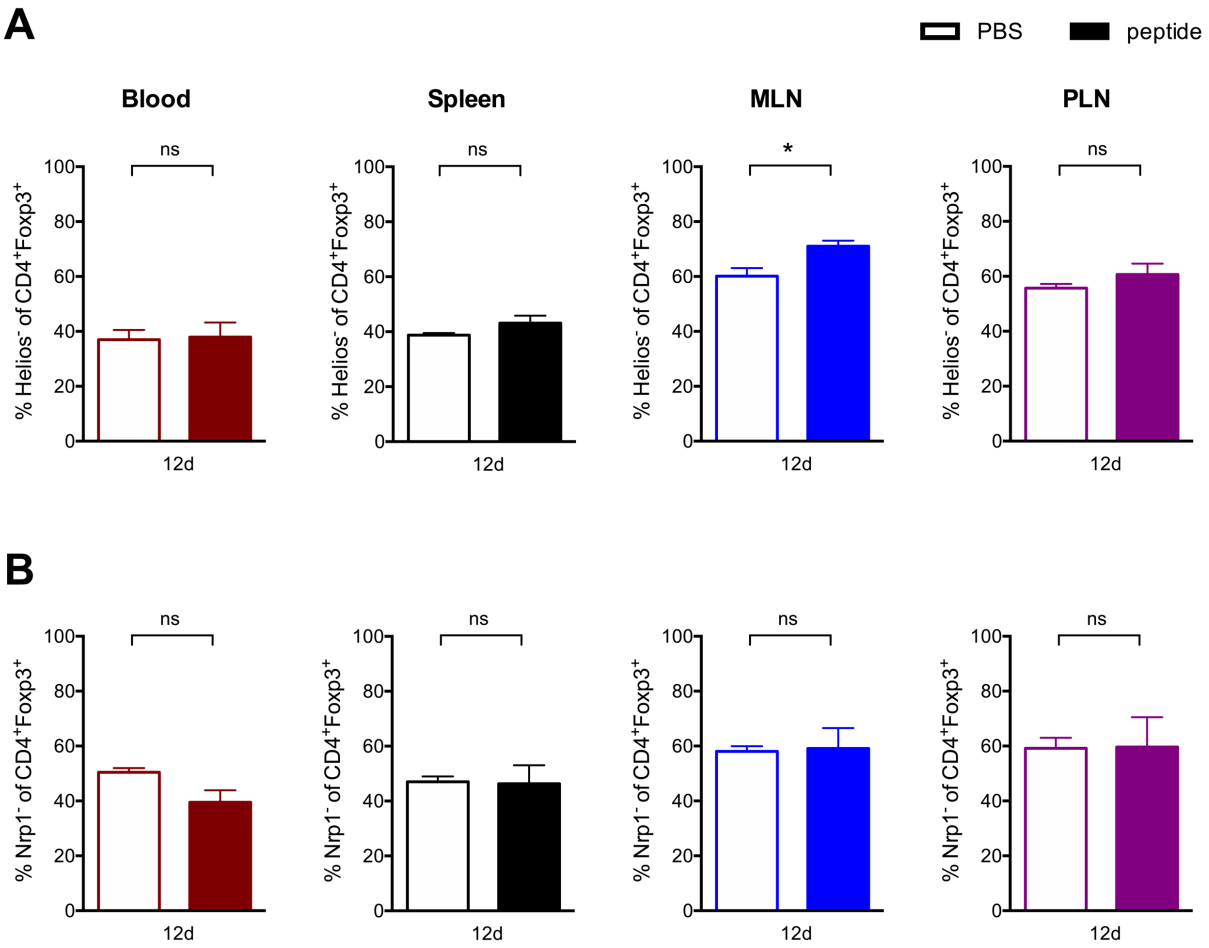

Figure 14: Expression of Helios and Nrp1 in *in vivo* induced CD4$^+$Foxp3$^+$ Tregs by single intravenous peptide administration

For induction of Foxp3 expression a single dose of 5 µg BDC2.5 mimetope peptide was applied intravenously. Samples from blood, spleen, MLN and PLN were taken 12 days after peptide administration and analyzed by flow cytometry. The full gating strategy is reported in Material and Methods. All samples were gated on live CD4$^+$CD8$^-$ lymphocytes. Results are shown as mean ± SEM with 3-4 animals per group.
A) Percentages of Helios$^-$ of CD4$^+$Foxp3$^+$ T cells in blood, spleen and lymph nodes are shown.
B) Percentages of Nrp1$^-$ of CD4$^+$Foxp3$^+$ T cells in blood, spleen and lymph nodes are shown.
Empty bars represent control animals, full bars depict the experimental group. * ($p < 0.05$)

3.2.2. *In vivo* induction of Foxp3 expression by prolonged subcutaneous application of agonist BDC2.5 peptide

Previous work from other groups showed that prolonged low-dose administration of agonist peptide can induce Foxp3 expression [136]. We therefore sought to investigate Foxp3 induction by prolonged BDC2.5 mimetope application through a subcutaneously implanted osmotic minipump compared to a single peptide injection.

Here, 5 µg BDC2.5 mimetope were administered daily for 14 days. Control mice were implanted with osmotic pumps perfusing PBS only. Blood was taken repeatedly and analyzed by flow cytometry (Figure 15, left panel). In contrast to what was seen after a single intravenous

mimetope application, significant changes in Foxp3 expression in blood were not observable early after pump implantation (day 3; p = 0.1445). However, at day 8 after pump implantation an absolute increase of 7.08 % ± 1.12 % SEM $Foxp3^+$ cells of $CD4^+$ cells in peptide-treated animals compared to controls receiving PBS only was seen (p = 0.0015) in peripheral blood. Accordingly, there was a significant increase in $CD4^+Foxp3^+$ T cells in peripheral blood in peptide-treated animals between day 3 and day 8 (paired students t-test p = 0.0055). 14 days after pump implantation, mice were sacrificed and Foxp3 expression levels were analyzed in samples from blood and spleen (Figure 15). Blood samples from day 14 showed elevated Foxp3 expression levels in peptide-treated animals compared to PBS controls (absolute increase of 9.34 % ± 3.29 % SEM, p = 0.0295). Yet, there was no further increase in $CD4^+Foxp3^+$ T cells between day 8 and day 14 in peripheral blood (paired students t-test p = 0.2233).

In spleen samples from day 14, there was a trend towards increased levels of $CD4^+Foxp3^+$ T cells upon peptide-treatment compared to PBS controls. However, this was not significant (absolute increase of $CD4^+Foxp3^+$ T cells in peptide-treated animals vs. PBS controls: 7.06 % ± 2.91, p = 0.0512) (Figure 15, right panel).

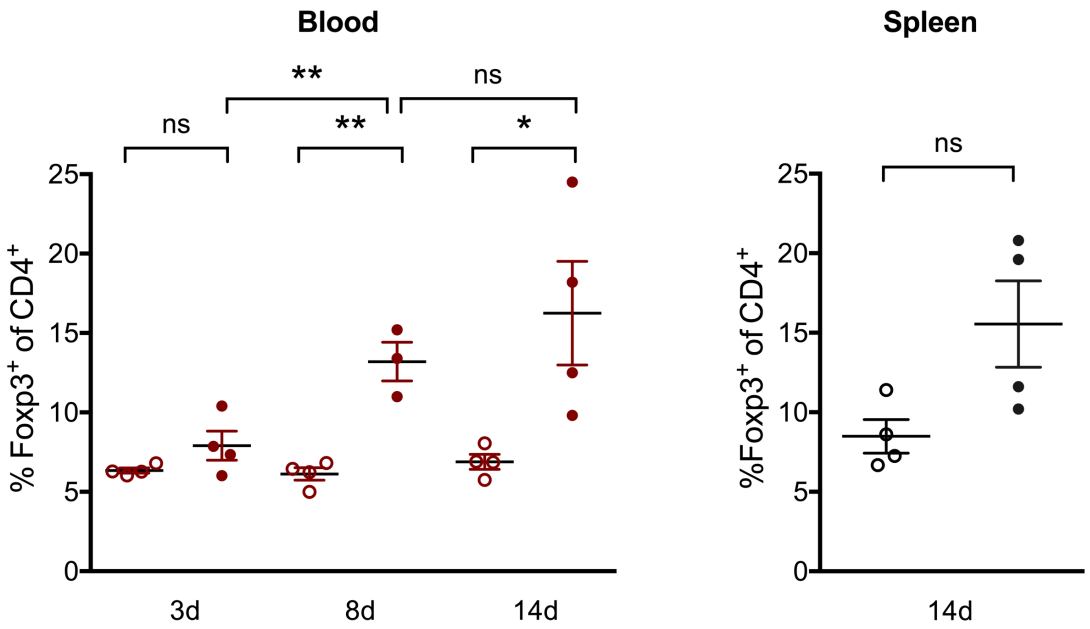

Figure 15: *In vivo* induction of $CD4^+Foxp3^+$ Tregs in BDC2.5 tg NOD by prolonged subcutaneous mimetope application

Mice were implanted with osmotic minipumps. Experimental mice received 5 µg BDC2.5 mimetope peptide daily, whereas control animals received an equivalent volume of PBS. Samples from blood and spleen were taken at indicated time points and analyzed by flow cytometry. Cell frequencies (mean ± SEM) for percentage of $Foxp3^+$ cells among $CD4^+$ cells are shown. The full gating strategy is reported in Material and Methods. All samples were gated on live $CD4^+CD8^-$ lymphocytes. Each circle represents one experimental animal. Empty circles represent control animals, full circles depict the experimental group. * ($p < 0.05$), ** ($p < 0.01$)

Helios and Nrp1 expression within Foxp3$^+$CD4$^+$ T cells were assessed at day 3, 8 and 14. Representative results from blood samples from day 8 can be found in Figure 16. In accordance with the observation for intravenous mimetope application, percentages of Helios$^-$ ($p = 0.0692$) and Nrp1$^-$ ($p = 0.1257$) of Foxp3$^+$CD4$^+$ T cells did not significantly change upon peptide stimulation.

There were significantly less Nrp1$^-$ of Foxp3$^+$CD4$^+$ T cells than Helios$^-$ of Foxp3$^+$CD4$^+$ T cells in both, untreated as well as in peptide stimulated groups (difference between means of Helios$^-$ and Nrp-1$^-$ of CD4$^+$Foxp3$^+$ upon control treatment: 22.30 % ± 5.12 % SEM, $p = 0.0048$; difference between means of Helios$^-$ and Nrp-1$^-$ of CD4$^+$Foxp3$^+$ upon peptide treatment: 24.02 % ± 6.18 % SEM, $p = 0.0302$).

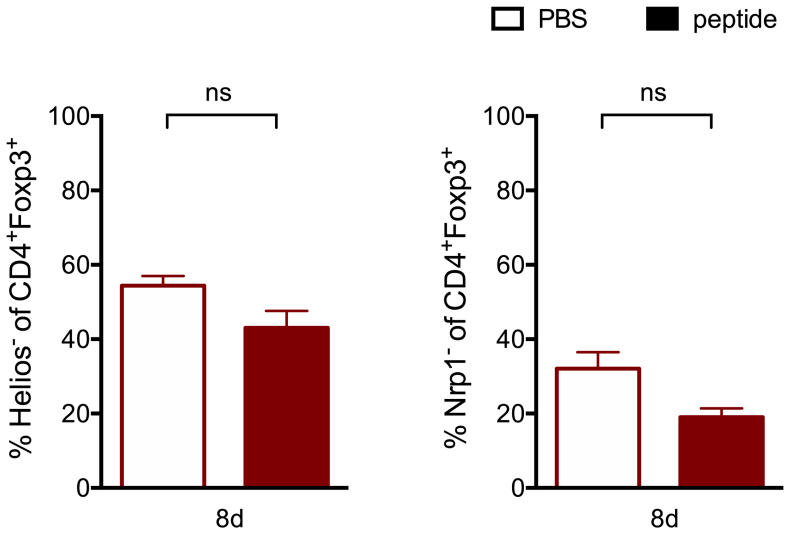

Figure 16: Expression of Helios and Nrp1 in *in vivo* induced CD4$^+$Foxp3$^+$ Tregs by prolonged subcutaneous mimetope application

Mice were implanted with osmotic minipumps. Experimental mice received 5 µg BDC2.5 mimetope peptide daily, whereas control animals received an equivalent volume of PBS. Blood samples were taken 8 days after pump implantation and analyzed for Helios and Nrp1 expression by flow cytometry. The full gating strategy is reported in Material and Methods. All samples were gated on live CD4$^+$CD8$^-$ lymphocytes. Results are shown as mean ± SEM with 2-4 animals per group.
Empty bars represent control animals, full bars depict the experimental group. * ($p < 0.05$)

3.2.3. *In vivo* induction of Foxp3 expression in adoptively transferred BDC2.5 tg CD4$^+$ donor cells by single intravenous application of agonist BDC2.5 peptide

To evaluate Foxp3 induction by BDC2.5 mimetope peptide stimulation more specifically in the CD4$^+$ T cell compartment, adoptive transfer experiments were performed. Splenic CD4$^+$ T cells from BDC2.5 tg donors were isolated and labeled with fixable Cell Proliferation Dye eFluor™ 670 to allow for long-term cell tracking. Donor cell suspensions were immediately

transferred into NOD WT recipients. One day after transfer, the experimental group was challenged with a single intravenous dose of 5 µg BDC2.5 mimetope peptide. Control animals were injected with an equivalent volume of PBS. All mice were sacrificed after seven days and spleen samples were taken. Foxp3 expression within transferred $CD4^+$ donor cells was analyzed by flow cytometry (Figure 17).

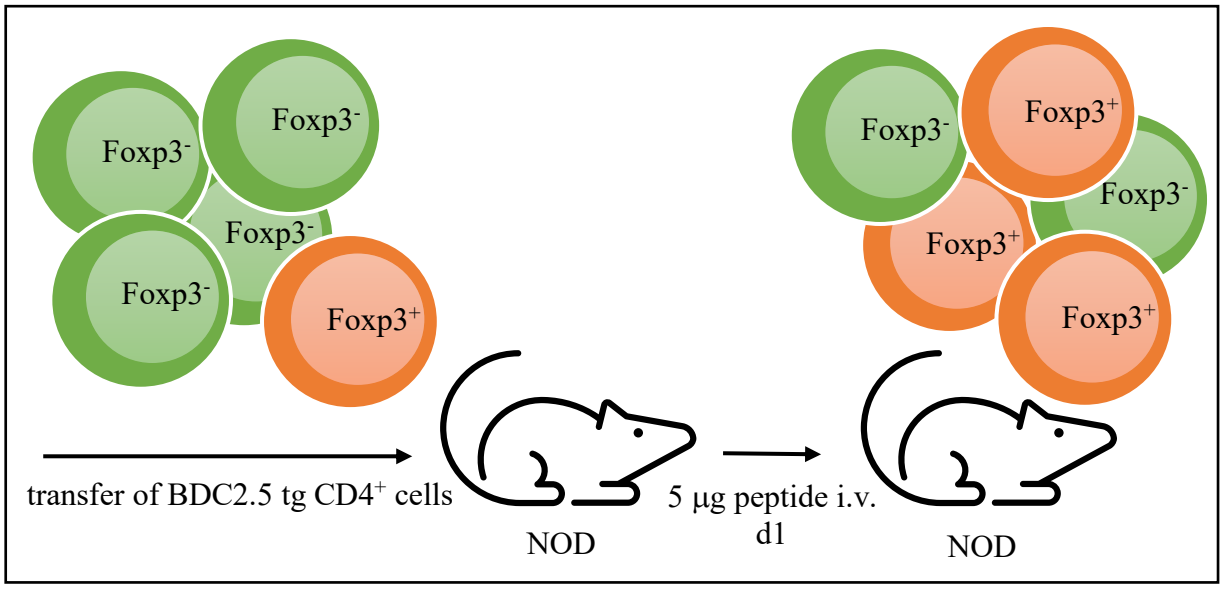

Figure 17: Experimental design: *In vivo* induction of Foxp3 expression in adoptively transferred BDC2.5 tg $CD4^+$ donor cells by single intravenous peptide application

$CD4^+$ donor cells from BDC2.5 tg mice were purified, labeled and transferred into NOD WT recipients. Recipient mice received a single intravenous dose of 5 µg BDC2.5 mimetope peptide one day after transfer (d1). Control animals were treated with an equivalent volume of PBS. After seven days, mice were sacrificed and spleens were harvested. Foxp3 expression within donor $CD4^+$ cells was analyzed by flow cytometry after seven days.
Symbols: Orange: $CD4^+Foxp3^+$ T cells; green: $CD4^+Foxp3^-$ T cells.

Among transferred $CD4^+$ donor cells, there was a significant increase in $CD4^+Foxp3^+$ T cells after seven days. In spleen samples from control animals, 12.87 % ± 1,32 % SEM of $CD4^+$ T cell were $Foxp3^+$, compared to 36.97 % ± 1.01 % $CD4^+Foxp3^+$ T cells in peptide-treated animals ($p = 0.0001$) (Figure 18 A).

Although retrieved numbers of transferred Foxp3 positive cells were low (mean control group: 35 / mean peptide treated group: 32), Helios and Nrp1 expression patterns were assessed (Figure 18 B). There was a significant increase in $Helios^-CD4^+Foxp3^+$ T cells when stimulated with agonist peptide compared to control animals (difference between means 20.23 % ± 6.58 % SEM; $p = 0.0371$). Nrp1 expression was not significantly altered ($p = 0.7434$).

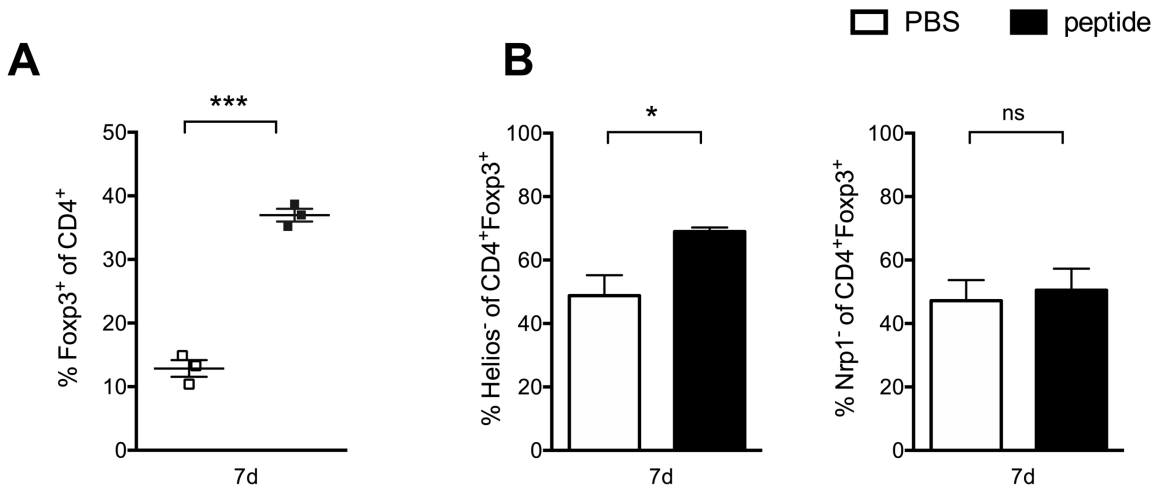

Figure 18: *In vivo* induction of Foxp3 expression in adoptively transferred BDC2.5 tg CD4$^+$ donor cells by single intravenous peptide application

CD4$^+$ cells were isolated from BDC2.5 tg mice, labeled and transferred into NOD mice. The following day, T cell recipients were injected intravenously with 5 µg BDC2.5 mimetope peptide. Controls were treated with an equivalent volume of PBS. Foxp3 expression within transferred CD4$^+$ BDC2.5 tg donor cells was measured by flow cytometry after seven days. Tregs were identified as being CD4$^+$Foxp3$^+$ T cells. All samples were gated on transferred live CD4$^+$CD8$^-$ lymphocytes. The full gating strategy is reported in Material and Methods.
A) Cell frequencies (mean ± SEM) for percentage of Foxp3$^+$ cells among CD4$^+$ cells are shown. Each symbol represents one experimental animal. Empty squares represent the control group, full squares depict the experimental group.
B) Nrp-1 and Helios expression within labeled CD4$^+$Foxp3$^+$ cells are shown (mean ± SEM).
Results are representative for three similar experiments. * ($p < 0.05$), ** ($p < 0.01$), *** ($p < 0.001$)

3.3. Dependency of *in vivo* Foxp3 induction on CNS1 and TGF-β

3.3.1. Peptide-induced Foxp3 expression in CNS1 WT CD4$^+$ vs. CNS1 KO CD4$^+$ cells

To test *in vivo* Foxp3 induction upon tolerogenic peptide stimulation in CNS1 deficient cells, NOD CNS1 WT and NOD CNS1 KO mice were bred with BDC2.5 tg NOD mice. The offspring was genotyped at weaning age. Female CNS1 WT BDC2.5 tg and CNS1 KO BDC2.5 tg mice were sacrificed when grown to adult age. Spleens from CNS1 WT BDC2.5 tg and CNS1 KO BDC2.5 tg donors, respectively, were pooled. CD4$^+$CD25$^-$ donor cells were enriched by magnetic purification and labelled with fixable Cell Proliferation Dye eFluor™ 670. Magnetic activated cell sorting (MACS) yielded 94.80 % Foxp3$^-$CD25$^-$ cells within CNS1 WT BDC2.5 tg CD4$^+$ donor cells and 94.60% Foxp3$^-$CD25$^-$ cells within CNS1 KO BDC2.5 tg CD4$^+$ donor cells. However, 2.08 % of CNS1 WT BDC2.5 tg CD4$^+$ donor cells and 2.18 % of CNS1 KO BDC2.5 tg CD4$^+$ donor cells were Foxp3$^+$CD25$^+$. In total, 4.38 % of transferred CNS1 WT BDC2.5 tg CD4$^+$ donor cells and 4.02 % of transferred CNS1 KO BDC2.5 tg CD4$^+$ donor cells remained positive for Foxp3 (Figure 19 A). Cell suspensions were directly transferred into NOD WT recipient mice. One day after transfer, experimental groups were challenged with a

single intravenous dose of 5 µg BDC2.5 mimetope peptide. Control animals were injected with an equivalent volume of PBS. All mice were sacrificed seven days after injections and spleens were analyzed by flow cytometry (Figure 17, Figure 19 B, C).

In spleen samples from control animals that received CNS1 WT BDC2.5 tg $CD4^+$ donor cells and PBS-treatment, 2.80 % ± 0.60 % SEM of transferred $CD4^+$ donor cells were positive for Foxp3. Correspondingly, in spleen samples from mice that received CNS1 KO BDC2.5 tg $CD4^+$ donor cells and PBS-injections, 4.33 % ± 0.18 % SEM of transferred $CD4^+$ donor cells were positive for Foxp3. No difference in Foxp3 expression within transferred $CD4^+$ donor cells upon PBS-control injections was found between transferred CNS1 WT BDC2.5 tg $CD4^+$ donor cells and CNS1 KO BDC2.5 tg $CD4^+$ donor cells after one week ($p = 0.0502$) (Figure 19 C).

Peptide treatment increased Foxp3 expression in transferred $CD4^+$ cells from both CNS1 WT BDC2.5 tg and CNS1 KO BDC2.5 tg donors. Peptide application induced Foxp3 expression in 17.33 % ± 0.77 % SEM of transferred CNS1 WT BDC2.5 tg $CD4^+$ donor cells (absolute increase of 14.53 % ± 0.98 % SEM, $p < 0.0001$). In transferred CNS1 KO BDC2.5 tg $CD4^+$ donor cells, peptide application induced Foxp3 expression in 11.28 % ± 1.52 % SEM of $CD4^+$ donor cells (absolute increase of 6.95 % ± 1.54 % SEM, $p = 0.0040$). Foxp3 induction upon peptide stimulation in transferred CNS1 KO BDC2.5 tg $CD4^+$ donor cells was significantly below Foxp3 induction in transferred CNS1 WT BDC2.5 tg $CD4^+$ donor cells ($p = 0.0122$) (Figure 19 C).

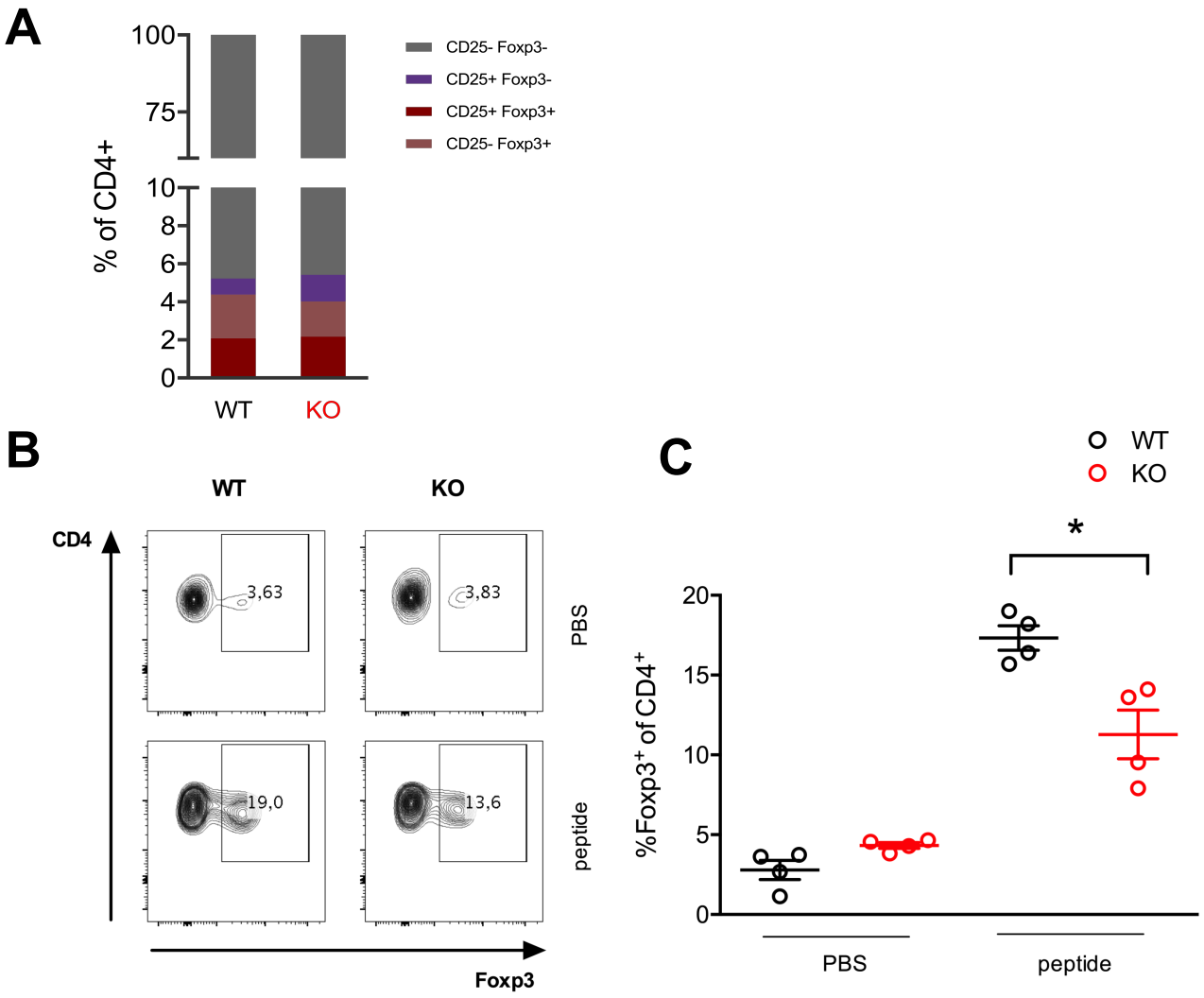

Figure 19: *In vivo* induction of Foxp3 expression in adoptively transferred CNS1 WT BDC2.5 tg CD4$^+$ cells vs. CNS1 KO BDC2.5 tg CD4$^+$ cells by single intravenous peptide application

Donor cells were isolated from CNS1 WT BDC2.5 tg or CNS1 KO BDC2.5 tg mice and enriched for CD4$^+$CD25$^-$ cells by magnetic purification. Purified cells were labelled and transferred into NOD WT mice. The following day, T cell recipients were injected intravenously with 5 µg BDC2.5 mimetope peptide. After one week, Foxp3 expression in labelled CD4$^+$ donor cells in full spleen samples was measured by flow cytometry. Tregs were identified as being CD4$^+$Foxp3$^+$ T cells. All samples were gated on transferred live CD4$^+$CD8$^-$ lymphocytes. The full gating strategy is reported in Material and Methods.
A) FACS analysis of transferred cells from either pooled CNS1 WT BDC2.5 tg or CNS1 KO BDC2.5 tg donors are shown. Columns show the expression of Foxp3 and CD25 after magnetic enrichment of CD4$^+$CD25$^-$ T cells.
B) Representative blots for Foxp3 expression in CNS1 WT BDC2.5 tg or CNS1 KO BDC2.5 tg donor cells are shown. NOD WT recipients were either treated with PBS or BDC2.5 mimetope peptide.
C) Cell frequencies (mean ± SEM) for percentage of Foxp3$^+$ cells among CD4$^+$ cells are shown. Each symbol represents one experimental animal. Black circles represent CNS1 WT BDC2.5 tg donors whereas red circles depict CNS1 KO BDC2.5 tg donors. Exact P-values are shown (unpaired t-test).
Results are representative for three similar experiments. * ($p < 0.05$)

3.3.2. Peptide-induced Foxp3 expression in CNS1 WT CD4$^+$ cells under TGF-β-blockade

TGF-β has been shown to facilitate induction of Foxp3 expression in pTregs [105, 140, 163, 164] as opposed to tTregs where TGF-β-signaling seems to play a minor role in upregulation

of Foxp3 expression [163, 165]. CNS1 contains a binding site for Smad3 downstream of TGF-β signaling [109, 111]. This raised the question, whether the observed impairment in induction of Foxp3 expression in CNS1 deficient BDC2.5 tg $CD4^+$ T cells upon stimulation with agonist peptide is due to perturbed TGF-β signaling.

To address this question, spleens from CNS1 WT BDC2.5 tg donors were pooled. Single cell suspensions were prepared and enriched for $CD4^+CD25^-$ donor cells by magnetic purification. Prior to transfer into NOD WT recipients, donor cells were labeled with fixable Cell Proliferation Dye eFluor™ 670. One day after transfer recipients were challenged with a single intravenous dose of 5 µg BDC2.5 mimetope peptide. *In vivo* TGF-β-blockade was done by intraperitoneal injection of 300 µg monoclonal antibody on day 1 and day 4 after cell transfer (final dose per mouse: 600 µg anti TGF-β). Control animals were injected with an equivalent volume of PBS. All mice were sacrificed after seven days and spleens were analyzed by flow cytometry (Figure 20).

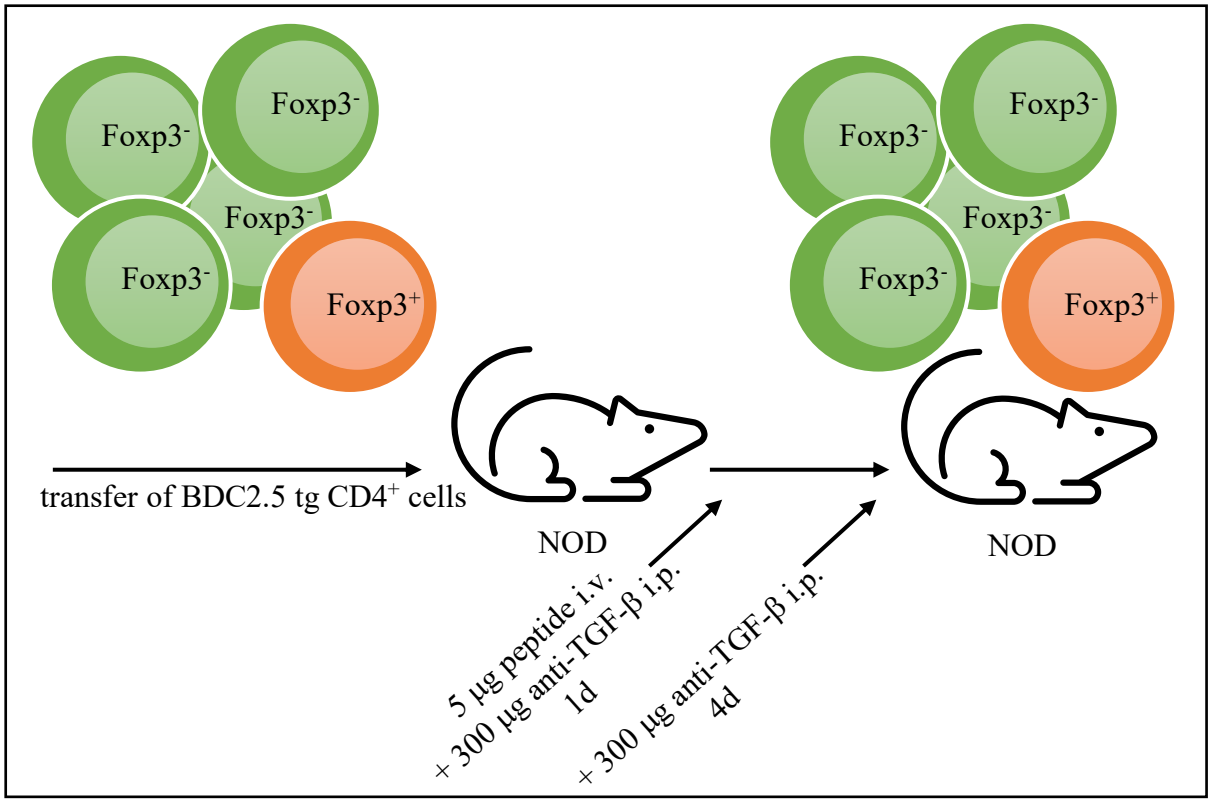

Figure 20: Experimental design: *In vivo* induction of Foxp3 in adoptively transferred BDC2.5 tg $CD4^+$ donor cells by single intravenous peptide application under TGF-β-blockade

CNS1 WT $CD4^+$ donor cells from BDC2.5 tg mice were purified, labeled and transferred into NOD WT recipients. Recipient mice received a single intravenous dose of 5 µg BDC2.5 mimetope peptide one day after transfer (d1). 300 µg of anti-TGF-β was injected intraperitoneally at day 1 (1d) and day 4 (4d). Control mice were treated with PBS instead. Foxp3 expression within donor $CD4^+$ cells was analyzed in in spleens by flow cytometry after seven days.
Symbols: Orange: $CD4^+Foxp3^+$ T cells; green: $CD4^+Foxp3^-$ T cells.

Magnetic activated cell sorting yielded 93.10 % $CD25^{-}Foxp3^{-}$ cells in CNS1 WT BDC2.5 tg $CD4^{+}$ donor cells. 2.29 % of the isolated CNS1 WT BDC2.5 tg $CD4^{+}$ donor cells remained double positive for CD25 and Foxp3. A total of 5.69 % of CNS1 WT BDC2.5 tg $CD4^{+}$ donor cells were $Foxp3^{+}$ (Figure 21 A).

In CNS1 WT BDC2.5 tg $CD4^{+}$ donor cells, application of agonist peptide led to an absolute increase of 11.21 % ± 0.90 % SEM in Foxp3 expression within $CD4^{+}$ donor cells compared to CNS1 WT BDC2.5 tg $CD4^{+}$ controls receiving PBS only ($p < 0.0001$) (Figure 21 C).

Notably, application of anti-TGF-β abrogated Foxp3 induction upon peptide stimulation: No increase in Foxp3 expression within transferred CNS1 WT BDC2.5 tg $CD4^{+}$ donor cells was found upon treatment with peptide + 600 µg anti-TGF-β compared to PBS control treatment ($p = 0.1436$). Accordingly, levels of $CD4^{+}Foxp3^{+}$ cells within transferred CNS1 WT BDC2.5 tg $CD4^{+}$ donor cells in animals treated with peptide + anti-TGF-β were significantly below levels of $CD4^{+}Foxp3^{+}$ T cells within transferred CNS1 WT BDC2.5 tg $CD4^{+}$ donor cells that received peptide treatment but no additional TGF-β-blockade (peptide: 16.63 % ± 0.88 % SEM vs. peptide + 600 µg anti-TGF-β: 9.04 % ± 2.15 % SEM; $p = 0.0170$) (Figure 21 C). Representative FACS blots can be found in Figure 21 B.

However, due to a lack of CNS1 KO BDC2.5 tg mice, no additional testing for *in vivo* TGF-β-blockade was performed in CNS1 KO donor cells.

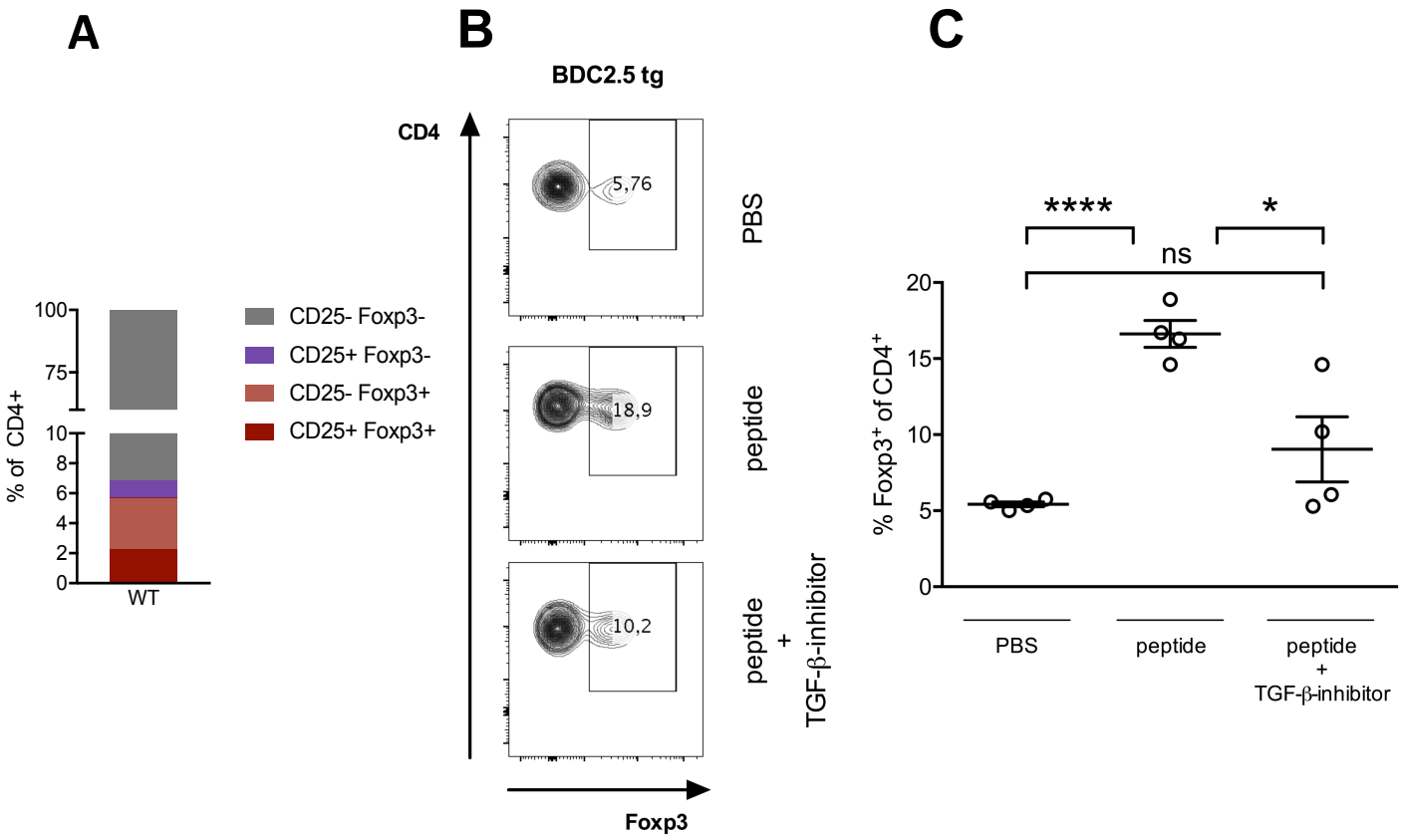

Figure 21: *In vivo* Foxp3 induction in adoptively transferred CNS1 WT BDC2.5 tg CD4$^+$ cells by single intravenous peptide application under TGF-β-blockade

CD4$^+$ T cells were isolated from CNS1 WT BDC2.5 tg mice and enriched for CD4$^+$CD25$^-$ T cells by magnetic purification. Purified cells were labeled and transferred into NOD mice. Recipients were treated with PBS only, BDC2.5 mimetope peptide or peptide plus 600 µg anti-TGF-β. Foxp3 expression in labeled BDC2.5 donor cells was measured by flow cytometry after seven days in full spleen samples. Tregs were identified as being CD4$^+$Foxp3$^+$ cells. All samples were gated on transferred live CD4$^+$CD8$^-$ lymphocytes. The full gating strategy is reported in Material and Methods.
A) FACS analysis of transferred cells from pooled CNS1 WT donors are shown. Columns show the expression of Foxp3 and CD25.
B) Representative blots for Foxp3 expression in CNS1 WT CD4$^+$ BDC2.5 tg cells are shown.
C) Cell frequencies are shown (mean ± SEM). Each symbol represents one experimental animal.
* ($p < 0.05$), ** ($p < 0.01$), *** ($p < 0.001$)

3.3.3. Foxp3 expression in adoptively transferred CNS1 WT CD4$^+$ cells vs. CNS1 KO CD4$^+$ cells in lymphopenic NOD SCID recipients

Foxp3 expression in naïve T cells can be induced by transfer into T cell deficient mice [110, 166, 167]. To evaluate CNS1 dependency in this setting, NOD CNS1 WT and CNS1 KO donor mice were sacrificed. Spleens from either CNS1 WT or CNS1 KO animals were pooled. Cell suspensions were magnetically depleted of CD4$^+$Foxp3$^+$ cells. FACS analysis demonstrated that magnetic depletion initially could decrease CD4$^+$Foxp3$^+$ cells only incompletely within CNS1 WT CD4$^+$ donor cells by 1.27 % and by 1.82 % for CNS1 KO CD4$^+$ donor cells. After MACS 87.1 % of CNS1 WT CD4$^+$ donor cells were CD25$^-$Foxp3$^-$ and 87.4 % of CNS1 KO

$CD4^+$ donor cells were $CD25^-Foxp3^-$. Thus, 11.69 % of the transferred CNS1 WT $CD4^+$ donor cells and 11.30 % of the transferred CNS1 KO $CD4^+$ donor cells were positive for Foxp3 (Figure 22 A). Cell suspensions were directly transferred into NOD SCID mice. Recipients were analyzed for changes in Foxp3 expression within transferred CNS1 WT $CD4^+$ donor cells and CNS1 KO $CD4^+$ donor cells in the blood every second week.

Two weeks after transfer into lymphopenic recipients, CNS1 WT but also CNS1 KO donor cells showed a drastic expansion of $Foxp3^+$ cells within $CD4^+$ cells (absolute increase of $Foxp3^+$ cells within CNS1 WT $CD4^+$ donor cells after two weeks compared to the initial level of $Foxp3^+$ cells within CNS1 WT $CD4^+$ donor cells: 17.29 % ± 1.52 % SEM vs. 14.43 % ± 1.29 % SEM for $Foxp3^+$ cells within CNS1 KO $CD4^+$ donor cells after two weeks compared to the initial level of $Foxp3^+$ cells within CNS1 KO $CD4^+$ donor cells). Yet, Foxp3 expression in CNS1 WT $CD4^+$ donor cells (mean $Foxp3^+$ of $CD4^+$: 28.98 % ± 1.52 % SEM) did not differ from Foxp3 expression in CNS1 KO $CD4^+$ donor cells (mean $Foxp3^+$ of $CD4^+$: 25.73 % ± 1.29 % SEM) two weeks after cell transfer ($p = 0.1293$, Figure 22 B).
Four weeks after transfer, Foxp3 expression levels decreased towards their initial level prior to transfer in both CNS1 WT and CNS1 KO $CD4^+$ donor cells (CNS1 WT: mean $Foxp3^+$ of $CD4^+$: 14.67 % ± 0.92 % SEM; CNS1 KO: mean $Foxp3^+$ of $CD4^+$: 15.70 % ± 1.22 % SEM). Again, Foxp3 expression in CNS1 WT $CD4^+$ donor cells did not differ from Foxp3 expression in CNS1 KO $CD4^+$ donor cells ($p = 0.5042$).
This level of $Foxp3^+$ cells within $CD4^+$ donor cells was maintained six weeks after transfer (CNS1 WT: mean $Foxp3^+$ of $CD4^+$: 15.53 % ± 1.19 % SEM; CNS1 KO: mean $Foxp3^+$ of $CD4^+$: 18.16 % ± 1.18 % SEM; $p = 0.1481$).
Accordingly, transfer-induced Diabetes did not differ between mice receiving CNS1 WT donor cells vs. mice that were transferred with CNS1 KO donor cells: Median disease onset was 48 days for both CNS1 WT and CNS1 KO groups (Log-rank test: $p = 0.6013$; Gehan-Breslow-Wilcoxon test: $p = 0.8812$) (Figure 22 C).

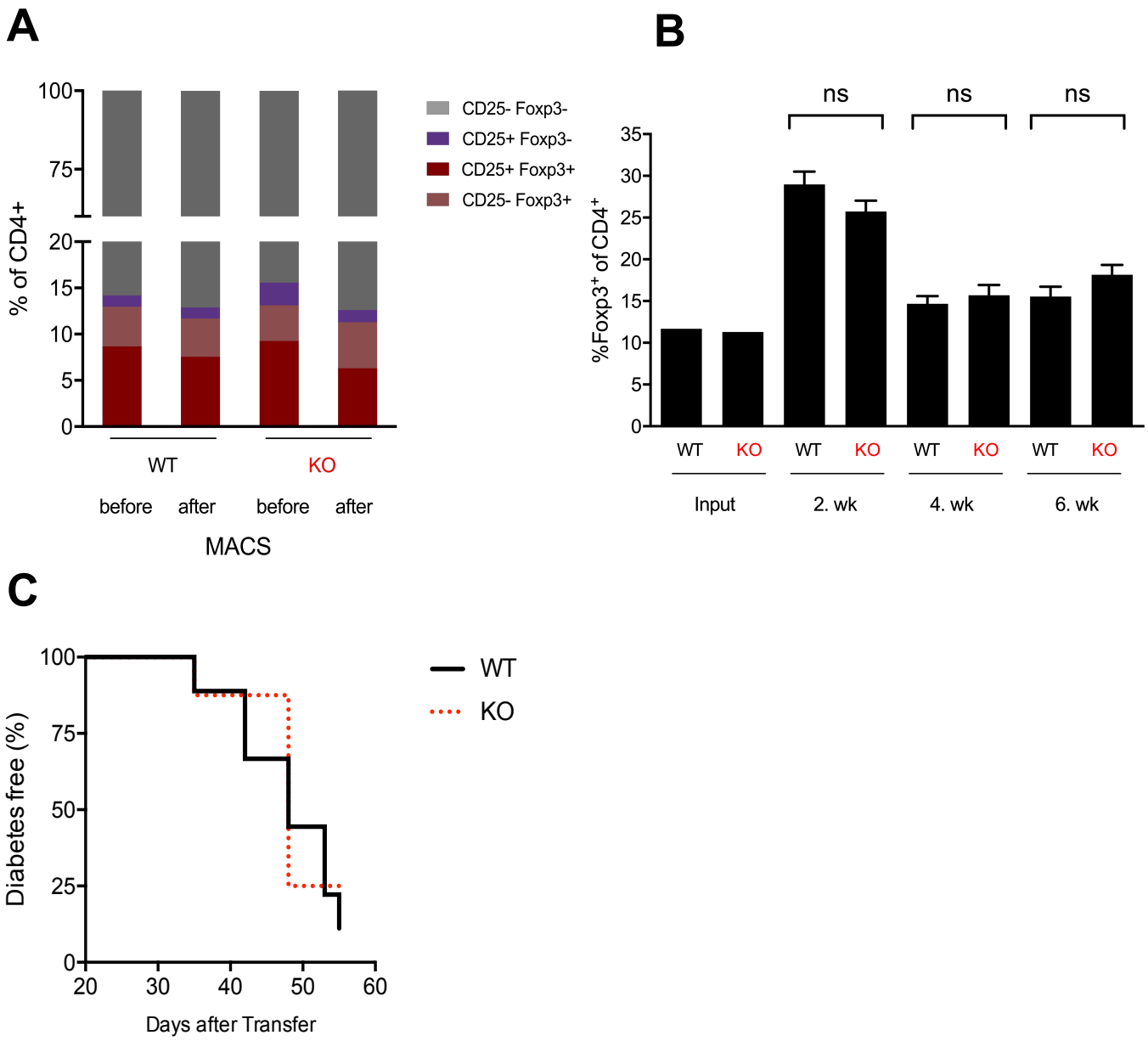

Figure 22: Foxp3 expression in CNS1 WT NOD CD4$^+$ donor cells vs. CNS1 KO NOD CD4$^+$ donor cells in lymphopenic NOD SCID recipients and diabetes onset after transfer

CD4$^+$ donor cells were isolated from CNS1 WT or CNS1 KO NOD mice and enriched for CD4$^+$CD25$^-$ cells by magnetic purification. Purified cells were transferred into SCID recipient mice. Foxp3 expression in transferred cells was measured by flow cytometry every second week in peripheral blood samples. Tregs were identified as being CD4$^+$Foxp3$^+$ cells. All samples were gated on transferred live CD4$^+$CD8$^-$ lymphocytes. The full gating strategy is reported in Material and Methods.
A) FACS analysis of transferred cells from pooled CNS1 WT or CNS1 KO donors are shown. Columns show the expression of Foxp3 and CD25 before and after magnetic purification.
B) Blood samples were taken from recipients that were either transferred with CNS1 WT or CNS1 KO donor cells. Foxp3 expression is depicted as proportion of all CD4$^+$ T cells at indicated time points. Cell frequencies (mean ± SEM) are shown. * ($p < 0.05$)
C) Cumulative diabetes onset of recipient mice after transfer of either CNS1 WT or CNS1 KO donor cells.

3.3.4. Foxp3 expression in adoptively transferred CNS1 WT BDC2.5 tg CD4$^+$ cells vs. CNS1 KO BDC2.5 tg CD4$^+$ cells in lymphopenic NOD SCID recipients under additional peptide stimulation

Further tests were done to evaluate the influence of BDC2.5 mimetope stimulation in this setting of homeostatic expansion pressure. Cell suspensions were prepared from CNS1 WT BDC2.5 tg or CNS1 KO BDC2.5 tg donors (see above) and magnetically enriched for CD4$^+$CD25$^-$ T cells. The use of an improved depletion protocol yielded relatively better purity of CD4$^+$Foxp3$^-$ T cells. FACS analyses of transferred cells demonstrated that 92.4 % of CNS1 WT BDC2.5 tg CD4$^+$ and 93.6 % of transferred CNS1 KO BDC2.5 tg CD4$^+$ donor cells were double negative for CD25 and Foxp3 expression. Yet, 6.55 % of transferred CNS1 WT BDC2.5 tg CD4$^+$ donor cells and 5.60 % of transferred CNS1 KO BDC2.5 tg CD4$^+$ donor cells remained positive for Foxp3 (Figure 23 A). Cell suspensions were directly transferred into NOD SCID mice. Recipients received either intravenous control injections one day after transfer or were treated with 5 µg agonist peptide. Blood samples from seven days after transfer as well as spleen and PLN samples taken thirteen days after transfer were analyzed for changes in Foxp3 expression in transferred CNS1 WT BDC2.5 tg and CNS1 KO BDC2.5 tg CD4$^+$ donor cells (Figure 23 B, C).

As described above, upon transfer into lymphopenic recipients, even in mice that did not experience peptide stimulation but were injected with PBS only, dramatic increases in Foxp3$^+$ cells were seen. This was the case for both, CD4$^+$ donor cells from CNS1 WT BDC2.5 tg and CNS1 KO BDC2.5 tg donors (Figure 23 B and A). In blood samples from seven days after transfer, Foxp3 expression within CD4$^+$ donor cells increased by 14.38 % ± 1.30 % SEM for CNS1 WT donor cells and by 6.00 % ± 0.42 % SEM for CNS1 KO donor cells upon transfer and control treatment only. Notably, as opposed to what was seen two weeks after transfer into lymphopenic recipients (compare Figure 22B), seven days after transfer blood samples from CNS1 WT BDC2.5 tg CD4$^+$ cell recipients showed higher levels of Foxp3$^+$ cells within CD4$^+$ cells compared to levels of Foxp3$^+$ cells within CD4$^+$ cells from mice that received CNS1 KO BDC2.5 tg CD4$^+$ donor cells ($p = 0.0005$) (Figure 23 B).

Analyses from solid organ samples taken thirteen days after transfer and control treatment as well showed higher Foxp3 expression within CD4$^+$ cells compared to the initial level of Foxp3$^+$ cells within transferred CD4$^+$ donor cells (Figure 23 B and A). In spleens, Foxp3 expression within transferred BDC2.5 tg CD4$^+$ donor cells was found to have increased by 11.35 % ± 2.10 % SEM for CNS1 WT BDC2.5 tg and by 5.23% ± 4.33 % SEM for CNS1 KO BDC2.5 tg cells compared to the initial fraction of Foxp3$^+$ cells within BDC2.5 tg CD4$^+$ donor

cells. Yet, in contrast to blood samples taken seven days after transfer, spleen samples taken thirteen days after transfer showed no difference in Foxp3$^+$ levels between CNS1 WT BDC2.5 tg CD4$^+$ and CNS1 KO BDC2.5 tg CD4$^+$cells ($p = 0.1921$) (Figure 23 B).
In contrast, PLN samples taken thirteen days after transfer of donor CNS1 WT BDC2.5 tg and CNS1 KO BDC2.5 tg CD4$^+$ cells into lymphopenic recipients and control treatment showed no increase in Foxp3 expression within BDC2.5 tg CD4$^+$ donor cells (Figure 23 B and A). Moreover, there was no difference between levels of Foxp3$^+$ cells from CNS1 WT BDC2.5 tg and CNS1 KO BDC2.5 tg CD4$^+$ donor cells ($p = 0.0676$, Figure 23 B).

Further observations were made on recipients of CNS1 WT BDC2.5 tg and CNS1 KO BDC2.5 tg CD4$^+$ donor cells that received 5 µg peptide instead of the control treatment (Figure 23 C). Notably, in contrast to what was observed for peptide-stimulation upon transfer into NOD WT recipients (Figure 19C), peptide treatment after transfer into lymphopenic recipients did not further boost expression of Foxp3 in BDC2.5 tg CD4$^+$ donor cells compared to PBS control injections (compare Figure 23 B and C). Analyses from both, mice that received CNS1 WT BDC2.5 tg CD4$^+$ or CNS1 KO BDC2.5 tg CD4$^+$ donor cells, showed no increase in Foxp3$^+$ cells within CD4$^+$ donor cells upon peptide-treatment compared to control injections when transferred into lymphopenic recipients. This observation was made in samples from blood (7 days after transfer), spleen and PLN (thirteen days after transfer). Solely blood samples from CNS1 KO BDC2.5 tg CD4$^+$ donor cell recipients taken seven days after transfer showed a moderate increase in Foxp3 expression upon peptide treatment compared to CNS1 KO donor cells receiving PBS only (difference between means: 4.13 % ± 0.69 % SEM; $p = 0.0018$).
Levels of Foxp3$^+$ cells within CNS1 WT BDC2.5 tg CD4$^+$ donor cells and CNS1 KO BDC2.5 tg CD4$^+$ donor cells after peptide-treatment were compared (Figure 23 C). Blood samples taken from peptide-treated animals seven days after transfer showed no difference in Foxp3 expression between CNS1 WT BDC2.5 tg CD4$^+$ and CNS1 KO BDC2.5 tg CD4$^+$ T cells (CNS1 WT BDC2.5 tg: mean Foxp3$^+$ of CD4$^+$: 17.98 % ± 2.30 % SEM; CNS1 KO BDC2.5 tg: mean Foxp3$^+$ of CD4$^+$: 15.73 % ± 0.56 % SEM; $p = 0.4540$). Similar observations were made for spleen samples taken thirteen days after transfer (CNS1 WT BDC2.5 tg: mean Foxp3$^+$ of CD4$^+$: 13.74 % ± 2.82 % SEM; CNS1 KO BDC2.5 tg: mean Foxp3$^+$ of CD4$^+$: 9.97 % ± 1.58; $p = 0.2876$).
In PLN samples, levels of Foxp3$^+$ cells within CNS1 WT BDC2.5 tg CD4$^+$ donor cells were significantly higher compared to Foxp3$^+$ cells within CNS1 KO BDC2.5 tg CD4$^+$ donor cells (WT: mean Foxp3$^+$ of CD4$^+$: 7.14 % ± 0.92 % SEM; KO: mean Foxp3$^+$ of CD4$^+$:

3.72 % SEM ± 0.31 % SEM; p = 0.0101). However, as mentioned above, in PLN levels of $Foxp3^+$ cells within transferred $CD4^+$ donor cells did not increase upon transfer into lymphopenic recipients.

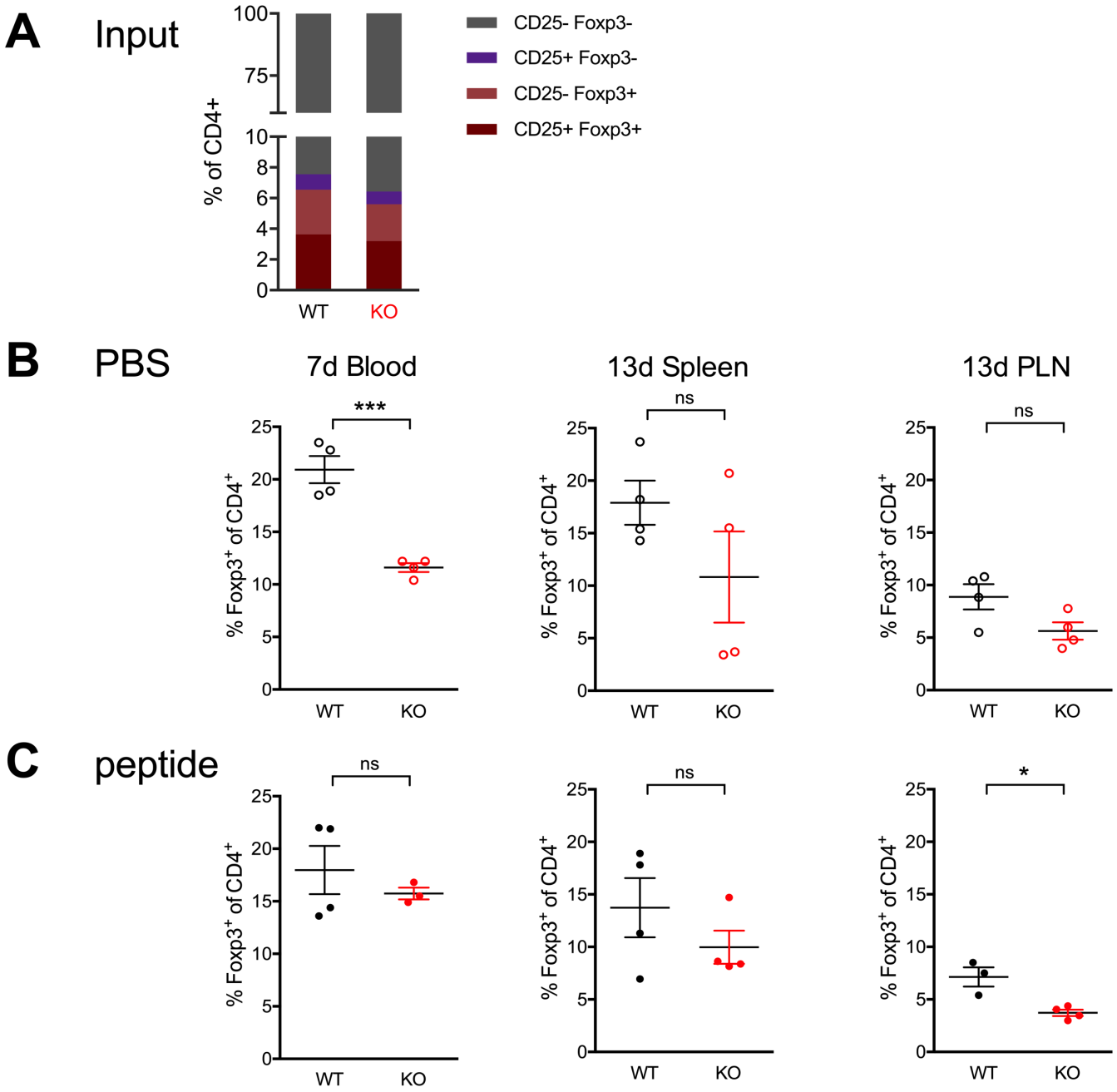

Figure 23: Foxp3 expression in CNS1 WT BDC2.5 tg CD4$^+$ cells vs. CNS1 KO BDC2.5 tg CD4$^+$ cells in lymphopenic NOD SCID recipients and additional mimetope stimulation

CD4$^+$ donor cells were isolated from CNS1 WT BDC2.5 tg or CNS1 KO BDC2.5 tg NOD mice and enriched for CD4$^+$CD25$^-$ T cells by magnetic purification. Purified cells were transferred into SCID mice. Foxp3 expression in transferred CD4$^+$ cells was measured by flow cytometry. Samples from blood, spleen and PLN were taken at indicated time points. Tregs were identified as being CD4$^+$Foxp3$^+$ cells. All samples were gated on transferred live CD4$^+$CD8$^-$ lymphocytes. The full gating strategy is reported in Material and Methods.
A) FACS analysis of transferred cells from either pooled CNS1 WT BDC2.5 tg or CNS1 KO BDC2.5 tg donor cells are shown. Columns show the expression of Foxp3 and CD25 after magnetic purification.
B) Blood and solid organ samples were taken from recipients that were either transferred with CNS1 WT BDC2.5 tg (black circles) or CNS1 KO BDC2.5 tg CD4$^+$ donor cells (red circles) and received intravenous control injections one day after transfer. Cell frequencies (mean ± SEM) for percentage of Foxp3$^+$ cells among CD4$^+$ cells at indicated time points are shown.
C) Blood and solid organ samples were taken from recipients that were either transferred with CNS1 WT BDC2.5 tg (black circles) or CNS1 KO BDC2.5 tg CD4$^+$ donor (red circles) cells and received intravenous peptide injections one day after transfer. Cell frequencies (mean ± SEM) for percentage of Foxp3$^+$ cells among CD4$^+$ cells at indicated time points are shown.
* ($p < 0.05$), ** ($p < 0.01$), *** ($p < 0.001$)

4. Discussion

4.1. Discussion of selected methods

4.1.1. Parenteral application of agonist BDC2.5 mimetope

For this project, we developed a protocol for the *in vivo* induction of $CD4^+Foxp3^+$ T cells in NOD BDC2.5 tg T cells. Previously, Thorstenson and colleagues [138] adoptively transferred DO11.10 TCR tg $CD4^+$ T cells into unirradiated BALB7c mice and applied a single dose of 5 µg OVA peptide intravenously. This limited antigen exposure was sufficient to induce antigen-specific $CD4^+CD25^+$ T cells. Similarly, Daniel and colleagues [142] transferred B:9-23 TCR tg T cells into congenic NOD $Thy1.1^+$ mice and applied agonist peptide daily for 14 days through subcutaneously implanted osmotic minipumps. A minute dose of 5 µg agonist peptide was sufficient to convert naïve $CD4^+$ B:9-23 TCR tg T cells into $CD4^+CD25^+Foxp3^+$ Tregs. With reference to these results, 5 µg agonist BDC2.5 peptide was used to induce Foxp3 expression in this project. Both, single intravenous and prolonged subcutaneous application of 5 µg BDC2.5 mimetope peptide induced $CD4^+Foxp3^+$ Tregs. However, single intravenous injection of peptide was not only more feasible than subcutaneous implantation of osmotic minipumps but also showed stronger induction of $CD4^+Foxp3^+$ Tregs.

4.1.2. Adoptive cell transfer

To evaluate Foxp3 induction in $CD4^+$ T cells only, adoptive transfer experiments were performed. $CD4^+$ cells from NOD BDC2.5 donor mice were isolated by magnetic purification and directly transferred into recipient mice to reduce cell death. Transfer into lymphopenic hosts was performed without labelling donor cells. In FACS analyses, transferred cells were identified as $CD4^+CD8^-$ cells. Transfers into NOD WT recipients however required labelling of donor cells in order to distinguish transferred cells from pre-existing $CD4^+CD8^-$ cells of recipient mice. Donor cells were fluorescently labelled with fixable Cell Proliferation Dye eFluor™ 670, which binds to any cellular protein containing primary amines. As cells divide it is equally distributed between daughter cells.

Similar to other protocols [139, 168], intravenous application of BDC2.5 agonist peptide was performed 24 hours after adoptive transfer of tg donor cells.

4.1.3. Depletion of pre-existing donor $CD4^+Foxp3^+$ Tregs

Some experiments required depletion of pre-existing donor $CD4^+Foxp3^+$ Tregs prior to transfer. However, $CD4^+Foxp3^+$ Tregs could not be directly depleted. This is as for intracellular Foxp3 staining, cells have to be fixed. Thus, expression of surface CD25 had to be used to identify donor Tregs. However, CD25 is an imperfect marker for the identification of Tregs: CD25 is not only highly expressed on Tregs, but also upregulated by activated T cells [70]. It became apparent that additionally to CD25 not being a specific characteristic of Tregs, this surface marker is not necessarily upregulated on all Tregs. To a certain extent, there are $CD25^-$ Tregs with transcriptional signatures and suppressive function similar to what is seen for $CD25^+$ Tregs that can be found in secondary lymphoid organs and other nonlymphoid tissue [71]. However, other Treg markers such as CTLA-4 or GITR (glucocorticoid-induced TNFR-related protein) are not specific for Tregs either [70].

Depletion of $CD4^+CD25^+$ Tregs was achieved by magnetic cell sorting. However, depending on the experiment 4.02 % to 11.69 % of transferred cells remained positive for Foxp3. To increase purity of the transferred cell suspensions, the initially used protocol for magnetic depletion of $CD25^+$ T cells was extended to primary depletion of $CD4^-$ cells. As intended, final cell suspensions contained less $CD4^+Foxp3^+$ T cells. Variable success rates are a well-known issue of magnetic separation kits [169]. More accurate depletion of $Foxp3^+$ T cells potentially could have been achieved by alternative isolation strategies such as FACS sorting of transferred cells. However, FACS sorting entails longer periods during which cells are subjected to suboptimal conditions including physical stress, as sorting requires high-pressure fluidics [170]. Low frequencies of vital purified cells might be the consequence. Although widely used, superiority of FACS sorting compared to magnetic separation thus remains questionable [170, 171]. Yet, as depletion of $CD4^+Foxp3^+$ Tregs prior to transfer was incomplete, it is not fully clear whether increased frequencies of Foxp3 expressing $CD4^+$ T cells upon transfer are due to an expansion of pre-existing donor $Foxp3^+$ Tregs or represent *de novo* differentiation from formerly $CD4^+Foxp3^-$ T cells. Presumably, both effects contributed to the observed increases in $CD4^+Foxp3^+$ Tregs frequencies.

4.1.4. *In vivo* TGF-β blockade

Common *in vivo* models of abrogated TGF-β-signaling rely on transgenic mice expressing a defective version of the TGF-β receptor [140, 163, 172]. Alternatively, *in vivo* blockade by monoclonal antibodies [137, 173] is commonly used. Complementary experiments were

performed by pulsed administration of exogenous TGF-β [174]. Similar to previous publications [175, 176], we performed repetitive intraperitoneal injections of anti-TGF-β (final dose of 600 μg anti-TGF-β) to abrogate TGF-β signaling *in vivo*.

4.1.5. Sample collection

For this study, Foxp3 induction was followed-up in peripheral blood from living animals throughout the entire time of experimental procedures. Additional solid organ samples from spleens, pancreatic and mesenteric lymph nodes were taken once the experimental endpoint was reached and mice were sacrificed.

Adoptive transfer experiments showed that numbers of retrieved labelled cells from solid organs were low. As relative numbers of transferred and labeled cells were low compared to residual cells of recipient mice, partial analysis of isolated organs was insufficient to obtain adequate numbers of transferred cells. As a consequence, in subsequent experiments full organ samples were taken and analyzed by flow cytometry. As absolute numbers of full organ samples were high, $CD4^+$ T cells had to be magnetically enriched prior to flow cytometry.

4.1.6. Flow cytometry

Expression levels of Foxp3 as well as expression of Nrp-1 and Helios were assessed by flow cytometry. Where applicable, transferred cells were positive for Cell Proliferation Dye eFluor™ 670. $CD4^+CD8^-$ cells were gated on CD25 and Foxp3 to identify Tregs. As mentioned above, for this study expression of surface CD25 was mainly used for depletion of donor Tregs prior to the transfer into recipients. In contrast to CD25 with its abovementioned disadvantages for Treg identification, intracellular expression of Foxp3 was found to be a more reliable Treg marker [71-73]. Hence, for this study Tregs were defined as $CD4^+CD8^-Foxp3^+$ cells whenever intracellular staining was possible.

4.1.7. Helios- and Nrp1-expression pattern for discrimination between p- and tTregs

Helios and Nrp-1 were assessed to characterize *in vivo* induced Tregs as both markers are used to discriminate between different Treg subsets [104, 112, 118]. While tTregs are considered $Helios^+$ and $Nrp\text{-}1^+$, pTregs have been shown to lack Helios and Nrp-1expression [104, 112, 118]. As we hypothesized that peptide induced Tregs share characteristics with naturally

occurring pTregs, the population of Helios$^-$ and Nrp-1$^-$ cells within induced Foxp3$^+$ Tregs was assessed. As expected for redundant markers, the fraction of Helios$^-$ of CD4$^+$Foxp3$^+$ T cells and Nrp-1$^-$ of CD4$^+$Foxp3$^+$ T cells was equal between same organ samples mostly. Yet, expression patterns of Helios and Nrp-1 within CD4$^+$Foxp3$^+$ cells were not fully identical in our experiments. Previous reports indeed showed Helios and Nrp-1 expression patterns to be influenced by the experimental protocol and the mouse strain being used [103, 115, 116, 118, 127, 177]. Taken together, Helios and Nrp-1 remain controversial markers for discrimination of p- and tTregs [178]. Yet, due to a lack of better alternative markers Helios and Nrp-1 were utilized for discrimination between p- and tTregs for this project.

4.2. Discussion of results

4.2.1. Dependency of *in vitro* induced CD4$^+$Foxp3$^+$ Tregs on CNS1 and TGF-β

Despite not being identical, *in vitro* generated Tregs share many characteristics of naturally *in vivo* occurring Tregs and thus are widely used to unravel underlaying functional and structural characteristics [103]. *In vitro* Treg differentiation and expansion is used to obtain sufficient numbers of Tregs for *in vivo* studies of Treg-based therapies in both rodents and humans [170]. Over the past decades, various protocols for *in vitro* generation of Tregs have been established [105, 179]. *In vitro* conversion of naïve CD4$^+$ T cells into Foxp3$^+$ Tregs has repeatedly been shown to be dependent on TGF-β [180, 181]. Beyond this, *in vitro* induction of Foxp3$^+$ Tregs in co-culture with co-stimulatory, non-proliferative APC was shown to be CNS1 dependent [110]. Similar studies confirmed CNS1 dependency in cultures without additional co-stimulatory APCs [111].

To validate *in vitro* CNS1 dependency, Foxp3 induction was examined under various conditions. Variations included co-culture of various amounts of co-stimulatory APC, incubation times, as well as different concentrations of anti-CD3 and/ or anti-CD28, IL-2 and additional TGF-β. Cultures lacking additional TGF-β application contained up to 21.30 % Foxp3$^+$ of CD4$^+$ T cells. This might be explained by the proliferation of pre-existing CD4$^+$Foxp3$^+$ T cells in the starting population due to incomplete purity of the initial cell suspension. Thus, observed increases in Treg frequencies may not be solely due to *de novo* differentiation of CD4$^+$Foxp3$^+$ Tregs from formerly naïve CD4$^+$ T cells. In addition, it cannot be ruled out that the culture media being used (RPMI CM with 10 % FBS) already contained sufficient amounts of TGF-β for *in vitro* induction of Foxp3 in naïve CD4$^+$ T cells without additional application of exogenous TGF-β [182]. However, the *in vitro* culture yielded a

notable induction of $CD4^+Foxp3^+$ Tregs. Foxp3 expression was strongly dependent on TGF-β in both, naïve $CD4^+$ T cells from CNS1 WT and CNS1 KO donors. In accordance with previously described findings, upon stimulation, naïve $CD4^+$ T cells from CNS1 KO donor cells clearly lagged behind Foxp3 induction compared to CNS1 WT cells (Figure 11) [111]. To test CNS1 dependency of antigen-specific $CD4^+Foxp3^+$ Tregs further experiments were conducted.

4.2.2. *In vivo* induction of Foxp3 expression by single intravenous application of agonist BDC2.5 peptide

BDC2.5 tg CNS1 WT mice were challenged with a low dose of agonist BDC2.5 mimetope to induce Foxp3 expression *in vivo*. A single injection of the BDC2.5 mimetope yielded a significant increase in $CD4^+Foxp3^+$ Tregs in peripheral blood samples that persevered over the observed time up to 12 days after peptide application. As early as four days after peptide administration the fraction of $CD4^+Foxp3^+$ Tregs in peripheral blood in peptide-treated animals had almost doubled compared to control mice receiving PBS only. Yet, at later time points after peptide injection, Treg levels in peptide-treated animals were decreasing and finally approached Treg levels of PBS-treated control animals. These kinetics are in line with results from Thorstenson and colleagues [138] in adoptive transfers of RAG-2-deficient DO11.10 CD4 T cells into BALB/c mice. Here, Tregs defined as $CD25^+KJ1\text{-}26^+CD4^+$ T cells peaked in spleens between day 3 and day 8 after antigen admission [138]. Reason for this decrease in $CD4^+Foxp3^+$ Tregs shortly after a temporary peak early after peptide administration might be the instability of induced cells or compartment shifts towards secondary lymphatic organs. Solid organ samples were taken once the experimental endpoint was reached 12 days after peptide administration. Indeed, levels of $CD4^+Foxp3^+$ Tregs were found to be increased in spleens of BDC2.5 tg mice after single intravenous peptide administration. However, as mice had to be sacrificed for this purpose and only a limited number of mice was available, the frequency of $CD4^+Foxp3^+$ T cells in solid organ samples was not assessed on its time dependency. This would have required additional experimental groups. Hence, it's not clear whether a compartment shift from blood towards solid organs can fully explain decreasing levels of $CD4^+Foxp3^+$ Tregs in peripheral blood. However, previous results from other groups suggest that this is not the case but are rather due to instability of induced cells [138, 140].

Naturally occurring pTregs are mainly found in the gut, likely due to promotion of Treg induction by residual gut microbiota [106-108]. As we hypothesized in this study that peptide induced Tregs share characteristics with naturally occurring pTregs, gut draining mesenteric

lymph nodes were analyzed for Foxp3 expression upon peptide treatment. Indeed, peptide treated animals showed elevated levels of $CD4^+Foxp3^+$ T cells in mesenteric lymph nodes. However, the relevance of this finding is not fully clear as the peptide was not applied enterally, but parenterally. Increases in $CD4^+Foxp3^+$ Tregs in MLN thus might be due to homing from the primary site of origin to these lymph nodes.

Pancreatic lymph nodes have been found to be the primary site of activation of beta cell-reactive T cells in autoimmune diabetes [183]. Recently, Daniel and colleagues could demonstrate that subimmunogenic administration of agonist peptide did not only significantly elevate levels of $CD4^+Foxp3^+$ Tregs in PLN of TCR tg mice but also protected peptide-treated animals from disease outbreak [142]. To assess the therapeutic potential of intravenous BDC2.5 peptide application, levels of $CD4^+Foxp3^+$ Tregs in PLN upon BDC2.5 mimetope application were analyzed. However, in contrast to what was seen in samples from peripheral blood, spleen and MLN, there was no significant increase $CD4^+Foxp3^+$ Tregs in PLN upon peptide treatment. Diabetes-onset was not awaited in this experimental protocol as mice had to be sacrificed for solid organ analyzes. Yet, it seems unlikely that this transient peak of $CD4^+Foxp3^+$ Tregs in peripheral blood would have a protective effect on active autoimmune processes in the pancreata of mice suffering from diabetes. To test long-term induction of immunosuppressive $CD4^+Foxp3^+$ Tregs, additional experiments with prolonged subcutaneous peptide application were performed (see below).

Helios and Nrp-1 expression were assessed to characterize the peptide-induced Tregs. Single intravenous application of agonist BDC2.5 mimetope did not affect expression levels of Helios and Nrp-1 within $CD4^+Foxp3^+$ Tregs in peripheral blood, spleen and pancreatic lymph nodes. Instead, Helios and Nrp-1 expression levels independently from peptide- or control-treatment were similar to what has been reported for untreated NOD WT mice [158]. Thus, peptide-application did not shift the ratio of $Helios^+$ towards $Helios^-$ $CD4^+Foxp3^+$ Tregs and $Nrp\text{-}1^+$ towards $Nrp\text{-}1^-$ $CD4^+Foxp3^+$ Tregs. Notably, in this setting the interpretation of Helios and Nrp-1 expression was complicated. Here, in contrast to later experiments where naïve $CD4^+$ T cells were adoptively transferred and peptide-stimulated, pre-existing Tregs were not depleted prior to treatment. Thus, it is not clear to which extent Helios and Nrp-1 expression levels reflect expression patterns of expanding pre-existing Tregs or expression levels of *de novo* generated Tregs upon peptide stimulation.

Surprisingly in one experiment, peptide administration led to a moderate, but significant shift towards $Helios^-$ cells within $CD4^+Foxp3^+$ cells in MLN. As this trend was not found in other

organ samples and did not go along with concordantly higher levels of $CD4^+Foxp3^+Nrp\text{-}1^-$ cells in MLNs, the relevance of this isolated finding is uncertain. Repetition of the experiment would be needed for validation.

4.2.3. *In vivo* induction of Foxp3 expression by prolonged subcutaneous application of agonist BDC2.5 peptide

It has been reported that prolonged treatment of TCR restricted animals with low doses of agonist peptide induces Tregs *in vivo*. These Tregs showed long-term stability and functionality [136, 184]. Using this protocol, Daniel et al. were able to show long-term efficacy in the prevention of experimental type I diabetes in NOD mice [142]. Due to these promising results we sought to test this method for Treg induction in our mouse model. Hereto, osmotic pumps that continuously released low doses of antigen were implanted subcutaneously. As expected, similar to what was seen for single intravenous peptide application, prolonged peptide administration induced Foxp3 expression in $CD4^+$ T cells. Unlike to what was seen after single peptide application, where levels of $CD4^+Foxp3^+$ T cells peaked at day 4 after peptide injection, in peripheral blood prolonged peptide-administration resulted in Foxp3 induction at later time points. The most significant increase was seen in peripheral blood at day 8 after pump implantation. As opposed to the kinetics after single peptide application, levels of $CD4^+Foxp3^+$ T cells in peptide-treated animals did not decrease over the observed time course. Instead, there was a significant increase of $CD4^+Foxp3^+$ T cells in peptide-treated animals between day 3 and day 8 in peripheral blood. This level of $CD4^+Foxp3^+$ T cells was maintained until mice were sacrificed 14 days after pump implantation. Thus, prolonged antigen application through osmotic minipumps allowed for elevated levels of $CD4^+Foxp3^+$ T cells for longer periods than what was seen after single peptide administration. Although induction of $CD4^+Foxp3^+$ T cells upon prolonged antigen application takes longer and is more complex than single peptide application, this method thus might be suitable for a more preserved induction of $CD4^+Foxp3^+$ T cells.

Unlike what was seen in blood, in spleens there was no significant induction of $CD4^+Foxp3^+$ T cells 14 days after pump implantation. Although there was a trend towards elevated levels of $Foxp3^+$ cells among $CD4^+$ T cells in peptide-treated animals compared to PBS controls, this effect was not significant ($p = 0.0512$). As there was a great variability of $CD4^+Foxp3^+$ T cells between tested animals, repetition of the experiment would be needed to evaluate the relevance of this finding.

Daniel and colleagues were able to induce long-term suppression of autoimmunity upon prolonged antigen application [142] suggesting a relevant survival of induced $CD4^+Foxp3^+$ Tregs. As for this project, mice were sacrificed 14 days after pump implantation it is not clear how the level of $CD4^+Foxp3^+$ T cells develops once the peptide application is discontinued. It remains unclear whether the observed changes in Foxp3 expression would be sufficient to prevent diabetes. Future research is needed to address this question.

Beyond that, Nrp-1 and Helios expression were assessed simultaneously to test whether prolonged *in vivo* peptide-stimulation had any impact on how these markers are distributed in peptide-induced $CD4^+Foxp3^+$ Tregs. As expected, similar to what was seen after single intravenous peptide admission, Helios and Nrp-1 expression levels were not significantly altered in peptide treated animals versus controls (see above). There was a significantly higher fraction of $Helios^-CD4^+Foxp3^+$ cells compared to $Nrp1^-CD4^+Foxp3^+$ in both, control and peptide-treated animals. As mentioned above, incomplete concordance of these redundant Treg markers is well known [103, 118]. However, as there was a great difference between expression levels of Helios and Nrp-1 in this experiment, additional factors such as methodological influences and inadequate staining results should be taken into account and may have biased these results. Replications of this experiment are be needed to identify potential confounding variables.

4.2.4. *In vivo* induction of Foxp3 expression in adoptively transferred BDC2.5 tg $CD4^+$ donor cells by single intravenous application of agonist BDC2.5 peptide

To evaluate Foxp3 induction in $CD4^+$ T cells only, additional adoptive transfer experiments were performed. $CD4^+$ cells from NOD BDC2.5 tg donor mice were isolated and fluorescently labeled followed by direct transfer into NOD recipient mice. Intravenous application of BDC2.5 peptide was performed 24 hours after transfer. One week after peptide application, spleens were taken and analyzed for induction of $CD4^+Foxp3^+$ Tregs. In accordance with what has been described previously [138], there was a dramatic increase of $CD4^+Foxp3^+$ Tregs in peptide-treated animals. By contrast, control mice that received PBS did not show increased levels of $CD4^+Foxp3^+$ Tregs. It was not clear whether the observed increases in $CD4^+Foxp3^+$ Tregs were due to formerly $CD4^+Foxp3^-$ cells that converted into $CD4^+Foxp3^+$ cells or whether pre-existing $CD4^+Foxp3^+$ cells expanded upon peptide application. To address this question, in subsequent experiments $CD4^+CD25^+$ Tregs were depleted prior to transfer (see below).

Similar to what was described above, Helios and Nrp-1 expression levels were assessed to characterize induced $CD4^+Foxp3^+$ T cells. Recipients that received peptide stimulation showed higher levels of $Helios^-CD4^+Foxp3^+$ T cells compared to controls that did not undergo peptide treatment. Yet, the fraction of $Nrp\text{-}1^-CD4^+Foxp3^+$ remained unchanged. This was surprising as Helios and Nrp-1 as redundant markers for pTregs were expected to equally respond to peptide stimulation [104, 112, 118]. Additionally, in the previously mentioned experiments Helios and Nrp-1 expression levels did not change upon peptide stimulation whenever appropriate cell counts could be analyzed. Taken together, this unilateral increase of $Helios^-CD4^+Foxp3^+$ Tregs remains to be questioned and might be due to low absolute numbers of analyzed $CD4^+Foxp3^+$ cells (mean control group: 35 / mean peptide treated group: 32). Repetition of the experiment including the analysis of full organ samples would be required to gain a valid impression of the properties of Helios and Nrp-1 expression patterns in Tregs that were induced upon peptide stimulation and adoptive transfer.

4.2.5. Impaired *in vivo* Foxp3 induction in CNS1 KO $CD4^+$ BDC2.5 tg cells

CNS1 deficient NOD mice were described previously by Schuster and colleagues [158]. CNS1 KO mice showed impaired *in vivo* generation of pTregs whereas tTregs as well as overall Treg frequencies remained stable [158]. In contrast, in this study we tested the *in vivo* induction of Foxp3 upon tolerogenic stimulation with an agonist peptide. For this purpose, NOD CNS1 WT and NOD CNS1 KO mice were mated with BDC2.5 tg NOD mice. $CD4^+$ T cells from adult CNS1 WT BDC2.5 tg NOD and CNS1 KO BDC2.5 tg NOD offspring were isolated, magnetically depleted for $CD25^+$ T cells, fluorescently labeled and transferred into CNS1 WT NOD recipients. One day after transfer, recipients were treated with BDC2.5 peptide or PBS as a control. Analyses of full spleen samples one week after cell transfer revealed significant increases in Foxp3 expression in both, CNS1 WT BDC2.5 tg and CNS1 KO BDC2.5 tg donor cells when treated with agonist BDC2.5 peptide. However, CNS1 deficient BDC2.5 tg donor cells showed significantly impaired induction of Foxp3 expression upon peptide treatment compared to what was observed for CNS1 WT BDC2.5 tg donor cells. Thus, the *in vivo* formation of peptide induced $Foxp3^+$ Tregs is dependent on CNS1 akin to what was described previously for naturally occurring pTregs [110, 111, 158]. Formation of *in vivo* induced Tregs upon peptide stimulation might follow molecular pathways similar to what holds true for naturally occurring pTregs.

Notably, neither in this study nor in similar experiments by others, CNS1 deficiency fully abrogated induction of Foxp3$^+$ Tregs [110, 111, 158]. One explanation for this observation might be an insufficient knock-out of the CNS1 gene. In this case, residual CNS1 expression could induce Foxp3 expression upon peptide application in some CD4$^+$ T cells. However, CNS1 KO mice that were used in this study were no offspring of the originally published C57BL/6 CNS1 KO from Zheng et al. [110], but generated and published by Schuster et al. [158]. Thus, it seems rather unlikely that a technically insufficient CNS1 KO can solely explain residual Foxp3 expression. Instead, CNS1 might indeed be critical, but not on its own decisive for the adequate formation of Foxp3$^+$ pTregs.

4.2.6. Impaired *in vivo* Foxp3 induction in CNS1 WT CD4$^+$ BDC2.5 tg cells under TGF-β-blockade

TGF-β signaling is involved in ensuring tolerance towards self-antigens. Mice lacking functional TGF-β signaling succumb to severe autoimmunity similar to what is seen in mice devoid of Foxp3 [185]. In particular, TGF-β has been shown to facilitate induction of Foxp3 expression in pTregs [105, 140, 163, 164]. In contrast, TGF-β-signaling seems to play a minor role for the upregulation of Foxp3 expression in tTregs [163, 165]. It has been suggested that TGF-β signaling has diverse effects on Tregs including improved survival and stability of Foxp3 expression [186]. *In vitro* studies on model cell lines expressing Foxp3 only when stimulated, showed Foxp3 induction to be dependent on Smad3 and NFAT. The authors suggested that induction of Foxp3 (which itself does not contain a TGF-β binding site) is mediated by TGF-β signaling through synergy of Smad3 and NFAT binding to a Foxp3 enhancer element [187]. The CNS1 enhancer in the Foxp3 promotor contains a binding site for Smad3 downstream of TGF-β signaling [109, 111, 188] providing a direct link between pTreg formation and TGF-β-signaling. Thus, binding of Smad3 to CNS1 together with NFAT might serve as an indirect mechanism to promote Foxp3 expression in peripheral Tregs by TGF-β [186]. Accordingly, subsequent studies performed on mice with perturbed binding of Smad3 to CNS1 confirmed impaired Treg generation in the gut whereas overall Treg development remained unaffected [189]. These findings raised the question as to whether CNS1 deficiency in our model of Foxp3 induction upon tolerogenic peptide stimulation leads to impaired Foxp3 expression due to abrogated TGF-β signaling. To test this hypothesis, CNS1 WT BDC2.5 tg NOD CD4$^+$CD25$^-$ T cells were isolated and adoptively transferred into NOD recipients

followed by BDC2.5 peptide stimulation plus additional blocking of TGF-β. Mice treated with blocking monoclonal antibodies indeed showed no increase in $CD4^+Foxp3^+$ within transferred donor cells compared to PBS treated controls as well as a significantly reduced Foxp3 induction compared to mice that were treated with stimulating peptide only. Hence, these results are in line with the hypothesis that CNS1 deficiency inhibits Foxp3 expression upon peptide stimulation due to perturbed TGF-β signaling. However, to prove this hypothesis as well as to quantify the importance of TGF-β for CNS1 signaling, further experiments using blocking monoclonal antibodies on peptide treated CNS1 deficient mice are necessary and should be subject of future investigations. Here, Foxp3 induction upon peptide administration would be expected to be similarly perturbed in both $CD4^+$ T cells from CNS1 WT donors treated with peptide + anti-TGF-β and $CD4^+$ T cells from CNS1 KO donors treated with peptide only. Moreover, additional TGF-β-blockade should not further inhibit Foxp3 induction in CNS1 KO $CD4^+$ T cells upon peptide stimulation.

4.2.7. Foxp3 expression in adoptively transferred CNS1 WT NOD $CD4^+$ vs. CNS1 KO NOD $CD4^+$ cells in lymphopenic NOD SCID recipients

It is well known that $CD4^+Foxp3^+$ Tregs proliferate *in vivo* under the influence of cytokine signaling and MHC-interactions when transferred into lymphopenic recipients [132]. Here, this model was employed to test the *in vivo* induction of Foxp3 in CNS1 deficient naïve T cells. CNS1 WT NOD $CD4^+CD25^-$ T cells and CNS1 KO NOD $CD4^+CD25^-$ T cells were magnetically purified and subsequently transferred into lymphopenic SCID recipients. As discussed above, depending on the protocol used for magnetic isolation, variable purity levels could be obtained. As expected, cell transfer into lymphopenic recipients led to a massive proliferation of $CD4^+Foxp3^+$ Tregs. CNS1 deficient donor cells showed significantly impaired proliferation of $CD4^+Foxp3^+$ T cells compared to CNS1 WT donor cells. However, this effect was only seen as early as seven days after transfer. At later time points, differences between CNS1 WT and CNS1 KO donor cells in Foxp3 expression were considerably reduced or not detectable anymore. However, this is in line with what has been reported previously by Josefowicz and colleagues [111] who could demonstrate impaired *in vivo* Treg generation in a comparable experimental setting: Josefowicz and colleagues transferred OVA-specific $OT\text{-}II^+$TCR-tg $Foxp3^-$ CNS1 KO or WT cells into lymphopenic recipients that were subsequently exposed to ad libitum administration for OVA in drinking water for six days. After this duration of antigen exposure, the authors were able to show a significantly impaired Foxp3 induction in

CNS1 KO cells in various organs, predominantly in spleens, Peyer's patches and lymph nodes, small and large intestine lamina propria. However, the stability of *in vivo* induced Tregs over longer time periods was not investigated in this setting [111]. In contrast, Zheng and colleagues [110] reported continuous impairment for *in vivo* Foxp3 induction in CNS1 deficient $CD4^+$ T cells: CNS1-deficient and CNS1-sufficient congenically labelled $CD4^+Foxp3^-$ naïve T cells were co-transferred into lymphopenic recipients and *in vivo* Foxp3 induction in transferred cells was assessed after 10 weeks. Impaired induction of Fox3 expression was found in Peyer's patches, intraepithelial lymphocytes and lamina propria lymphocytes but not in spleens. Notably, percentages of $Foxp3^+$ cells within $CD4^+$ T cells generally were very low in this setting (less than 1 % $Foxp3^+$ of $CD4^+$). Thus, long-term stability of *in vivo* induced Foxp3 expression upon transfer into lymphopenic recipients remains questionable.

As in this study, no persistent difference in levels of potentially protective $CD4^+Foxp3^+$ Tregs was found, also no difference in transfer-induced diabetes between CNS1 WT and KO groups was detected.

4.2.8. Foxp3 expression in adoptively transferred CNS1 WT NOD $CD4^+$ vs. CNS1 KO NOD $CD4^+$ cells in lymphopenic NOD SCID recipients under additional peptide stimulation

To test peptide-driven induction of $CD4^+Foxp3^+$ Tregs in this setting of homeostatic proliferation, additional groups of lymphopenic SCID recipients received either CNS1 WT BDC2.5 tg or CNS1 KO BDC2.5 tg donor cells followed by BDC2.5 peptide treatment. However, peptide stimulation did not yield higher frequencies of $CD4^+Foxp3^+$ Tregs compared to control animals receiving PBS as a control. Only blood samples taken from CNS1 KO BDC2.5 tg T cell recipients seven days after transfer showed a mild increase in Foxp3 expression upon peptide treatment compared to PBS treated CNS1 KO BDC2.5 tg controls. It remains unclear why peptide treatment inconsistently boosted Foxp3 expression in this setting. Potentially, the drastic stimulation of Foxp3 expression upon this massive expansion pressure biased the peptide stimulation of naïve $CD4^+$ CNS1 KO or WT T cells.

Interestingly, PLN from mice receiving CNS1 KO BDC2.5 tg donor cells followed by BDC2.5 peptide stimulation showed lower levels of $CD4^+Foxp3^+$ cells compared to control animals that received CNS1 WT BDC2.5 tg donor cells prior to BDC2.5 peptide stimulation. However, in contrast to what was seen for samples from blood and spleen, expression levels of Foxp3 within $CD4^+$ T cells in PLN were similar or even below levels of $CD4^+Foxp3^+$ Tregs of the initially

transferred cell suspensions. Thus, no relevant expansion of $CD4^+Foxp3^+$ Tregs upon transfer and peptide-treatment took place in PLNs. The observed differences between $CD4^+Foxp3^+$ Tregs levels in CNS1 WT and CNS1KOs thus might rather be due to the difference in the level of transferred pre-existing Tregs than due to any effects mediated by transfer, peptide-treatment or CNS1 deficiency.

4.3. Future directions

$CD4^+Foxp3^+$ Tregs are an attractive candidate for drug development due to their capability to circulate through the organism and to perform antigen-specific immunosuppression [190, 191]. Current clinical approaches mainly focus on adoptive transfer of freshly isolated [96, 192, 193] or *ex vivo* expanded immunosuppressive cells [97, 99, 100, 194-198]. Alternative protocols include for instance the therapeutic administration of low-dose Il-2 for in situ Treg induction [56-58].

Here, we have shown that the *in vivo* generation of antigen-specific $CD4^+Foxp3^+$ Tregs is dependent on CNS1. These results, indicating that *in vivo* induced Tregs share mechanistic characteristics with naturally occurring pTregs, lead to further questions: These include whether peptide-induced Tregs also share similar functional characteristics with their naturally occurring counterparts. Further work should explore the *in vivo* effects of these peptide-induced Tregs and their potential for clinical usage complementing current approaches for Treg based therapies. Additional questions regarding how and where exactly in the periphery peptide-induced $CD4^+Foxp3^+$ Tregs develop *in vivo* and which factors contribute to their long-term stability and function remain to be answered. Further evaluation of Treg biology will be fundamental for the targeted development of new clinical strategies. Evaluation of the biological relevance of *in vivo* induced antigen-specific Tregs may be done in experimental models of autoimmunity such as the NOD mice as a model of spontaneous autoimmune diabetes.

5. Summary

$CD4^+Foxp3^+$ Tregs can be induced *in vitro* by TGF-β stimulation. Here, CNS1 deficient $CD4^+$ T cells were found to show compromised Foxp3 upregulation *in vitro* compared to CNS1 WT $CD4^+$ T cells. Moreover, we could demonstrate that antigen-specific $CD4^+Foxp3^+$ Tregs can be induced *in vivo* by tolerogenic antigen stimulation. Parenteral application of agonist BDC2.5 mimetope induced Foxp3 expression in $CD4^+$ BDC2.5 tg cells. We could show that induction of Foxp3 expression by tolerogenic peptide stimulation is impaired in CNS1 deficient $CD4^+$ BDC2.5 tg cells compared to CNS1 WT $CD4^+$ BDC2.5 tg controls. These results indeed indicate that *in vivo* induced Tregs share mechanistic characteristics with naturally occurring pTregs.

Additional *in vivo* experiments with blocking monoclonal anti-TGF-β demonstrated that high dosage TGF-β blockade abrogated peptide-induced Foxp3 expression in CNS1 WT BDC2.5 tg $CD4^+$ cells, akin to what is seen for impaired Foxp3 upregulation in peptide-stimulated CNS1 KO BDC2.5 tg $CD4^+$ cells without anti-TGF-β-treatment.

Adoptive transfer of $CD4^+CD25^-$ T cells in T cell deficient recipients dramatically increased $CD4^+Foxp3^+$ Treg frequencies in both CNS1 WT $CD4^+$ and CNS1 KO $CD4^+$ donor cells. Despite an initially lower increase in Foxp3 expression in CNS1 KO donor cells compared to CNS1 WT donor cells early after transfer, in this setting impaired Treg induction in CNS1 deficient cells was not preserved over time. Consequently, diabetes onset and progression were indistinguishable between mice that received CNS1 WT or CNS1 KO donor cells. Additional Foxp3 induction by peptide stimulation of immunodeficient recipients after transfer of CNS1 WT BDC2.5. tg or CNS1 KO BDC2.5 tg donor cells was not detectable.

6. Zusammenfassung

$CD4^+Foxp3^+$ Tregs können *in vitro* mittels TGF-β-Stimulation induziert werden. Im Rahmen dieses Projekts konnte bestätigt werden, dass CNS1-defiziente $CD4^+$ T-Zellen im Vergleich zu $CD4^+$ CNS1 WT-Zellen *in vitro* eine eingeschränkte Foxp3-Hochregulation zeigen. Des Weiteren konnten wir Antigen-spezifische $CD4^+Foxp3^+$ Tregs mittels tolerogener Antigenstimulation *in vivo* induzieren. Parenteral appliziertes BDC2.5-Mimetop induzierte die Foxp3 Expression in $CD4^+$ BDC2.5 transgenen T-Zellen. Hierbei zeigten CNS1 KO BDC2.5 transgene $CD4^+$ T-Zellen im Vergleich zu CNS1 WT BDC2.5 transgenen $CD4^+$ T-Zell-Kontrollen eine eingeschränkte Hochregulation der Foxp3 Expression nach Mimetop-Stimulation. Peptid-induzierte $CD4^+Foxp3^+$ Tregs verhalten sich somit ähnlich wie natürlich vorkommende pTregs.

Unter Verwendung höherer Dosen von anti-TGF-β zeigte sich bei Mimetop-Stimulation im *in vivo* Experiment eine eingeschränkte Foxp3-Hochregulation der CNS1 WT $CD4^+$ BDC2.5 transgenen T-Zellen, ähnlich wie es bei CNS1 KO $CD4^+$ BDC2.5 transgenen T-Zellen ohne anti-TGF-β-Behandlung zu beobachten war.

Ein adoptiver Zelltransfer von $CD4^+CD25^-$ T-Zellen in immundefiziente Empfänger-Mäuse ohne funktionsfähige T- und B-Zellen führte zu einem deutlichen Anstieg von $CD4^+Foxp3^+$ Tregs. Hierbei zeigte sich nur kurz nach dem Zelltransfer ein signifikant geringerer Anstieg der induzierten CNS1 KO $CD4^+Foxp3^+$ T-Zellen gegenüber den CNS1 WT $CD4^+Foxp3^+$ T-Zellen. Langfristig blieb dieser Unterschied jedoch nicht erhalten. Entsprechend konnte kein Unterschied bezüglich des Diabetes-Beginns bzw. -Progression zwischen CNS1 WT- und CNS1 KO-Mäusen festgestellt werden. Eine zusätzliche Foxp3-Induktion durch Peptid-Stimulation nach Transfer von CNS1 WT BDC2.5 transgenen bzw. CNS1 KO BDC2.5 transgenen Spender-Zellen in immundefiziente Empfänger-Mäuse war nicht nachweisbar.

7. Bibliography

1. Atkinson, M.A., G.S. Eisenbarth, and A.W. Michels, *Type 1 diabetes.* The Lancet, 2014. **383**(9911): p. 69-82.
2. Parkin, J. and B. Cohen, *An overview of the immune system.* Lancet, 2001. **357**(9270): p. 1777-89.
3. Plitas, G. and A.Y. Rudensky, *Regulatory T Cells: Differentiation and Function.* Cancer Immunol Res, 2016. **4**(9): p. 721-5.
4. Josefowicz, S.Z., L.F. Lu, and A.Y. Rudensky, *Regulatory T cells: mechanisms of differentiation and function.* Annu Rev Immunol, 2012. **30**: p. 531-64.
5. Janeway, C.A., Jr., Travers, P., Walport, M., Shlomchik, M. J., *The front line of host defense*, in *Immunobiology: The Immune System in Health and Disease. 5th edition.* 2001, Garland Science: New York.
6. Delves, P.J. and I.M. Roitt, *The immune system. Second of two parts.* N Engl J Med, 2000. **343**(2): p. 108-17.
7. Delves, P.J. and I.M. Roitt, *The immune system. First of two parts.* N Engl J Med, 2000. **343**(1): p. 37-49.
8. Arstila, T.P., et al., *A direct estimate of the human alphabeta T cell receptor diversity.* Science, 1999. **286**(5441): p. 958-61.
9. Goodnow, C.C., et al., *Cellular and genetic mechanisms of self tolerance and autoimmunity.* Nature, 2005. **435**(7042): p. 590-7.
10. Klein, L., et al., *Positive and negative selection of the T cell repertoire: what thymocytes see (and don't see).* Nat Rev Immunol, 2014. **14**(6): p. 377-91.
11. O'Garra, A. and P. Vieira, *Regulatory T cells and mechanisms of immune system control.* Nat Med, 2004. **10**(8): p. 801-5.
12. Sakaguchi, S., et al., *Immunologic tolerance maintained by CD25+ CD4+ regulatory T cells: their common role in controlling autoimmunity, tumor immunity, and transplantation tolerance.* Immunol Rev, 2001. **182**: p. 18-32.
13. Zhang, Q. and D.A. Vignali, *Co-stimulatory and Co-inhibitory Pathways in Autoimmunity.* Immunity, 2016. **44**(5): p. 1034-51.
14. Sakaguchi, S., et al., *Regulatory T cells and immune tolerance.* Cell, 2008. **133**(5): p. 775-87.
15. Cooper, G.S., M.L. Bynum, and E.C. Somers, *Recent insights in the epidemiology of autoimmune diseases: improved prevalence estimates and understanding of clustering of diseases.* J Autoimmun, 2009. **33**(3-4): p. 197-207.
16. Jacobson, D.L., et al., *Epidemiology and estimated population burden of selected autoimmune diseases in the United States.* Clin Immunol Immunopathol, 1997. **84**(3): p. 223-43.
17. Eisenbarth, G.S., *Type I diabetes mellitus. A chronic autoimmune disease.* N Engl J Med, 1986. **314**(21): p. 1360-8.
18. Stadinski, B., J. Kappler, and G.S. Eisenbarth, *Molecular targeting of islet autoantigens.* Immunity, 2010. **32**(4): p. 446-56.
19. Dabelea, D., *The accelerating epidemic of childhood diabetes.* Lancet, 2009. **373**(9680): p. 1999-2000.
20. Farag, Y.M. and M.R. Gaballa, *Diabesity: an overview of a rising epidemic.* Nephrol Dial Transplant, 2011. **26**(1): p. 28-35.
21. Santamaria, P., *The long and winding road to understanding and conquering type 1 diabetes.* Immunity, 2010. **32**(4): p. 437-45.
22. Herold, K.C., et al., *Type 1 diabetes: translating mechanistic observations into effective clinical outcomes.* Nat Rev Immunol, 2013. **13**(4): p. 243-56.

23. Herold, G., *Diabetes Mellitus*, in *Innere Medizin*. 2016.
24. Orchard, T.J., et al., *Type 1 diabetes and coronary artery disease.* Diabetes Care, 2006. **29**(11): p. 2528-38.
25. Maser, R.E., et al., *Cardiovascular disease and arterial calcification in insulin-dependent diabetes mellitus: interrelations and risk factor profiles. Pittsburgh Epidemiology of Diabetes Complications Study-V.* Arterioscler Thromb, 1991. **11**(4): p. 958-65.
26. Nathan, D.M., et al., *Intensive diabetes treatment and cardiovascular disease in patients with type 1 diabetes.* N Engl J Med, 2005. **353**(25): p. 2643-53.
27. American Diabetes, A., *(2) Classification and diagnosis of diabetes.* Diabetes Care, 2015. **38 Suppl**: p. S8-S16.
28. Foulis, A.K. and J.A. Stewart, *The pancreas in recent-onset type 1 (insulin-dependent) diabetes mellitus: insulin content of islets, insulitis and associated changes in the exocrine acinar tissue.* Diabetologia, 1984. **26**(6): p. 456-61.
29. Willcox, A., et al., *Analysis of islet inflammation in human type 1 diabetes.* Clin Exp Immunol, 2009. **155**(2): p. 173-81.
30. Ziegler, A.G. and G.T. Nepom, *Prediction and pathogenesis in type 1 diabetes.* Immunity, 2010. **32**(4): p. 468-78.
31. Ziegler, A.G., E. Bonifacio, and B.-B.S. Group, *Age-related islet autoantibody incidence in offspring of patients with type 1 diabetes.* Diabetologia, 2012. **55**(7): p. 1937-43.
32. Lieberman, S.M. and T.P. DiLorenzo, *A comprehensive guide to antibody and T-cell responses in type 1 diabetes.* Tissue Antigens, 2003. **62**(5): p. 359-77.
33. Concannon, P., S.S. Rich, and G.T. Nepom, *Genetics of type 1A diabetes.* N Engl J Med, 2009. **360**(16): p. 1646-54.
34. Cooper, J.D., et al., *Inherited variation in vitamin D genes is associated with predisposition to autoimmune disease type 1 diabetes.* Diabetes, 2011. **60**(5): p. 1624-31.
35. Knip, M., S.M. Virtanen, and H.K. Akerblom, *Infant feeding and the risk of type 1 diabetes.* Am J Clin Nutr, 2010. **91**(5): p. 1506S-1513S.
36. Blanton, D., et al., *Reduced serum vitamin D-binding protein levels are associated with type 1 diabetes.* Diabetes, 2011. **60**(10): p. 2566-70.
37. Rosenblum, M.D., et al., *Treating human autoimmunity: current practice and future prospects.* Sci Transl Med, 2012. **4**(125): p. 125sr1.
38. Serra, P. and P. Santamaria, *Antigen-specific therapeutic approaches for autoimmunity.* Nat Biotechnol, 2019. **37**(3): p. 238-251.
39. Kroger, C.J., et al., *Therapies to Suppress beta Cell Autoimmunity in Type 1 Diabetes.* Front Immunol, 2018. **9**: p. 1891.
40. Simmons, K.M. and A.W. Michels, *Type 1 diabetes: A predictable disease.* World J Diabetes, 2015. **6**(3): p. 380-90.
41. Herold, K.C., et al., *Anti-CD3 monoclonal antibody in new-onset type 1 diabetes mellitus.* N Engl J Med, 2002. **346**(22): p. 1692-8.
42. Daifotis, A.G., et al., *Anti-CD3 clinical trials in type 1 diabetes mellitus.* Clin Immunol, 2013. **149**(3): p. 268-78.
43. Pescovitz, M.D., et al., *Rituximab, B-lymphocyte depletion, and preservation of beta-cell function.* N Engl J Med, 2009. **361**(22): p. 2143-52.
44. Orban, T., et al., *Co-stimulation modulation with abatacept in patients with recent-onset type 1 diabetes: a randomised, double-blind, placebo-controlled trial.* Lancet, 2011. **378**(9789): p. 412-9.

45. Orban, T., et al., *Costimulation modulation with abatacept in patients with recent-onset type 1 diabetes: follow-up 1 year after cessation of treatment.* Diabetes Care, 2014. **37**(4): p. 1069-75.
46. Mastrandrea, L., et al., *Etanercept treatment in children with new-onset type 1 diabetes: pilot randomized, placebo-controlled, double-blind study.* Diabetes Care, 2009. **32**(7): p. 1244-9.
47. McGuire, H.M., et al., *Interleukin-21 is critically required in autoimmune and allogeneic responses to islet tissue in murine models.* Diabetes, 2011. **60**(3): p. 867-75.
48. Murri, M., et al., *Gut microbiota in children with type 1 diabetes differs from that in healthy children: a case-control study.* BMC Med, 2013. **11**: p. 46.
49. Tai, N., F.S. Wong, and L. Wen, *The role of gut microbiota in the development of type 1, type 2 diabetes mellitus and obesity.* Rev Endocr Metab Disord, 2015. **16**(1): p. 55-65.
50. de Goffau, M.C., et al., *Fecal microbiota composition differs between children with beta-cell autoimmunity and those without.* Diabetes, 2013. **62**(4): p. 1238-44.
51. Kostic, A.D., et al., *The dynamics of the human infant gut microbiome in development and in progression toward type 1 diabetes.* Cell Host Microbe, 2015. **17**(2): p. 260-73.
52. Endesfelder, D., et al., *Compromised gut microbiota networks in children with anti-islet cell autoimmunity.* Diabetes, 2014. **63**(6): p. 2006-14.
53. Giongo, A., et al., *Toward defining the autoimmune microbiome for type 1 diabetes.* ISME J, 2011. **5**(1): p. 82-91.
54. Marino, E., et al., *Gut microbial metabolites limit the frequency of autoimmune T cells and protect against type 1 diabetes.* Nat Immunol, 2017. **18**(5): p. 552-562.
55. Trzonkowski, P., et al., *Hurdles in therapy with regulatory T cells.* Sci Transl Med, 2015. **7**(304): p. 304ps18.
56. Todd, J.A., et al., *Regulatory T Cell Responses in Participants with Type 1 Diabetes after a Single Dose of Interleukin-2: A Non-Randomised, Open Label, Adaptive Dose-Finding Trial.* PLoS Med, 2016. **13**(10): p. e1002139.
57. Hartemann, A., et al., *Low-dose interleukin 2 in patients with type 1 diabetes: a phase 1/2 randomised, double-blind, placebo-controlled trial.* Lancet Diabetes Endocrinol, 2013. **1**(4): p. 295-305.
58. Rosenzwajg, M., et al., *Low-dose interleukin-2 fosters a dose-dependent regulatory T cell tuned milieu in T1D patients.* J Autoimmun, 2015. **58**: p. 48-58.
59. Smith, E.L. and M. Peakman, *Peptide Immunotherapy for Type 1 Diabetes-Clinical Advances.* Front Immunol, 2018. **9**: p. 392.
60. McIntire, K.R., S. Sell, and J.F. Miller, *Pathogenesis of the Post-Neonatal Thymectomy Wasting Syndrome.* Nature, 1964. **204**: p. 151-5.
61. Nishizuka, Y. and T. Sakakura, *Thymus and reproduction: sex-linked dysgenesia of the gonad after neonatal thymectomy in mice.* Science, 1969. **166**(3906): p. 753-5.
62. Gershon, R.K. and K. Kondo, *Cell interactions in the induction of tolerance: the role of thymic lymphocytes.* Immunology, 1970. **18**(5): p. 723-37.
63. Gershon, R.K. and K. Kondo, *Infectious immunological tolerance.* Immunology, 1971. **21**(6): p. 903-14.
64. Kerbel, R.S. and D. Eidinger, *Enhanced immune responsiveness to a thymus-independent antigen early after adult thymectomy: evidence for short-lived inhibitory thymus-derived cells.* Eur J Immunol, 1972. **2**(2): p. 114-8.
65. Sakaguchi, S., et al., *Immunologic self-tolerance maintained by activated T cells expressing IL-2 receptor alpha-chains (CD25). Breakdown of a single mechanism of self-tolerance causes various autoimmune diseases.* J Immunol, 1995. **155**(3): p. 1151-64.

66. Sakaguchi, S. and N. Sakaguchi, *Regulatory T cells in immunologic self-tolerance and autoimmune disease.* Int Rev Immunol, 2005. **24**(3-4): p. 211-26.
67. Gavin, M. and A. Rudensky, *Control of immune homeostasis by naturally arising regulatory CD4+ T cells.* Curr Opin Immunol, 2003. **15**(6): p. 690-6.
68. Shevach, E.M., *Regulatory T cells in autoimmmunity*.* Annu Rev Immunol, 2000. **18**: p. 423-49.
69. Bluestone, J.A., *FOXP3, the Transcription Factor at the Heart of the Rebirth of Immune Tolerance.* J Immunol, 2017. **198**(3): p. 979-980.
70. Fontenot, J.D., et al., *Regulatory T cell lineage specification by the forkhead transcription factor foxp3.* Immunity, 2005. **22**(3): p. 329-41.
71. Fontenot, J.D., M.A. Gavin, and A.Y. Rudensky, *Foxp3 programs the development and function of CD4+CD25+ regulatory T cells.* Nat Immunol, 2003. **4**(4): p. 330-6.
72. Hori, S., T. Nomura, and S. Sakaguchi, *Control of regulatory T cell development by the transcription factor Foxp3.* Science, 2003. **299**(5609): p. 1057-61.
73. Khattri, R., et al., *An essential role for Scurfin in CD4+CD25+ T regulatory cells.* Nat Immunol, 2003. **4**(4): p. 337-42.
74. Brunkow, M.E., et al., *Disruption of a new forkhead/winged-helix protein, scurfin, results in the fatal lymphoproliferative disorder of the scurfy mouse.* Nat Genet, 2001. **27**(1): p. 68-73.
75. Kim, J.M., J.P. Rasmussen, and A.Y. Rudensky, *Regulatory T cells prevent catastrophic autoimmunity throughout the lifespan of mice.* Nat Immunol, 2007. **8**(2): p. 191-7.
76. Bennett, C.L., et al., *The immune dysregulation, polyendocrinopathy, enteropathy, X-linked syndrome (IPEX) is caused by mutations of FOXP3.* Nat Genet, 2001. **27**(1): p. 20-1.
77. Wildin, R.S., et al., *X-linked neonatal diabetes mellitus, enteropathy and endocrinopathy syndrome is the human equivalent of mouse scurfy.* Nat Genet, 2001. **27**(1): p. 18-20.
78. Gambineri, E., T.R. Torgerson, and H.D. Ochs, *Immune dysregulation, polyendocrinopathy, enteropathy, and X-linked inheritance (IPEX), a syndrome of systemic autoimmunity caused by mutations of FOXP3, a critical regulator of T-cell homeostasis.* Curr Opin Rheumatol, 2003. **15**(4): p. 430-5.
79. Smith, K.A., *The interleukin 2 receptor.* Annu Rev Cell Biol, 1989. **5**: p. 397-425.
80. Gavin, M.A., et al., *Single-cell analysis of normal and FOXP3-mutant human T cells: FOXP3 expression without regulatory T cell development.* Proc Natl Acad Sci U S A, 2006. **103**(17): p. 6659-64.
81. Gavin, M.A., et al., *Foxp3-dependent programme of regulatory T-cell differentiation.* Nature, 2007. **445**(7129): p. 771-5.
82. Williams, L.M. and A.Y. Rudensky, *Maintenance of the Foxp3-dependent developmental program in mature regulatory T cells requires continued expression of Foxp3.* Nat Immunol, 2007. **8**(3): p. 277-84.
83. Kwon, H.K., et al., *Different molecular complexes that mediate transcriptional induction and repression by FoxP3.* Nat Immunol, 2017. **18**(11): p. 1238-1248.
84. Liu, W., et al., *CD127 expression inversely correlates with FoxP3 and suppressive function of human CD4+ T reg cells.* J Exp Med, 2006. **203**(7): p. 1701-11.
85. Ohkura, N., Y. Kitagawa, and S. Sakaguchi, *Development and maintenance of regulatory T cells.* Immunity, 2013. **38**(3): p. 414-23.
86. Tang, Q., et al., *Central role of defective interleukin-2 production in the triggering of islet autoimmune destruction.* Immunity, 2008. **28**(5): p. 687-97.
87. Ehrenstein, M.R., et al., *Compromised function of regulatory T cells in rheumatoid arthritis and reversal by anti-TNFalpha therapy.* J Exp Med, 2004. **200**(3): p. 277-85.

88. Viglietta, V., et al., *Loss of functional suppression by CD4+CD25+ regulatory T cells in patients with multiple sclerosis.* J Exp Med, 2004. **199**(7): p. 971-9.
89. Denning, T.L., G. Kim, and M. Kronenberg, *Cutting edge: CD4+CD25+ regulatory T cells impaired for intestinal homing can prevent colitis.* J Immunol, 2005. **174**(12): p. 7487-91.
90. Maul, J., et al., *Peripheral and intestinal regulatory CD4+ CD25(high) T cells in inflammatory bowel disease.* Gastroenterology, 2005. **128**(7): p. 1868-78.
91. Mayne, C.G. and C.B. Williams, *Induced and natural regulatory T cells in the development of inflammatory bowel disease.* Inflamm Bowel Dis, 2013. **19**(8): p. 1772-88.
92. Schneidawind, D., A. Pierini, and R.S. Negrin, *Regulatory T cells and natural killer T cells for modulation of GVHD following allogeneic hematopoietic cell transplantation.* Blood, 2013. **122**(18): p. 3116-21.
93. Edinger, M., et al., *CD4+CD25+ regulatory T cells preserve graft-versus-tumor activity while inhibiting graft-versus-host disease after bone marrow transplantation.* Nat Med, 2003. **9**(9): p. 1144-50.
94. Sabatos-Peyton, C.A., J. Verhagen, and D.C. Wraith, *Antigen-specific immunotherapy of autoimmune and allergic diseases.* Curr Opin Immunol, 2010. **22**(5): p. 609-15.
95. Nishikawa, H. and S. Sakaguchi, *Regulatory T cells in cancer immunotherapy.* Curr Opin Immunol, 2014. **27**: p. 1-7.
96. Di Ianni, M., et al., *Tregs prevent GVHD and promote immune reconstitution in HLA-haploidentical transplantation.* Blood, 2011. **117**(14): p. 3921-8.
97. Brunstein, C.G., et al., *Infusion of ex vivo expanded T regulatory cells in adults transplanted with umbilical cord blood: safety profile and detection kinetics.* Blood, 2011. **117**(3): p. 1061-70.
98. Gliwinski, M., D. Iwaszkiewicz-Grzes, and P. Trzonkowski, *Cell-Based Therapies with T Regulatory Cells.* BioDrugs, 2017. **31**(4): p. 335-347.
99. Brunstein, C.G., et al., *Adoptive transfer of umbilical cord blood-derived regulatory T cells and early viral reactivation.* Biol Blood Marrow Transplant, 2013. **19**(8): p. 1271-3.
100. Theil, A., et al., *Adoptive transfer of allogeneic regulatory T cells into patients with chronic graft-versus-host disease.* Cytotherapy, 2015. **17**(4): p. 473-86.
101. Abbas, A.K., et al., *Regulatory T cells: recommendations to simplify the nomenclature.* Nat Immunol, 2013. **14**(4): p. 307-8.
102. Hsieh, C.S., et al., *An intersection between the self-reactive regulatory and nonregulatory T cell receptor repertoires.* Nat Immunol, 2006. **7**(4): p. 401-10.
103. Shevach, E.M. and A.M. Thornton, *tTregs, pTregs, and iTregs: similarities and differences.* Immunol Rev, 2014. **259**(1): p. 88-102.
104. Yadav, M., et al., *Neuropilin-1 distinguishes natural and inducible regulatory T cells among regulatory T cell subsets in vivo.* J Exp Med, 2012. **209**(10): p. 1713-22, S1-19.
105. Chen, W., et al., *Conversion of peripheral CD4+CD25- naive T cells to CD4+CD25+ regulatory T cells by TGF-beta induction of transcription factor Foxp3.* J Exp Med, 2003. **198**(12): p. 1875-86.
106. Ostman, S., et al., *Impaired regulatory T cell function in germ-free mice.* Eur J Immunol, 2006. **36**(9): p. 2336-46.
107. Atarashi, K., et al., *Induction of colonic regulatory T cells by indigenous Clostridium species.* Science, 2011. **331**(6015): p. 337-41.
108. Atarashi, K., et al., *Treg induction by a rationally selected mixture of Clostridia strains from the human microbiota.* Nature, 2013. **500**(7461): p. 232-6.
109. Samstein, R.M., et al., *Extrathymic generation of regulatory T cells in placental mammals mitigates maternal-fetal conflict.* Cell, 2012. **150**(1): p. 29-38.

110. Zheng, Y., et al., *Role of conserved non-coding DNA elements in the Foxp3 gene in regulatory T-cell fate.* Nature, 2010. **463**(7282): p. 808-12.
111. Josefowicz, S.Z., et al., *Extrathymically generated regulatory T cells control mucosal TH2 inflammation.* Nature, 2012. **482**(7385): p. 395-9.
112. Thornton, A.M., et al., *Expression of Helios, an Ikaros transcription factor family member, differentiates thymic-derived from peripherally induced Foxp3+ T regulatory cells.* J Immunol, 2010. **184**(7): p. 3433-41.
113. Kelley, C.M., et al., *Helios, a novel dimerization partner of Ikaros expressed in the earliest hematopoietic progenitors.* Curr Biol, 1998. **8**(9): p. 508-15.
114. Hahm, K., et al., *Helios, a T cell-restricted Ikaros family member that quantitatively associates with Ikaros at centromeric heterochromatin.* Genes Dev, 1998. **12**(6): p. 782-96.
115. Akimova, T., et al., *Helios expression is a marker of T cell activation and proliferation.* PLoS One, 2011. **6**(8): p. e24226.
116. Gottschalk, R.A., E. Corse, and J.P. Allison, *Expression of Helios in peripherally induced Foxp3+ regulatory T cells.* J Immunol, 2012. **188**(3): p. 976-80.
117. Serre, K., et al., *Helios is associated with CD4 T cells differentiating to T helper 2 and follicular helper T cells in vivo independently of Foxp3 expression.* PLoS One, 2011. **6**(6): p. e20731.
118. Weiss, J.M., et al., *Neuropilin 1 is expressed on thymus-derived natural regulatory T cells, but not mucosa-generated induced Foxp3+ T reg cells.* J Exp Med, 2012. **209**(10): p. 1723-42, S1.
119. Sarris, M., et al., *Neuropilin-1 expression on regulatory T cells enhances their interactions with dendritic cells during antigen recognition.* Immunity, 2008. **28**(3): p. 402-13.
120. Delgoffe, G.M., et al., *Stability and function of regulatory T cells is maintained by a neuropilin-1-semaphorin-4a axis.* Nature, 2013. **501**(7466): p. 252-6.
121. Solomon, B.D., et al., *Neuropilin-1 attenuates autoreactivity in experimental autoimmune encephalomyelitis.* Proc Natl Acad Sci U S A, 2011. **108**(5): p. 2040-5.
122. Corbel, C., et al., *Neuropilin 1 and CD25 co-regulation during early murine thymic differentiation.* Dev Comp Immunol, 2007. **31**(11): p. 1082-94.
123. Yadav, M., S. Stephan, and J.A. Bluestone, *Peripherally induced tregs - role in immune homeostasis and autoimmunity.* Front Immunol, 2013. **4**: p. 232.
124. Shevach, E.M., *Mechanisms of foxp3+ T regulatory cell-mediated suppression.* Immunity, 2009. **30**(5): p. 636-45.
125. Vignali, D.A., L.W. Collison, and C.J. Workman, *How regulatory T cells work.* Nat Rev Immunol, 2008. **8**(7): p. 523-32.
126. Chinen, T., et al., *An essential role for the IL-2 receptor in Treg cell function.* Nat Immunol, 2016. **17**(11): p. 1322-1333.
127. Thornton, A.M. and E.M. Shevach, *CD4+CD25+ immunoregulatory T cells suppress polyclonal T cell activation in vitro by inhibiting interleukin 2 production.* J Exp Med, 1998. **188**(2): p. 287-96.
128. Wing, K., et al., *CTLA-4 control over Foxp3+ regulatory T cell function.* Science, 2008. **322**(5899): p. 271-5.
129. von Boehmer, H., *Mechanisms of suppression by suppressor T cells.* Nat Immunol, 2005. **6**(4): p. 338-44.
130. Chaudhry, A., et al., *Interleukin-10 signaling in regulatory T cells is required for suppression of Th17 cell-mediated inflammation.* Immunity, 2011. **34**(4): p. 566-78.
131. Wan, Y.Y. and R.A. Flavell, *'Yin-Yang' functions of transforming growth factor-beta and T regulatory cells in immune regulation.* Immunol Rev, 2007. **220**: p. 199-213.

132. Gavin, M.A., et al., *Homeostasis and anergy of CD4(+)CD25(+) suppressor T cells in vivo.* Nat Immunol, 2002. **3**(1): p. 33-41.
133. Annacker, O., et al., *CD25+ CD4+ T cells regulate the expansion of peripheral CD4 T cells through the production of IL-10.* J Immunol, 2001. **166**(5): p. 3008-18.
134. Jordan, M.S., et al., *Thymic selection of CD4+CD25+ regulatory T cells induced by an agonist self-peptide.* Nat Immunol, 2001. **2**(4): p. 301-6.
135. Walker, L.S., et al., *Antigen-dependent proliferation of CD4+ CD25+ regulatory T cells in vivo.* J Exp Med, 2003. **198**(2): p. 249-58.
136. Apostolou, I. and H. von Boehmer, *In vivo instruction of suppressor commitment in naive T cells.* J Exp Med, 2004. **199**(10): p. 1401-8.
137. Mucida, D., et al., *Oral tolerance in the absence of naturally occurring Tregs.* J Clin Invest, 2005. **115**(7): p. 1923-33.
138. Thorstenson, K.M. and A. Khoruts, *Generation of anergic and potentially immunoregulatory CD25+CD4 T cells in vivo after induction of peripheral tolerance with intravenous or oral antigen.* J Immunol, 2001. **167**(1): p. 188-95.
139. Unger, W.W., et al., *Early events in peripheral regulatory T cell induction via the nasal mucosa.* J Immunol, 2003. **171**(9): p. 4592-603.
140. Kretschmer, K., et al., *Inducing and expanding regulatory T cell populations by foreign antigen.* Nat Immunol, 2005. **6**(12): p. 1219-27.
141. Akbarpour, M., et al., *Insulin B chain 9-23 gene transfer to hepatocytes protects from type 1 diabetes by inducing Ag-specific FoxP3+ Tregs.* Sci Transl Med, 2015. **7**(289): p. 289ra81.
142. Daniel, C., et al., *Prevention of type 1 diabetes in mice by tolerogenic vaccination with a strong agonist insulin mimetope.* J Exp Med, 2011. **208**(7): p. 1501-10.
143. Reed, J.C. and K.C. Herold, *Thinking bedside at the bench: the NOD mouse model of T1DM.* Nat Rev Endocrinol, 2015. **11**(5): p. 308-14.
144. van Belle, T.L., K.T. Coppieters, and M.G. von Herrath, *Type 1 diabetes: etiology, immunology, and therapeutic strategies.* Physiol Rev, 2011. **91**(1): p. 79-118.
145. Anderson, M.S. and J.A. Bluestone, *The NOD mouse: a model of immune dysregulation.* Annu Rev Immunol, 2005. **23**: p. 447-85.
146. Wenzlau, J.M., et al., *The cation efflux transporter ZnT8 (Slc30A8) is a major autoantigen in human type 1 diabetes.* Proc Natl Acad Sci U S A, 2007. **104**(43): p. 17040-5.
147. Zucchelli, S., et al., *Defective central tolerance induction in NOD mice: genomics and genetics.* Immunity, 2005. **22**(3): p. 385-96.
148. Wicker, L.S., J.A. Todd, and L.B. Peterson, *Genetic control of autoimmune diabetes in the NOD mouse.* Annu Rev Immunol, 1995. **13**: p. 179-200.
149. Serreze, D.V. and E.H. Leiter, *Genetic and pathogenic basis of autoimmune diabetes in NOD mice.* Curr Opin Immunol, 1994. **6**(6): p. 900-6.
150. Maier, L.M. and L.S. Wicker, *Genetic susceptibility to type 1 diabetes.* Curr Opin Immunol, 2005. **17**(6): p. 601-8.
151. Serreze, D.V., J.W. Gaedeke, and E.H. Leiter, *Hematopoietic stem-cell defects underlying abnormal macrophage development and maturation in NOD/Lt mice: defective regulation of cytokine receptors and protein kinase C.* Proc Natl Acad Sci U S A, 1993. **90**(20): p. 9625-9.
152. Greeley, S.A., et al., *Elimination of maternally transmitted autoantibodies prevents diabetes in nonobese diabetic mice.* Nat Med, 2002. **8**(4): p. 399-402.
153. Kagohashi, Y., et al., *Maternal factors in a model of type 1 diabetes differentially affect the development of insulitis and overt diabetes in offspring.* Diabetes, 2005. **54**(7): p. 2026-31.

154. Katz, J.D., et al., *Following a diabetogenic T cell from genesis through pathogenesis.* Cell, 1993. **74**(6): p. 1089-100.
155. Kikutani, H. and S. Makino, *The murine autoimmune diabetes model: NOD and related strains.* Adv Immunol, 1992. **51**: p. 285-322.
156. Bach, J.F., *Insulin-dependent diabetes mellitus as an autoimmune disease.* Endocr Rev, 1994. **15**(4): p. 516-42.
157. Shoda, L.K., et al., *A comprehensive review of interventions in the NOD mouse and implications for translation.* Immunity, 2005. **23**(2): p. 115-26.
158. Schuster, C., et al., *Peripherally induced regulatory T cells contribute to the control of autoimmune diabetes in the NOD mouse model.* Eur J Immunol, 2018. **48**(7): p. 1211-1216.
159. Gonzalez, A., et al., *Damage control, rather than unresponsiveness, effected by protective DX5+ T cells in autoimmune diabetes.* Nat Immunol, 2001. **2**(12): p. 1117-25.
160. Van Belle, T.L., P. Taylor, and M.G. von Herrath, *Mouse Models for Type 1 Diabetes.* Drug Discov Today Dis Models, 2009. **6**(2): p. 41-45.
161. Blunt, T., et al., *Defective DNA-dependent protein kinase activity is linked to V(D)J recombination and DNA repair defects associated with the murine scid mutation.* Cell, 1995. **80**(5): p. 813-23.
162. Rohane, P.W., et al., *Islet-infiltrating lymphocytes from prediabetic NOD mice rapidly transfer diabetes to NOD-scid/scid mice.* Diabetes, 1995. **44**(5): p. 550-4.
163. Marie, J.C., et al., *TGF-beta1 maintains suppressor function and Foxp3 expression in CD4+CD25+ regulatory T cells.* J Exp Med, 2005. **201**(7): p. 1061-7.
164. Li, M.O., S. Sanjabi, and R.A. Flavell, *Transforming growth factor-beta controls development, homeostasis, and tolerance of T cells by regulatory T cell-dependent and -independent mechanisms.* Immunity, 2006. **25**(3): p. 455-71.
165. Schallenberg, S., et al., *Identification of an immediate Foxp3(-) precursor to Foxp3(+) regulatory T cells in peripheral lymphoid organs of nonmanipulated mice.* J Exp Med, 2010. **207**(7): p. 1393-407.
166. Curotto de Lafaille, M.A., et al., *CD25- T cells generate CD25+Foxp3+ regulatory T cells by peripheral expansion.* J Immunol, 2004. **173**(12): p. 7259-68.
167. Knoechel, B., et al., *Sequential development of interleukin 2-dependent effector and regulatory T cells in response to endogenous systemic antigen.* J Exp Med, 2005. **202**(10): p. 1375-86.
168. Sun, J., et al., *Antigen-specific T cell activation and proliferation during oral tolerance induction.* J Immunol, 1999. **162**(10): p. 5868-75.
169. Flaherty, S. and J.M. Reynolds, *Mouse Naive CD4+ T Cell Isolation and In vitro Differentiation into T Cell Subsets.* J Vis Exp, 2015(98).
170. Akkaya, B., et al., *Ex-vivo iTreg differentiation revisited: Convenient alternatives to existing strategies.* J Immunol Methods, 2017. **441**: p. 67-71.
171. Karlsson, F., et al., *Ex vivo generation of regulatory T cells: characterization and therapeutic evaluation in a model of chronic colitis.* Methods Mol Biol, 2011. **677**: p. 47-61.
172. Huber, S., et al., *Cutting edge: TGF-beta signaling is required for the in vivo expansion and immunosuppressive capacity of regulatory CD4+CD25+ T cells.* J Immunol, 2004. **173**(11): p. 6526-31.
173. Cobbold, S.P., et al., *Induction of foxP3+ regulatory T cells in the periphery of T cell receptor transgenic mice tolerized to transplants.* J Immunol, 2004. **172**(10): p. 6003-10.

174. Peng, Y., et al., *TGF-beta regulates in vivo expansion of Foxp3-expressing CD4+CD25+ regulatory T cells responsible for protection against diabetes.* Proc Natl Acad Sci U S A, 2004. **101**(13): p. 4572-7.
175. Komai, T., et al., *Transforming Growth Factor-beta and Interleukin-10 Synergistically Regulate Humoral Immunity via Modulating Metabolic Signals.* Front Immunol, 2018. **9**: p. 1364.
176. Clemente-Casares, X., et al., *Expanding antigen-specific regulatory networks to treat autoimmunity.* Nature, 2016. **530**(7591): p. 434-40.
177. Schliesser, U., et al., *Generation of highly effective and stable murine alloreactive Treg cells by combined anti-CD4 mAb, TGF-beta, and RA treatment.* Eur J Immunol, 2013. **43**(12): p. 3291-305.
178. Szurek, E., et al., *Differences in Expression Level of Helios and Neuropilin-1 Do Not Distinguish Thymus-Derived from Extrathymically-Induced CD4+Foxp3+ Regulatory T Cells.* PLoS One, 2015. **10**(10): p. e0141161.
179. Fantini, M.C., et al., *In vitro generation of CD4+ CD25+ regulatory cells from murine naive T cells.* Nat Protoc, 2007. **2**(7): p. 1789-94.
180. Fantini, M.C., et al., *Cutting edge: TGF-beta induces a regulatory phenotype in CD4+CD25- T cells through Foxp3 induction and down-regulation of Smad7.* J Immunol, 2004. **172**(9): p. 5149-53.
181. Shevach, E.M., et al., *The critical contribution of TGF-beta to the induction of Foxp3 expression and regulatory T cell function.* Eur J Immunol, 2008. **38**(4): p. 915-7.
182. Oida, T. and H.L. Weiner, *Depletion of TGF-beta from fetal bovine serum.* J Immunol Methods, 2010. **362**(1-2): p. 195-8.
183. Hoglund, P., et al., *Initiation of autoimmune diabetes by developmentally regulated presentation of islet cell antigens in the pancreatic lymph nodes.* J Exp Med, 1999. **189**(2): p. 331-9.
184. Daniel, C., H. Ploegh, and H. von Boehmer, *Antigen-specific induction of regulatory T cells in vivo and in vitro.* Methods Mol Biol, 2011. **707**: p. 173-85.
185. Li, M.O. and R.A. Flavell, *TGF-beta: a master of all T cell trades.* Cell, 2008. **134**(3): p. 392-404.
186. Josefowicz, S.Z. and A. Rudensky, *Control of regulatory T cell lineage commitment and maintenance.* Immunity, 2009. **30**(5): p. 616-25.
187. Tone, Y., et al., *Smad3 and NFAT cooperate to induce Foxp3 expression through its enhancer.* Nat Immunol, 2008. **9**(2): p. 194-202.
188. Rudensky, A.Y., *Regulatory T cells and Foxp3.* Immunol Rev, 2011. **241**(1): p. 260-8.
189. Schlenner, S.M., et al., *Smad3 binding to the foxp3 enhancer is dispensable for the development of regulatory T cells with the exception of the gut.* J Exp Med, 2012. **209**(9): p. 1529-35.
190. Verhagen, J., A. Wegner, and D.C. Wraith, *Extra-thymically induced T regulatory cell subsets: the optimal target for antigen-specific immunotherapy.* Immunology, 2015. **145**(2): p. 171-81.
191. Esensten, J.H., et al., *Regulatory T-cell therapy for autoimmune and autoinflammatory diseases: The next frontier.* J Allergy Clin Immunol, 2018. **142**(6): p. 1710-1718.
192. Martelli, M.F., et al., *HLA-haploidentical transplantation with regulatory and conventional T-cell adoptive immunotherapy prevents acute leukemia relapse.* Blood, 2014. **124**(4): p. 638-44.
193. Edinger, M. and P. Hoffmann, *Regulatory T cells in stem cell transplantation: strategies and first clinical experiences.* Curr Opin Immunol, 2011. **23**(5): p. 679-84.
194. Geissler, E.K., *The ONE Study compares cell therapy products in organ transplantation: introduction to a review series on suppressive monocyte-derived cells.* Transplant Res, 2012. **1**(1): p. 11.

195. Marek-Trzonkowska, N., et al., *Factors affecting long-term efficacy of T regulatory cell-based therapy in type 1 diabetes.* J Transl Med, 2016. **14**(1): p. 332.
196. Marek-Trzonkowska, N., et al., *Therapy of type 1 diabetes with CD4(+)CD25(high)CD127-regulatory T cells prolongs survival of pancreatic islets - results of one year follow-up.* Clin Immunol, 2014. **153**(1): p. 23-30.
197. Marek-Trzonkowska, N., et al., *Administration of CD4+CD25highCD127- regulatory T cells preserves beta-cell function in type 1 diabetes in children.* Diabetes Care, 2012. **35**(9): p. 1817-20.
198. Bluestone, J.A., et al., *Type 1 diabetes immunotherapy using polyclonal regulatory T cells.* Sci Transl Med, 2015. **7**(315): p. 315ra189.

Appendix

Publication

Schuster, C., **Jonas, F.**, Zhao F., Kissler, S. *Peripherally induced regulatory T cells contribute to the control of autoimmune diabetes in the NOD mouse model.* Eur J Immunol, 2018. 48(7): p. 1211-1216.

Affidavit

I hereby confirm that my thesis entitled "CNS1-dependency of *in vivo* peptide-induced $CD4^+Foxp3^+$ regulatory T cells" is the result of my own work. I did not receive any help or support from commercial consultants. All sources and / or materials applied are listed and specified in the thesis.

Furthermore, I confirm that this thesis has not yet been submitted as part of another examination process neither in identical nor in similar form.

Würzburg Signature

Acknowledgments

First of all, I want to thank Dr. Stephan Kissler of the Joslin Diabetes Center at Harvard Medical School who gave me the unique opportunity to work as a part of his research group and who guided me throughout this project. I am very grateful for this great support and academic input.

I also want to thank my primary supervisor for this project Prof. Dr. Manfred Lutz of the Institute for Virology and Immunobiology at Julius-Maximilians-Universität Würzburg and Prof. Dr. Martin Fassnacht at University Hospital Würzburg as further member of my thesis committee for their helpful contribution and survey.

I also would like to thank Dr. Cornelia Schuster for her daily supervision and teaching in the laboratory.

Thanks also to all other members of the research group for their valuable feedback.

I wish to extend my special thanks to the Graduate School of Life Sciences at Julius-Maximilians-Universität Würzburg and the Max Weber-Program of the State of Bavaria. Without their financial funding I could not have finalised this project.

Finally, I particularly want to thank my family and friends for their support.